Bettina Hoser

Analysis of Asymmetric Communication Patterns in Computer Mediated Communication Environments

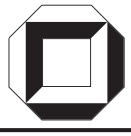

universitätsverlag karlsruhe

Bettina Hoser

Analysis of Asymmetric Communication Patterns in Computer Mediated Communication Environments

Analysis of Asymmetric Communication Patterns in Computer Mediated Communication Environments

von
Bettina Hoser

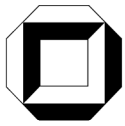

universitätsverlag karlsruhe

Dissertation, genehmigt von der Fakultät für Wirtschaftswissenschaften
der Universität Fridericiana zu Karlsruhe, 2004
Referenten: Prof. Dr. Andreas Geyer-Schulz, Prof. Dr. Karl-Heinz Waldmann

Impressum

Universitätsverlag Karlsruhe
c/o Universitätsbibliothek
Straße am Forum 2
D-76131 Karlsruhe

www.uvka.de

Print on Demand

ISBN 3-937300-49-X

Acknowledgement

To Doris Hoser.

But from the Sage it is so hard at any price to get a single word
That when his task is accomplished, his work done,
Throughout the country every one says: "It happened of its own accord".
(Lao-zi, The Dao De Jing)

Contents

Notation

$\mathbb{R}$	set of real numbers
$\mathbb{C}$	set of complex numbers
$\mathbf{A}$	matrix: capital letters
a_{kl}	matrix entry in the k-th row and l-th column
$\mathbf{V}$	vector space: bold capital letters
$\mathbf{x}$	vector: bold letters
$\mathbf{x}_{kl}$	: l-th component of vector $\mathbf{x}_k$
λ	eigenvalue: greek letters
$G\{V, E, A\}$	graph G with vertices $v \in V$, edges $e \in E$ and adjacency matrix A
$\langle \mathbf{x} \mid \mathbf{y} \rangle$	inner product of vectors $\mathbf{x}$ and $\mathbf{y}$
$\lvert x \rvert$	absolute value of x
$\parallel \mathbf{x} \parallel$	norm of vector $\mathbf{x}$
$\parallel H \parallel$	norm of matrix $\mathbf{A}$

Chapter 1

Introduction

Many predictions about the ways new technologies will transform society fade quickly - the telegraph, radio, movies, and television did create revolutions, but not the ones we expected. Hence, it is especially important that we turn from opinions and predictions to the serious analysis and description of online groups. (M. Smith and P. Kollock, 1999) [SK99, p.23]

As people transfer part of their social life to the Internet (see for example online communities like friendster [Fri04], linkedin [Lin04], orkut [Ork04], . . .), the question arises if the use of computer mediated communication (CMC) changes the way communities are built and kept alive, or if the known dynamics of social life are just being adapted to the new technology [Wel02]. One focus of interest is the notion of a center of a network. The question is how the way people build groups around certain "very important people" is transfered to CMC. Not only is this question of interest to the sociologist (see for example [Wel01]), but it has become increasingly interesting for security reasons on the one hand, and for its possible economic impact on the other.

Some applications have gained wide publicity, e.g. the hunt for terrorist networks, or the use of network dynamics for political goals. Since the terrorist attacks on New York on september 11th, 2001 the idea of using methods drawn from social network analysis have gained a wide interest [Kre02]. For the suicide attack on New York the terrorists had used modern communication channels, e.g. email and mobile phones, to plan and execute their dreadful attack. Thus interest in the development and enhancement of methods to detect communication patterns of such networks well in advance has grown dramatically.

In the 2004 U.S. presidential elections the campaign used the possibilities of the Internet to reach out to communities by "snowballing " (see [Ker04],

[Bus04]). The aim is to motivate people to participate in the elections, and to use the social networks of supporters to win over even more potential voters.

In the world of economics Hayek [Hay45, p.519-520] points to one of the major problems which researchers try to solve by using network analysis. He explicitly states, that *the peculiar character of the problem of a rational economic order is determined precisely by the fact that the knowledge of the circumstances of which we must make use never exists in concentrated or integrated form, but solely as the dispersed bits of incomplete and frequently contradictory knowledge which all the separate individuals possess*. Thus communication is at the heart of economic success, as well as the efficient allocation of information within a network. To know the patterns of such communication offers the possibility to act according to the needs of the organization. Hayek´s example is an illustration that the knowledge gained about social networks and how they are analyzed might be useful in understanding economic processes like markets.

Thus on the business side the opportunity to view customer, employee, supplier or trader behavior via their use of new media becomes ever more interesting, tempting and revealing. The availability of huge data sets, e.g. email server data or market log files, has opened the possibility to analyze behavior without the drawback of having to explicitly ask the observed subjects about their behavior. The discussion about privacy in this context and the legal aspects of the use of data without the explicit consent of the observed subjects is still on going. The legal systems of Germany and the United States for example have different approaches to privacy, which has the effect, that while in Germany emails in a company environment fall under strict laws protecting the privacy of the author, this is not the case in the U.S. Thus data like this is not easily accessible in Germany. Messages posted to newsgroups or any other open communication plattform are not protected by law neither in the U.S. nor in Germany. The scientific community though tends to either ask permission of any such group before using the data, or afterwards.

The way email, for example in an organization, is being used can reveal if the organizational structure of the company is reflected in the groups that can be detected out of the CMC [KH93]. On the customer side on the other hand the analysis of customer newsgroups or chat rooms could help identify those customers who can swing opinions, and thus help in marketing efforts. An application here is for example viral marketing. Another example of a network is given when one looks at supply chain management. Here a network of suppliers has to perform the difficult task of bringing parts and components together at the right time, in the required amount to the manufacturer. In this context informational efficiency plays a major role to cut costs or to stay on budget. If one now looks at even larger structures, one can see, that information efficiency is highly correlated with efficient markets. And these again can be viewed as social networks in the sense,

that agents interact via communication to trade goods or information.

As can be seen from these few examples the impact of CMC on communities and social interaction is strong. Consequently the interest of researchers, and subsequently, the use of their results for business applications, is growing rapidly.

There are many different angles from which these interactions can be analyzed. The one that will be in the focus in the course of this book is the question of centrality of a member within his or her social network. Centrality characterizes the fact, that a member plays a very important role within a given network and with respect to the interaction observed. The methods that have been developed in such until now unrelated fields as sociology, computer science, psychology, mathematics, operations research, physics, and signal intelligence have been brought together to yield insight into subject behavior in the Internet age by analyzing communication structures and dynamics in virtual communities using CMC.

1.1 Motivation

It´s who you know. Really.
(D. Gross, 2004) [Gro04]

To find structure in "uncharted" communities has been of interest for sociologists and intelligence service researchers for many years and, due to the effect the Internet has on marketing it has gained growing interest in the business world. The interest of sociologists is to find out, who is "important" within a community, who "leads", who corresponds with whom, thus putting the focus on relationships within a group in a sociological sense. The interest of intelligence services is to identify the links within a communication network, that, if shut down, most effectively hurt the targeted network. Lastly the interest of companies lies on the one hand in the knowledge about the behavior of their customers, which can be an integral part of customer relationship management efforts. On the other hand the knowledge of the existence of so called "hidden organizations" is of importance for the business processes within the company when process optimization is the goal. Thus the knowledge of communication structure has been of major importance for these fields.

Making all communication structures with respect to social interaction visible has been made possible by applying different methods to different "views" of the communication of a given community. Some of these views are: hierarchy, friendship, communication with, etc. Some of the employed methods are: graph theory, hubs and authority algorithms and stochastic processes.

But one major aspect of communication has been very difficult to analyze due to difficulties which arise from the mathematical tools used to explain communication structure through communication behavior. Communication is *a process by which information is exchanged between individuals through a common system of symbols, signs, or behavior* [Dic04]. Thus by definition it is bilateral. Several questions arise from this fact. For one there is the large field of signal processing, which looks at the way signals can be transmitted from one point, the source, to another, the destination. When signals are combined to create meaningful messages, the question of semantic and information arise. Information has been the focus of mathematical information theory which was founded by Shannon in 1948 [SW63].

Communication in the course of this book will be seen as the bilateral process of exchange of messages between to members of a network. Neither will the question be discussed whether the information transmitted has been understood by the recipient, nor will there be any discussion about the technical measures of information. The focus will be on the question how to identify patterns of communication in a given network if all exchanges are included in the analysis simultaneously. This has until now posed several problems when trying to use standard procedures as for example eigensystem analysis. The underlying data had to be represented in a real valued so called adjacency matrix.

Real numbers can only store data on one communication direction instead of two when looking at bilateral communication. To encode two components, data had to be for example dichotomized to represent the dominant direction of communication. This led to asymmetric matrices. These matrices are difficult to use in eigensystem analysis, since their spectrum can yield negative or even imaginary eigenvalues, which are difficult to interpret.

To circumvent this, matrices are being preprocessed in different ways to make them symmetric, because in this case the eigensystem is easier to interpret. One way is to multiply these matrices with their transposed matrices, which makes the result symmetric, and thus better behaved. Another method is to use matrix decomposition for square matrices to construct a symmetric matrix.

Another problem arises from the fact that real valued matrices use Euclidean space. Thus distances are interpreted in a way, that is often inappropriate for the subject. Especially in cases of non-transitivity, where distances in Euclidean space suggest that there should be transitivity, give rise to some difficulties in interpretation.

All these methods have one problem in common. Information is lost or is prone to noise-induced errors. Another problem is the fact, that some of these methods only use the principal eigenpair for interpretation, thus neglecting the information that the rest of the eigensystem might reveal about the underlying structure.

The objective of this book is to introduce a generalized method to analyze completely the structure of an asymmetric communication network, to validate this method using standard data sets and to point out some applications that might benefit from these findings. The data sets used consist of two way email communication within a community. The results will be obtained by using complex Hermitian adjacency matrices instead of real valued adjacency matrices. A complex number can store both communication directions in one number. The eigensystem of complex Hermitian matrices yields a powerful tool to explain the communication structure of a community based on its often asymmetric communication pattern structure, due to the mathematical properties of this class of matrices. Several points are noteworthy, and will be discussed in the course of this work:

- The Hermitian matrix can be decomposed into a Fourier sum of its subspaces weighted with the respective eigenvalue.
- All eigenvalues of Hermitian matrices are real and depend on the amount of communication within the group: This makes interpretation of these eigenvalues as “energy levels” intuitive.
- The eigenvalues can also be used to interpret the relevance of patterns due to the fact that they explain the part of the total variance contained in a subspace.
- The eigenvalues are at the same time also coordinates in Hilbert space, showing the relevance of the subspace in reference to the original matrix.
- The eigenvectors form an orthogonal (e.g. pairwise independent) system: all eigenvectors can be used for interpretation purposes.
- The orthogonal projector, derived from the eigenvector, reveals the similarity pattern between different members in respect of the subspace pattern.
- To show stability or instability of a matrix eigensystem when disturbances take place - for example flame wars - perturbation theory can be used to explain what happens and why.
- No ex ante notion has to be used or filters applied to preprocess the data: No loss of information has to be accepted.

These characteristics give rise to a clearer view on communication patterns in substructures within virtual communities (VC) based on the communication traffic volume and communication behavior within the group.

1.2 Guide to the Reader

In chapter 2 of this book a review of the research done in this field will be given and the relevant literature will be surveyed to introduce the reader to the topic of the use of eigensystem analysis in communication structure analysis. A short excursion at the end of that chapter will show how communication is analyzed using graph-theoretical approaches or tools used in physics. Also some applications from economics will be presented.

After this introduction to the field, chapter 3 will establish the theoretical basis on which this book is grounded. Complex eigensystem analysis of Hermitian matrices will be the main subject.

Chapter 4 will present the main idea of this book. The construction of the complex Hermitian adjacency matrix will be explained and some examples of artificially constructed communication patterns will be discussed to make the reader familiar with the approach.

Chapter 5 describes the data sets that have been used. In order to compare the results of the proposed method to those already existing, the EIES (Electronic Information Exchange System) data set of L. and S. Freeman [FF79] has been used as well as a subset thereof [Fre97].

After that the results obtained with the proposed method will be presented and results will be discussed extensively in chapter 6. Here the eigensystems gained from the data are shown and interpretations will be given based on the insights gained in chapter 4. In addition a comparative interpretation will be given, which points out the advantages of the proposed method with regard to the standard methods.

Chapter 7 summarizes the results of this book, refers to some interesting applications and points out problems that might be of interest for further research.

Chapter 2

Related Work

The aim of this chapter is to provide an overview of research done in the field of communication structure analysis with the help of eigensystem analysis of social networks, especially in email networks. To achieve that, a short review of literature on rank, prestige and status indices as well as eigenvector centrality will be given. This will provide the background for the generalized approach for communication structure analysis presented in this book.

In section 2.2 degree based measurements will be discussed, which give an intuitive introduction into section 2.3 about eigensystem analysis, which starts with rank and prestige or status measurements and goes on to other eigenvector centrality methods. As a side track a short overview of approaches toward network analysis from a physics point of view will be given. Section 2.4 will the point out some applications of the methods described in the preceding sections.

2.1 Social Network Analysis

A recent standard text book for SNA is by Wasserman and Faust [WF94]. Social network analysis (SNA) offers many tools to describe and/or evaluate relationship within a given network or group of people. It *focuses on patterns of relations among people, organizations, states, etc.* [GHW97]. This tool set allows to test theories about the concepts that describe these relationships. For a more elaborate definition of SNA see [WF94, p.16]. This tool set has over time grown and become more elaborate.

The basic concept, that is investigated, is that of choice, meaning, that the underlying sociomatrix is built up from the communication choices that the members within a network make. The importance of choice in an economical setting has first been emphasized in A. Samuelson´s Revealed Preference Theory [Sam48]. Choice can be interpreted in a broad sense. As early as 1984 Freeman [Fre84]

showed how CMC, and thus "choice" of email partners, could help to form and strengthen ties within a scientific community. Also Garton and Wellman [GW95] give a review on how the use of electronic mail has an impact on organizations. In 2001 Wellman [Wel01, p.2032] points out, that the fact that one person writes an email to another person can also be seen as a form of choice.

2.2 Degree based Measurements

The intuitive explanation of centrality and prestige of a network member is based on the number and direction of choices members in a network make. In addition to intuitiveness it is also easy to encode. A network can be viewed as a graph G where a line/edge connects two vertices k and l if those two vertices are related in any sense. If the connection has a direction, then the edge is transformed into an arrow starting at the vertex that made the choice and ends at the vertex that was chosen.

One of the first to introduce a centrality measure was Bavelas [Bav48], who in the field of psychology transfered ideas from topology to describe group structure and possible behavior.

In graph theory it is known that graphs can be encoded in so called adjacency matrices [Jun99]. The entries in that matrix are either 1 if a connection exists between two vertices, or 0 if it does not exist. Thus this matrix is either symmetric, if no direction is apparent, or asymmetric, if the choice has an inherent direction.

A standard approach for the measurement of centrality is based on degree measurements (see section. 3.2.1). The degree is the number of edges (choices made), that go out of (out-degree) or come into (in-degree) a vertex of a graph. It focuses on the question who (or which group) can be seen as most central with respect to their in- or out-degree with respect to their capacity to transfer for example messages within a network. These measurements can either be used as a stand alone characterization of a network, or in conjunction with other tools. Everett and Borgatti [EB99] give an overview of these measures and even extend it further to help analyze groups. To use these tools, measurements like degree, closeness, betweenness centrality and flow betweenness have been defined. The major drawback lies in the fact that either in-degree or out-degree can be used, but not both simultaneously.

A branch of the degree based approach looks at large networks and their evolution. Erdös and Renyi described in their 1959 paper on random graphs how such systems can be described. They proposed, that networks (or graphs) are built by the attachment of new vertices to an existing graph, and that the probability with which the new vertex attaches to an existing vertex is equally distributed. In 1999 Barabasi and Albert found [ALB99], that for real world networks, such as

the World Wide Web or the nervous system, the assumption of equally distributed attachment probability does not hold. They found that such networks show a scale-free degree distribution in contrast to the distribution expected by the random graph theory of Erdös and Renyi. Scale-free networks are described by the fact that the probability $p(d)$ that a vertex is connected to d other vertices follows a power law distribution $p(d) \sim d^{-\gamma}$. This means that vertices with almost any degree can be found in such a network. A special interest of this branch of research is in the vulnerability of networks, since in a large scale-free network there are nodes that have a very high degree that, when attacked, could cause a complete network breakdown. Large in this context means that the number of nodes/members in a networks exceeds 10^3. As an example see, Ebel et al. [EMB02]. They describe an email network of size $N = 59,912$ nodes. They use email addresses as nodes and exchanged messages as links. For instant messaging Smith [Smi02] shows also the scale-free characteristic and points towards aspects of vulnerability.

Based on degree measurements there is also research in the field of community analysis. There have been two approaches. One approach looks for densely knit groups within a network, which translates into high degree centrality, while the other looks for those members who have a high betweenness centrality (see section. 3.2.1) and then cut the network at that point, repeating this procedure until the network decomposes. See for example [ADDG$^+$04].

A slightly different standard approach is based on the more graph-theoretical approaches, even though it is closely connected to the degree measurements. It focuses mainly on the identification of subgroups within a given network/graph.

Recent research by Tyler et al. [TWH03] showed that they could identify subgroups in email networks by analyzing betweenness centrality in the form of inter-community edges with a large betweenness value. These edges are then removed until the graph decomposes into separate communities, thus re-organizing the graph structure. This is a min-cut-max-flow approach as discussed for example in Ford and Fulkerson [FF62]. The graph representing the network was generated by defining a cut-off number of emails that must be exchanged between members, and a minimum number of emails that had to be exchanged, so that a member was included into the graph. As discussed above, this could mean loss of information For example, it is not possible later on to find out who were the real “lurkers” in that network, since the threshold eliminated these. Lurkers are those network members who stand at the sidelines and observe what happens. In a newsgroup this could mean that these are members that read all messages, but only rarely participate, or do not get answers to their postings.

2.3 Eigensystem Analysis in Social Network Analysis

The use of eigensystem analysis in SNA started in the late 1940s and early 1950s when social relationships were encoded in so called sociomatrices which were closely related to adjacency or incidence matrices already well known from graph theory at that time.

In 1953 Katz [Kat53] presented an index based on this idea, namely that the rank of a group member depends on the rank of the members he or she is connected to by choice. These choices were represented in a binary so called adjacency matrix. This index does not only take into account the direct path between two members, but also longer paths that connect two members via other members. Stated in mathematical terms this yields the eigenvalue equation (for an eigenvalue equal to 1). The components of the principal eigenvector are the status indices of each group member. The highest ranked member, the one with the largest status index, is the one who is either chosen by few but high ranking co-members, or by many relatively low ranked co-members. This approach though did not present a solution to the problem that choice need not be mutual. In 1965 Hubbell [Hub65] extended this approach based on the Leontief Input-Output model to also include weighted or unilateral choices. Thus the idea of using eigensystem analysis to define the relevance of group members by comparing their individual status with those of other members they are connected to is in itself not a new idea.

Since the early 1950s the interpretation of the results of such methods have been enhanced and its applications broadened. Richards and Seary [RS00], [SR03a] give a very good overview of the different approaches used in the eigensystem analysis of social networks. Goh et al. [GKK01] show how the largest eigenvalue depends on system size, and that the eigenfunction (eigenvector) points toward the node with the highest degree. They use eigensystem analysis to further investigate scale-free networks, but not as a tool by itself.

One finding in the course of research was that distances in networks (between members) are very difficult to describe, since it may be the case that member i knows members j and k, but the members j and k have absolutely no knowledge about each other, thus denying transitivity of the relation of knowing each other. Transitivity, however, is a key factor in the concept of distances. This leads to the assumption of non-Euclidean distances in networks. Barnett and Rice [BR85] showed that if the matrix is for example defined as a distance matrix, triads (triangles of members) formed between three network members need not be Euclidean. If such a matrix is converted by multi dimensional scaling (non-linear principal component analysis) into Cartesian coordinates, eigenvalues may become negative and complex eigenspaces can emerge. To avoid this, such asymmetric be-

havior is normally excluded by designing the matrix in such a way that distances are dichotomized. But this evidently means loss of information. Barnett and Rice show that these negative eigenvalues $\lambda \leq 0$ yield information, for example about the homogeneity of the structure of the group. For this purpose they define the *warp* as the ratio of the real variance (all positive eigenvalues) and the total variance (all eigenvalues). If this warp equals 1, then the space is Euclidean. The larger it gets, the more non-Euclidean the space becomes, which means, that more and more interaction is done through less and less nodes. Thus they found a way to interpret the negative eigenvalues that had been a problem in the field.

Multi dimensional scaling is also the starting point of Chino [Chi98], He was the first to introduce the use of Hilbert space theory in the analysis of preference data in psychology. He found that with the help of Hilbert space theory asymmetric relationships between subjects could be better described. The interpretation of negative eigenvalues has also been discussed in his work. He proposes that the sign gives a hint on symmetric and asymmetric relations between subjects.

Eigensystem analysis has thus been pushed considerably towards the explanation of negative eigenvalues. On the other hand there were problems, already discussed by Katz, about the general question of what status is supposed to mean, and where it comes from.

Bonacich and Lloyd [BL01] present an introduction of the use of eigenvector-like measurements of centrality for unpreprocessed asymmetric data that broadens the eigensystem interpretation in that direction. For asymmetric relations they show that for some networks the standard eigenvector measures for network centrality do not lead to meaningful results. As a solution they suggest the notion of α-centrality which combines an individual's own inherent status with a weight α for the relative importance of the perceived status and a vector e of exogenous sources of status. In their conclusion they find that this α-centrality could be seen as a generalization of the standard eigenvector centrality measure.

This approach, to use an external or node inherent status effect, was also taken up by physicists who use Ising models to explain the behavior of networks. On the basis of the Ising model which describe the interaction between spins often used in condensed matter physics, some researchers (for example Herrero [Her02]) have also achieved some good insights into interactions within a social network using this model. These methods focus on transition of a network from one state into another and they try to determine the exact system characteristics (e.g. temperature) that lead to a phase transition of the system.

There have been other approaches to the interpretation of asymmetric communication behavior with the use of such indices. Freeman [Fre97] used it to show hierarchies within a group. He, like Chino [Chi98] and Barnett and Rice [BR85], generates the matrices that are then the basis for the eigenvalue analysis by splitting a given asymmetric real sociomatrix into its symmetric and skew-symmetric

part. While Barnett and Rice and Freeman remain in the real space, Chino uses this approach to shift into Hilbert space.

One last aspect is that of structural stability when looking at the communication pattern structure. This problem is at the center of perturbation theory. There is no literature about this topic in SNA. Still it is of interest to find out how much perturbation a network can "digest" without changing its structure. In the course of this book therefore general literature about perturbation of Hermitian eigensystems will be introduced. There are two aspects to keep in mind:

- Perturbation of the eigenvalues. This is closely related to traffic volume and relevance of pattern.
- Perturbation of the eigenspaces. This is closely related to a change in relevance of the members within the structure.

A general and extensive introduction into perturbation theory of linear operators is given in Kato [Kat95] (originally published in 1966). Kato gives an introduction into Banach and Hilbert space, and on this basis goes on to describe perturbation theory. As an application of special interest he gives examples from quantum mechanics. Here the results of perturbation theory in Hilbert space have an application for example when looking at Dirac operators or the Schrödinger equation.

A modern, more mathematical approach to perturbation bounds of eigensystems of Hermitian matrices can be found for example in Dopico et al. [DMM00], Mathias [Mat97], Barlow and Slapnicar [BS00], Fonseca [dF00] and Ipsen [Ips03] .

In a graph-theoretical setting Cvetkovic et al. [CS97] give an introduction into the effects of perturbation on the eigenvectors and eigenvalues of graphs represented by real valued adjacency matrices. Appendix B [CS97, p.235-238] provides a table of eigenvalue and eigenvector configurations for different kinds of graphs up to 5 vertices.

As a last set of methods we present those used to describe topology and evolution of large networks. For a good overview of these methods see Barabasi and Albert [BA02] and Barabasi and Bianconi [BB01]. Here different methods are being described ranging from random graphs to percolation theory and Bose-Einstein condensation. These methods have been taken from different fields in physics such as condensed matter physics, solid state physics and statistical mechanics. The idea is that in all of these fields there exist extensive methods to describe the evolution and behavior of either lattices or particle aggregates. It is only a short step from these concepts to the idea that human networks might follow similar laws as those described in physics.

A field of physics that also has much to offer when looking at the behavior of networks is nonlinear dynamics. Smale and Hirsch [HS74] or Strogatz [Str01] give an introduction to the field. These methods play an important role for example in the application to viral marketing, where the nonlinear behavior on nearly scale-free networks is a necessary condition for success.

2.4 Other Applications of Eigenvector Centrality

One of those many applications not within SNA, which will not be further discussed in the course of this work, has been presented by Kleinberg [Kle99], [GKR98] who showed how web sites on the internet are linked to form groups in view of their common context. In a hypertext context the fact that one web site features a link to another web site can be defined as a choice, and thus the link defines an entry in the adjacency matrix. In this context the matrix explains a directed graph, at that point without weights attached to the edges. Kleinberg uses the concept of hub and authority, which he derives from incrementally computing and approximating the principal eigenvalue and the left and right hand eigenvector belonging to the principal eigenvalue. The interpretation is limited due to the fact that it identifies only the major hub and the major authority, but does not reveal much about the substructure. Page et al. [PBMW98] used this approach to create the PageRank algorithm which is now the basis of the Google search engine. A good review of these methods and results can be found in Park and Thalwall [PT03]. A collection of algorithms that are being used in that field is given in Borodin et al. [BRRT01].

Another Internet related research was done by Yaltaghian and Behnak [YC02], who use different methods to analyze the results of the Google search engine.

Applications in organization research have already been pointed out in 1945 by Simon (see [Sim00]). He suggests that the use of email in organizations will change the way information is being distributed, and that it may well cause a different way of information diffusion than before. An example that this is the case is given in a paper by Krackhardt [KH93], who uses methods of SNA to uncover hidden structures within an organization compared to those given by the formal organization. In management sience the evolution of organizations is of some importance. This behavior can also be analyzed using methods described above as for example in Guimera et al. [GDDG$^+$02]. A good overview of the application of social network analysis in organizational research can be found in Borgatti and Foster [BF03].

In a more communication method based article Smith [Smi02] applies some of the above mentioned methods to instant messaging systems just as Ebel [EMB02] applied them to email networks. The largest email network is most probably the

USENET. A thorough analysis of this large network can be found in Choi and Danowski [CD02].

The idea to to use the communication flow between different points (or vertices) to detect patterns and act according to these results played a major role in naval warfare during the second World War when signal intelligence was used to find from the patterns of communication the whereabouts of targets. The idea to analyze communication structures with mathematical methods dates back to the 1950s and has since grown in relevance and capability. Yet the simultaneous analysis of inbound and outound communication between two members/nodes has posed difficulties, as well as the fact that the eigensystem analysis used up to now does not provide a complete interpretation of the eigenspace that could yield a detailed view on the pattern structure.

Chapter 3

Theoretical Foundations for Pattern Analysis in Social Networks

In this chapter the theoretical and methodological background for the analysis of communication patterns in social networks will be presented. In section 3.1 notations and definitions necessary for SNA will be given. Section 3.2.1 will explain the concepts of rank and status and how they can be measured in a given network. The last section 3.3 will present the mathematical and graph-theoretical concepts that will be needed. The main focus of this last section is to make the reader familiar with complex Hilbert space and the behavior of linear operators in that space.

3.1 Social Networks

3.1.1 Definitions

A *social network* will be defined as in Wasserman and Faust [WF94, p.20] as a *finite set or sets of actors and the relation or relations defined on them*. (Social Network.)

The relation in the cases discussed here will be the sending of and answering to emails. The next smaller unit is the group.

Wellman [Wel01] defines a *group* as a *special type of social network; one that is heavily interconnected and clearly bounded.*(Group.)

A *subgroup* is a substructure of a group, that is defined by the relation towards its *anchor* (see below).(Subgroup.)

A *virtual community* (VC) following Rheingold [Rhe00, p.xvii] is a group of people who *use words on screens to exchange pleasantries and argue, engage in intellectual intercourse* .... (Virtual Community.)

A more formalized definition of an online community can be found in Preece [Pre00, p.10]. Such a community consists of

- people who have any kind of social interaction,
- have a common goal, as for example information exchange,
- perform their exchanges within certain rules or social norms,
- and use computers to communicate.

Thus a VC is a special kind of a social network.

In the context of this work an *anchor* is defined as the most prominent member of a subgroup.(Anchor.)

This prominence is expressed by the fact that the complex rank prestige index has the highest absolute value in the eigenvector under inspection. The term anchor can be used arbitrarily either for the most prominent member of the whole group, or the most prominent member of a subgroup. The network‘s anchor is the member with the highest absolute eigenvector component value belonging to the highest absolute value eigenvalue.

Networks, and thus communication networks, will be represented as weighted directed graphs $G = \{V, E, A\}$ where the n members of the network are the vertices $v \in V$. Connections between members will be mapped as weighted edges $e \in E$. The graph G will be described by a weighted $n \times n$ adjacency matrix A. An entry of this matrix $a_{kl} \neq 0$ if there is a connection between two vertices v_k and v_l, which is equivalent to $e(k, l) \in E$. In the unweighted and undirected case the adjacency matrix has entries $a_{kl} = 1$ if $e(k, l) \in E$ and 0 otherwise.

3.2 Rank and Status

This section will introduce rank and status as terms and concepts that are relevant to this book. After a discussion of several definitions of these terms different measurements for these concepts will be given.

In Tab.(3.1) definitions of the concepts by different authors are given. The german texts have been translated for better understanding. No standard definition can be given for either of the concepts. In addition Tab.(3.2) shows how some of the concepts are the foundations for other concepts (represented by “$\rightarrow$”) or are derived on the basis of another concept (‘”$\leftarrow$”), or are used in a similar way or even synonymical (“$\sim$”). Only the upper triangular of this matrix is filled for clearer visibility.

Concept	**Schäfers** [Sch95]	**Burghardt** [Bur79]	**Giddens** [Gid95]	**Wasserman and Faust** [WF94]
Social position		[Bur79, p.91] a rateable function that a person has in a given social structure		[WF94, p.348] position refers to a collection of individuals who are similarly embedded in networks of relations
Role	[Sch95, p.290] expectations about behavior a group appoints to the bearer of a social position within that group	[Bur79, p.92] expectations of the environment or even the society as a whole about how a person is supposed to behave when holding a certain position		[WF94, p.348] role refers to the patterns of relations which obtain between actors or between positions.
Status	[Sch95, p.380] the more or less high standing that a person has in comparison to all other members of a society	[Bur79, p.97] social status is the visible or recognizable result of an evaluation of the attribute of a position	[Gid95, p.237] differences in perception by others that a social group has in comparison to other groups	
Rank		[Bur79, p.91] relative importance of a position on a vertical importance scale		
Prestige		[Bur79, p.103] subjective: the speculation of a person that a certain behavior yields social acceptance and a gain of estimation		[WF94, p.174] a prestigeous actor (is) one who is the object of extensivet ties, thus focusind solely on the actor as recipient

Table 3.1: Definitions of role, status, rank, prestige

	social position	Role	Status	Rank	Prestige
social position	-	$\rightarrow$			
Role		-	$\rightarrow$	$\sim$	
Status			-	$\sim$	$\sim$
Rank				-	$\rightarrow$
Prestige					-

Table 3.2: Order and Synonymity of role, status, rank, prestige

Rank and status are related in the sense that since the word status is mostly used in conjunction with a rating like “high” or “low”, or that the context yields this information these two are used synonymical. Sometimes even the word “prestige” is used as a synonym. But all these three are based on the role a member holds in a given community.

In the context of this book these abstract concepts will be used to describe results of mathematical evaluation with respect to the communication behavior of a member of the group. The following view is adopted: a member can have different roles, for example anchor or lurker (see later for a detailed explanation). The role has an inherent rank or status and at the same time an inherent prestige. Both depend on the mathematical computation defined on the communication traffic generated by each member.

3.2.1 Degree based Rank

In this subsection the rank based on in- or out-degree will be described. Thus an intuitive introduction to the concept of rank is given even though the proposed method is not restricted to degree centrality. Degree in this context when directed weighted graphs are observed is the number of edges e that either depart from a vertex v (out-degree: $d_k^o \in \mathbb{R}$) or are pointed towards the vertex (in-degree: $d_k^i \in \mathbb{R}$). In the case of weighted graphs we also define the strength following Barrat et al. [BBV04] as s_k^o and s_k^i as the number of messages that either go out from vertex k or come into vertex k over all connected vertices.

Centrality

There are several definitions for centrality $c_k \in \mathbb{R}$. Centrality here is defined following Wasserman and Faust [WF94] by the fact that in a non-directional setting a member is said to be central, if he is connected to many other members. In a directional setting centrality is defined by the choices the member makes. This is reflected in the number of different other members he communicates with.

Degree centrality as defined in Wasserman and Faust [WF94, p.199] focuses on the choices that are being made by the members of a network, thus the centrality in that case is based on the out-degree. A central member is thus a member that has many outgoing connections to different members within the network. d_k^o of vertex k is defined as the number of vertices that k is connected to as given in Eq.(3.1)

$$d_k^o = \sum_{l=1}^{n} q_{kl} \tag{3.1}$$

with $q_{kl} = 1$ if $a_{kl} \neq 0$ and $q_{kl} = 0$ if $a_{kl} = 0$. Thus the standardized centrality in a directed unweighted graph can be defined as in Eq.(3.2):

$$c_k = \frac{d_k^o}{(n-1)} \quad \text{with} \quad c_k \in \mathbb{R} \tag{3.2}$$

In the weighted case it is not possible to standardize anymore, since the number of possible connections is no longer known. In that case just the row sum is taken. This then has the problem of comparability between networks. (Degree centrality.)

Strength is the concept in the weighted case. The standardized form is given in Eq.(3.3). It is given as the row sum of the weighted adjacency matrix divided by the total sum of matrix entries, with $a_{kl} \in \mathbb{R}$ and n the number of vertices or members in the network.

$$s_k^o = \frac{\sum_{l=1}^{n} a_{kl}}{\sum_{k=1}^{n}\sum_{l=1}^{n} a_{kl}} \quad \text{with} \quad s_k^o \in \mathbb{R} \tag{3.3}$$

There are several derived concepts of centrality which will be presented without further explanation. We will present here only those that are relevant in the context of directional relationships. It should also be noted that all of these centrality measures can be generalized to group centrality measures. This can be achieved for example by defining hypernodes that contain the vertices that belong to that group.

Standardized closeness centrality is defined following again [WF94, p.200] for a directional and unweighted graph as in Eq.(3.4):

$$cl_k = \frac{n-1}{\sum_{l=1}^{n} dist(k,l)} \quad \text{with} \quad cl_k \in \mathbb{R} \tag{3.4}$$

with $dist(k,l)$ denoting the shortest distance between node k and l. Closeness centrality gives an indication of how close a member is to the other members of the group. This can intuitively be derived from the distances between vertex k and all other members. It should be mentioned though that if the actor is an isolate,

meaning, that he has no connections at all, the sum of distances becomes 0 and thus the index is undefined. (Closeness centrality.)

Betweenness centrality $bc_k \in \mathbb{R}$ puts the focus on the fact that a vertex v with a high betweenness centrality is like a bottleneck. All (or much) of the communication within a given network has to go through this vertex. Betweenness centrality as defined by Eq.(3.5) is thus based on the number of paths that go through a certain vertex when connecting two vertices in relation to all paths within a network that connect these two vertices.

$$bc_k = \frac{\sum_{l=1,k<l}^{n} g_{kl}^i / g_{kl}}{(n-1)(n-2)} \quad \text{with} \quad bc_k \in \mathbb{R} \tag{3.5}$$

with g_{kl} the number of paths between vertex k and l and g_{kl}^i the number of paths between vertex k and l that contain vertex i. This view requires the assumption that the choice of communication channel/path is equally distributed. That might not be the case, if preferential behavior is taken into account. Betweenness centrality has been used to detect clusters within networks [GN02], [NG03]. (Betweenness centrality.)

Information centrality is a stronger version of betweenness centrality, in that it now takes into account that paths between two vertices might not be taken for the transport of information on an equally distributed basis. Latora [LM04] extended this index to incorporate some notions from flows in non-directional and weighted or unweighted graphs, specifically the notion that information might take the shortest possible path available between two vertices. Thus the efficiency $\epsilon_{kl} \in \mathbb{R}$ of two vertices regarding information transfer is presumed to be proportional to $\frac{1}{min_l dist(k,l)}$. The efficiency of the network is then the average $\xi = \frac{\sum_{k \neq j \in G} \epsilon_{kl}}{n(n-1)}$. If now a graph G_k' is constructed where all edges incident to vertex k have been removed, then the information centrality ic_k is defined as in Eq.(3.6)

$$ic_k = \frac{\xi - \xi_k}{\xi} \in \mathbb{R} \tag{3.6}$$

Information centrality is thus *the relative drop in the network efficiency caused by the removal of* edges incident to the observed vertex.(Information centrality.)

α-centrality as defined by Bonacich [BL01] given in Eq.(3.7) adds an exante status, given as a vector $\mathbf{e}$ to the centrality measure and weighs the relative importance of the grouped-derived rank in comparison to the member inherent status by a coefficient α .

$$\mathbf{x} = \alpha A^t \mathbf{x} + \mathbf{e} \tag{3.7}$$

with A the unweighted, directed adjacency matrix.(α-centrality.)

In a graph-theoretical setting, on the other hand, a *center* can be defined as in Jungnickel [Jun99, p.91]. A vertex v is *central* if it has minimal excentricity. Excentricity ex being defined as $ex_k = max_l \quad dist(k,l)$. Thus a vertex k is seen as at the center of a graph if Eq.(3.8) is calculated,

$$gc_k = min_k ex_k \quad \text{with} \quad gc_k \in \mathbb{R} \tag{3.8}$$

which expresses the fact that this vertex has the minimal longest distance $dist(k,l)$ of all vertices in the network. This measure is defined for both non-directional and directional settings. It is a generalization of degree centrality, in that all distances are used, not only those to the nearest neighbors.(Graph centrality.)

Prestige

Following [WF94, p.202] prestige in comparison to centrality represents the degree to which a vertex is chosen by other vertices within a directed and possibly weighted network. It is calculated as in Eq.(3.9). Thus a vertex has a high prestige, if it has a high in-degree, defined analogous to the out-degree for centrality with $d_k^i = \sum_{l=1}^{n} q_{lk}$ the column sum as the in-degree of vertex k:

$$p_k = \frac{d_k^i}{(n-1)} \quad \text{with} \quad p_k \in \mathbb{R} \tag{3.9}$$

The strength in this case is defined analogous to the the outbound strength. It is the column sum of matrix A, as in Eq.(3.10).

$$s_k^i = \frac{\sum_{k=1}^{n} a_{kl}}{\sum_{k=1}^{n}\sum_{l=1}^{n} a_{kl}} \tag{3.10}$$

Proximity prestige is the in-bound analogon to closeness centrality. It is defined as in Wasserman and Faust [WF94, p.204] by Eq.(3.11):

$$pp_k = \frac{I_k/(n-1)}{\sum dist(l,k)/I_k} \quad \text{with} \quad pp_k \in \mathbb{R} \tag{3.11}$$

with I_k representing the number of members who are in the influence range of vertex k, which means members who can reach vertex k. Thus proximity prestige as defined over directed unweighted graphs. (Proximity prestige.)

3.2.2 Rank Prestige or Status index and eigenvector centrality

As was shown in section 3.2.1 neither centrality nor prestige by itself give a complete picture of the relevance of a vertex within a network. By finding an index that combines both views, this can be achieved. *Status* in the sense that will

be used in this work will have the meaning that a vertex is central and prestigious at the same time. Since [WF94] use status and rank prestige as synonyms, this will also be the case for the rest of this work. Status or rank thus in this work will be defined by the traffic in email volume that is exchanged and by the pattern that becomes visible in the eigensystem.

The status index as defined by Katz uses for the calculation not only the direct paths between two neighbors, but also all paths connecting two vertices since the k-th power of the adjacency matrix A has as its entries the numbers of paths of length k between two vertices. This leads to the interpretation that the rank of one member depends on the rank of those he is connected to.

In general this is referred to as eigenvector centrality, since this is calculated as follows:

The idea of the rank prestige index is based on the idea that not only the direct neighborhood of a vertex influences the rank of a vertex, but also the rank of the vertices that are connected to vertex l by way of other vertices. This holds also in a directed graph. This can be represented by the sum of an adjacency matrix A powered to $p = 1 \ldots \infty$. That the power of an adjacency matrix gives the number of k-length paths between two vertices is known from graph theory [Jun99, p.96]. Now the question is, how to find the rank index given for each member of a network based on the sum of the powered matrices. This can be solved with the help of two mathematical properties. For one every function of a diagonalizable matrix leads to a function of its eigenvalues and second the fact is used, that a power series converges under certain conditions. These two results will be introduced in section 3.3.4.

The components of the corresponding eigenvectors are the indices that represent the rank of the member.

Status as proposed by Katz [Kat53] is *defined by the question asked*. In the course of this work status is thus high if one member is identified as an *anchor*. The member with the highest overall status will be identified as the *anchor* corresponding to the highest absolute eigenvalue of the system.

3.2.3 Communication Patterns

In addition to eigenvector centrality the projectors derived form the eigenvectors yield an interpretation. As will be explained in more detail in section 3.3.5 the orthogonal projector in Eq.(3.58) gives a representation of structural similarity for members within a subspace and the pattern structure of the original space. See [BL04] for a discussion of the case for $G\{V, E, A\}$ with $A \in \mathbb{R}$.

3.3 Linear Operators in Hilbert Space

In this section the mathematical background is presented. As the method proposed in this book is based on the complex valued representation of communication, complex numbers will first be introduced in section 3.3.1. As a second step the construct of Hilbert space will be presented in section 3.3.2. Section 3.3.3 will introduce Hermitian operators in Hilbert space, followed by eigensystem analysis of such operator in section 3.3.4 . In section 3.3.5 orthogonal projectors are defined, which are computed from the eigenvectors, and the interpretation of these projectors in the context of communication pattern analysis is given. Since Hermitian operators behave very predictable under perturbation, which is of interest when analyzing communication patterns, section 3.3.6 will introduce those characteristics of Hermitian operators. Finally section 3.4 will present the application of the proposed method to two types of graphs, namely the star graph and the complete graph. Results in the bidirectional symmetric case will be compared to the undirected case, and results from Cvetcovic, Rowlinson and Simic [CS97] will be used for validation. Also eigensystems of asymmetric bidirectional graphs and perturbed graphs are given and discussed.

3.3.1 Complex Numbers and Hermitian Matrices

Unless otherwise stated all numbers are complex ($\in \mathbb{C}$). Column vectors will be written in bold face $\mathbf{x}$, with components $x_j, j = 1 \ldots n$. The vector space will be denoted by $\mathbf{V} = \mathbb{C}^n$. Capital letters will represent matrices A with a_{kl} denoting the entry in the k-th row and the l-th column ($k, l = 1 \ldots n$). Greek letters will stand for the eigenvalues with λ_k representing the k-th eigenvalue. $\mathbf{x}_k$ will denote the eigenvector corresponding to the k-th eigenvalue. The complex conjugate transpose of a vector $\mathbf{x}$ will be given as $\mathbf{x}^*$. The transpose of a vector $\mathbf{x}$ will be denoted as $\mathbf{x}^t$.

The equation $x^2 + 1 = 0$ has no solution in $\mathbb{R}$. By introducing the imaginary unit i with $i^2 = -1$ this equation is solvable. The set of the real numbers $\mathbb{R}$ augmented by the imaginary unit i and the operations $+$ and $*$ defined such that $(a+ib)+(c+id) = (a+c)+i(b+d)$ and $(a+ib)*(c+id) = (ac-bd)+i(ad+bc)$ with $a, b, c, d \in \mathbb{R}$ is defined as the field of the complex numbers $\mathbb{C}$.

As an intuitive alternative introduction to complex numbers consider a vector $\mathbf{p}$ in a 2-dimensional plane in $\mathbb{R}$ as in Fig.(3.1).

When we now rename the x-axis to “real” and the y-axis to “imaginary”, the transition to the Gauss-plane has been achieved as can be seen in Fig.(3.2).

It can thus easily be seen that the complex number z can be represented like a vector in algebraic form or equivalently in polar form:

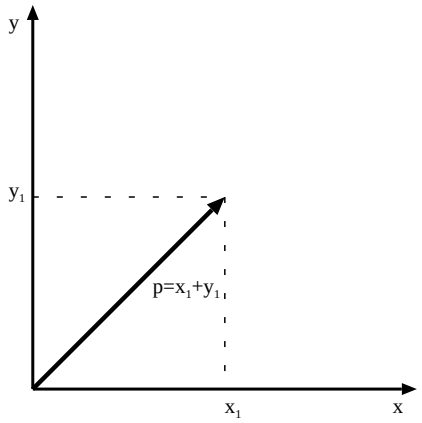

Figure 3.1: Two component vector in $\mathbb{R}^2$

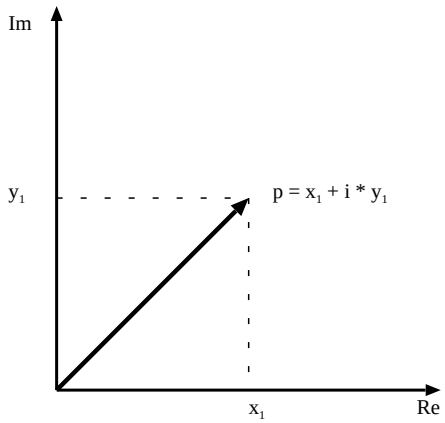

Figure 3.2: Two component vector in the Gauss plane

$$z = a + ib = |z|e^{i\phi} \tag{3.12}$$

with the real part of z being denoted as $Re(z) = a$, the imaginary part as $Im(z) = b$, with i the imaginary unit ($i^2 = -1$). $\overline{z}$ denotes the complex conjugate $\overline{z} = a - ib$ of z. The absolute value and phase are defined by Eqs.(3.13) and (3.14).

$$|z| = \sqrt{a^2 + b^2} \tag{3.13}$$

$$\phi = \arccos \frac{Re(z)}{|z|} \quad 0 \leq \phi \leq \pi \tag{3.14}$$

The following five equations are helpful when dealing with complex numbers:

$$z_1 z_2 = |z_1||z_2| e^{i(\phi_1+\phi_2)} \tag{3.15}$$

$$z = \overline{z} \qquad \text{if and only if} \quad z \in \mathbb{R} \tag{3.16}$$

$$\overline{z} z = |z|^2 \tag{3.17}$$

$$z + \overline{z} = 2Re(z) \tag{3.18}$$

$$\begin{aligned} z_1 \overline{z_2} = (&Re(z_1)Re(z_2) + Im(z_1)Im(z_2)) \\ &+ i(Re(z_2)Im(z_1) - Re(z_1)Im(z_2)) \end{aligned} \tag{3.19}$$

Eq.(3.15) shows that the multiplication of two complex numbers is achieved by multiplying the absolute values and adding the phases of the two complex numbers. Multiplication by a complex number is thus equivalent to a rotation about ϕ_2 and scaling by $|z_2|$ as can be seen in Fig.(3.3).

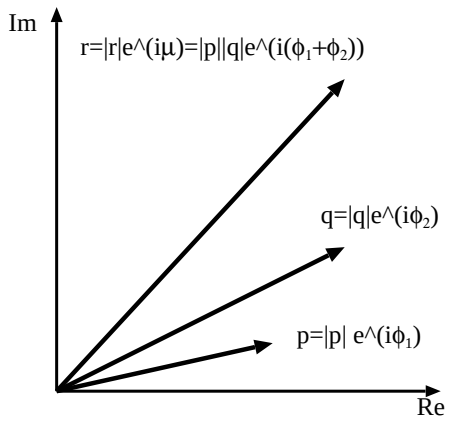

Figure 3.3: Multiplication of two complex numbers q and p

Eq.(3.16) states that a complex number and its complex conjugate (or adjoint) number are equal if and only if z is real. Eq.(3.17) expresses that the multiplication of a complex number with its complex conjugate gives the the square of the absolute value of that number, which can also be expressed as $Re(z)^2 + Im(z)^2$. This again is a real non-negative number. Eq.(3.18) states the fact, that the sum of a complex number and its complex conjugate is two times the real part of the complex number. Eq.(3.19) gives a representation of the product of a complex number and a complex conjugate number. This will be relevant when interpreting the orthogonal projectors.

In analogy to complex numbers we now introduce Hermitian matrices, since scalars can be viewed as 1×1 matrices.

A matrix H is called Hermitian, if and only if

$$H^* = H \tag{3.20}$$

with H^* representing the complex conjugate transpose of H. The complex conjugate transpose of a matrix H is found, when the original matrix H is either first transposed and then each entry is complex conjugated, or vice versa. Eq.(3.20) means that the matrix entries can be written as $h_{lk} = \overline{h_{kl}}$. The analogon in $\mathbb{R}$ is the symmetric matrix. Hermitian matrices are also normal (Eq. 3.21) as follows from Eq.(3.20):

$$HH^* = H^*H \tag{3.21}$$

A matrix H is unitarily similar ($X^*HX = D$, with X unitary and D diagonal) to a diagonal matrix if it is normal. This means that for normal matrices the eigenvectors form an orthogonal system.

Any matrix $M \in \mathbb{C}^n$ can be written as in Eq.(3.22). With the first part giving a hermitian part and the second a skew-hermitian ($M^* = -M$).

$$M = \frac{1}{2}(M + M^*) + \frac{1}{2}(M - M^*) \tag{3.22}$$

The characteristics of Hermitian matrices which are of special interest in this work are those of their eigensystem. These characteristics will be discussed in section 3.3.4.

3.3.2 Hilbert Space as a special Vector Space

Hilbert space is a

- complete
- normed
- inner product

vector space. In the following these characteristics will be introduced.

For any given vector space $\mathbf{V}$ on any field the following equations have to hold:

$$\mathbf{x}+\mathbf{y}\in V \qquad \forall \mathbf{x},\mathbf{y}\in \mathbf{V}\text{(closure)} \tag{3.23}$$

$$(\mathbf{x}+\mathbf{y})+\mathbf{z}=\mathbf{x}+(\mathbf{y}+\mathbf{z}) \qquad \forall \mathbf{x},\mathbf{y},\mathbf{z}\in \mathbf{V}\text{(associativity)} \tag{3.24}$$

$$\mathbf{x}+\mathbf{y}=\mathbf{y}+\mathbf{x} \qquad \forall \mathbf{x},\mathbf{y}\in \mathbf{V}\text{(commutativity)} \tag{3.25}$$

$$\exists \mathbf{0}\rightarrow \mathbf{x}+\mathbf{0}=\mathbf{x} \qquad \forall \mathbf{x}\in \mathbf{V}\text{(neutral element)} \tag{3.26}$$

$$\exists 1\rightarrow 1\mathbf{x}=\mathbf{x} \qquad \forall \mathbf{x}\in \mathbf{V}\text{(neutral element)} \tag{3.27}$$

$$\exists(-\mathbf{x})\rightarrow \mathbf{x}+(-\mathbf{x})=\mathbf{0} \qquad \forall \mathbf{x}\in \mathbf{V} \quad \text{(additive inverse)} \tag{3.28}$$

$$a\mathbf{x}\in V \qquad \forall a\in\mathbb{C},\mathbf{x}\in\mathbf{V} \tag{3.29}$$

$$(ab)\mathbf{x}=a(b\mathbf{x}) \qquad \forall a,b\in\mathbb{C}, \quad \forall \mathbf{x}\in \mathbf{V}\text{(associativity)} \tag{3.30}$$

$$a(\mathbf{x}+\mathbf{y})=a\mathbf{x}+a\mathbf{y} \qquad \forall a\in\mathbb{C},\forall \mathbf{x},\mathbf{y}\in \mathbf{V}\text{(distributivity)} \tag{3.31}$$

$$(a+b)\mathbf{x}=a\mathbf{x}+b\mathbf{x} \qquad \forall a,b\in\mathbb{C};\forall \mathbf{x},\mathbf{y}\in \mathbf{V}\text{(distributivity)} \tag{3.32}$$

A norm p on a given vector space $\mathbf{V}\subset\mathbb{C}^n$ is given by

$$\parallel \mathbf{x} \parallel_p = (\sum_{k=1}^{n} \mid x_k \mid^p)^{1/p} \tag{3.33}$$

The norms most often used are the 1-norm ($\parallel \mathbf{x} \parallel_1 = \sum_{k=1}^{n} \mid x_k \mid$), the 2-norm ($\parallel \mathbf{x} \parallel_2 = (\sum_{k=1}^{n} \mid x_k \mid^2)^{1/2}$) and the ∞-norm ($\parallel \mathbf{x} \parallel_\infty = max_k \mid x_k \mid$).

In Hilbert space the norm is analog to the 2-norm, but is based on the inner product, as defined in Eq.(3.34). The inner product of $\mathbf{x}$ and $\mathbf{y}$ is a semilinear (conjugate-linear in the first part and linear in the second) form on a given vector space $\mathbf{V}$ and is represented as

$$\langle \mathbf{x} \mid \mathbf{y} \rangle = \mathbf{x}^*\mathbf{y} = \sum_{k=1}^{n} \overline{x_k} y_k \tag{3.34}$$

The inner product norm is consequently defined by Eq.(3.35):

$$\sqrt{\langle \mathbf{x} \mid \mathbf{x} \rangle} = \parallel \mathbf{x} \parallel \tag{3.35}$$

This is the analogon to the Euclidean or 2-norm $\| \mathbf{x} \|_2 = \sqrt{\sum_{k=1}^{n} | x_k |^2}$ which by Eq.(3.17) is the same as $\sqrt{\sum_{k=1}^{n} \overline{x_k} x_k}$, which following Eq.(3.34) is the same as Eq.(3.35).
For a given arbitrary norm the following rules must hold:

$$\| \mathbf{x} \| \geq 0 \tag{3.36}$$
$$\| \mathbf{x} \| = 0 \Leftrightarrow \mathbf{x} = \mathbf{0} \tag{3.37}$$
$$\| a\mathbf{x} \| = | a | \| \mathbf{x} \|, \quad \forall a \in \mathbb{C} \tag{3.38}$$
$$\| \mathbf{x} + \mathbf{y} \| \leq \| \mathbf{x} \| + \| \mathbf{y} \| \tag{3.39}$$

A vector space $\mathbf{V}$ is said to be complete, if every sequence $\{x_n\}$ converges. In a complete normed space the Cauchy condition
$\lim_{min(n,m)\to\infty} \| \mathbf{x_n} - \mathbf{x_m} \| \to 0$
is satisfied.

The matrix norm $\| A \|$ is an induced norm for a given vector norm. Thus the matrix norm induced by the inner-product-norm is stated in Eq.(3.40). It explains to what extent a vector is stretched by A or shrunk by A^{-1} if A is nonsingular.

$$\| A \| = max_{\|\mathbf{x}\|=1} \| A\mathbf{x} \| \tag{3.40}$$

There are two matrix norms, which are of interest in this context:

- The Frobenius norm as defined in Eq.(3.41)

$$\| A \|_F^2 = \sum_{k,l} | a_{kl} |^2 = trace(A^* A) \tag{3.41}$$

- The 2-norm as defined in Eq.(3.42) following Eq.(3.40) and Eq.(3.52). This norm will be the one used as the standard matrix norm, if not otherwise stated.

$$\| A \| = | \lambda_{max} | \tag{3.42}$$

If A is nonsingular then $\| A^{-1} \| = \frac{1}{|\lambda_{min}|}$.

Eq.(3.42) defines at the same time the spectral radius, which will be introduced in more detail in section 3.3.4.

In Hilbert space thus the following equations hold:

$$\langle \mathbf{x} \mid \mathbf{x} \rangle \geq 0 \quad \text{with} \quad \langle \mathbf{x} \mid \mathbf{x} \rangle = 0 \quad \text{if and only if} \quad \mathbf{x} = 0 \tag{3.43}$$

$$\langle a\mathbf{x} \mid \mathbf{y} \rangle = \overline{a}\langle \mathbf{x} \mid \mathbf{y} \rangle; \quad \langle \mathbf{x} \mid a\mathbf{y} \rangle = a\langle \mathbf{x} \mid \mathbf{y} \rangle \qquad a \in \mathbb{C} \tag{3.44}$$

$$\langle \mathbf{x} + \mathbf{y} \mid \mathbf{z} \rangle = \langle \mathbf{x} \mid \mathbf{z} \rangle + \langle \mathbf{y} \mid \mathbf{z} \rangle \tag{3.45}$$

$$\langle \mathbf{x} \mid \mathbf{y} \rangle = \overline{\langle \mathbf{y} \mid \mathbf{x} \rangle} \tag{3.46}$$

3.3.3 Hermitian Operators in Hilbert Space

A linear operator on a given field is defined as a function that sends every vector $\mathbf{x} \in \mathbf{X}$ into another vector $\mathbf{y} \in \mathbf{X}$ by a linear transformation. Thus the transformation in

$$\begin{aligned} \mathbf{x}_1 &= \sum_{i=1}^{n} c_{1i}\mathbf{y}_i \\ &\dots \\ \mathbf{x}_n &= \sum_{i=1}^{n} c_{ni}\mathbf{y}_i \end{aligned} \tag{3.47}$$

with $c_{kl} \in C$ can also be written as $\mathbf{x} = C\mathbf{y}$ with c_{kl} the entries of the matrix C. C is then called a linear operator.

The adjoint space $\mathbf{V}^*$ of a vector space $\mathbf{V}$ is the set of all semilinear forms (e.g. inner product Eq.(3.44)) on a vector space $\mathbf{V}$ [Kat95, p.11] (Please note that Kato uses row vectors and thus the inner product is defined as linear in the first part and semi-linear in the second). A selfadjoint linear operator is called Hermitian. In Hilbert space the adjoint space $\mathbf{V}^*$ can be identified with the vector space $\mathbf{V}$ itself. For a proof see [Kat95, p.252-253]. Linear operators as defined in Eq.(3.20) will be of interest for the rest of this book.

The following (in)equalities hold in a normed inner product space:

- Cauchy-Schwarz inequality:

$$|\langle \mathbf{h} \mid \mathbf{x} \rangle| \leq \sqrt{\langle \mathbf{h} \mid \mathbf{h} \rangle}\sqrt{\langle \mathbf{x} \mid \mathbf{x} \rangle} \tag{3.48}$$

  with equality if $\mathbf{x} = a\mathbf{h}, a \in \mathbb{C}$.

- Bessel inequality: for any vector $\mathbf{h}$ and an orthonormal basis $\mathbf{x_j}$ with $j = 1, \dots, n$ of a vector space $\mathbf{X}$

$$\sum_{j=1}^{n} |\langle \mathbf{h} \mid \mathbf{x_j} \rangle|^2 \leq \| \mathbf{h} \|^2 \tag{3.49}$$

If the $\mathbf{x_j}$ form a complete orthonormal system the Bessel inequality becomes Parseval's equality:

$$\sum_{j=1}^{n} |\langle \mathbf{h} \mid \mathbf{x_j} \rangle|^2 = \| \mathbf{h} \|^2 \tag{3.50}$$

- Triangle inequality Eq.(3.39)

$$\| \mathbf{h} + \mathbf{x} \| = \sqrt{\langle \mathbf{h} + \mathbf{x} \mid \mathbf{h} + \mathbf{x} \rangle} \leq \| \mathbf{h} \| + \| \mathbf{x} \| = \sqrt{\langle \mathbf{h} \mid \mathbf{h} \rangle} + \sqrt{\langle \mathbf{x} \mid \mathbf{x} \rangle} \tag{3.51}$$

with equality if $\mathbf{x} = a\mathbf{h}$ as in Eq.(3.48) and in addition $a \in \mathbb{R}$.

In Hilbert space Eq.(3.48) becomes an equality and Eq.(3.50) holds due to the fact the condition for equality hold.

Thus Hilbert space is a very convenient vector space for Hermitian operators, since for the purposes of this book, many features help to lead to a quite natural interpretation in the context of SNA.

3.3.4 Eigensystem analysis of Hermitian Operators

In this section the main part of the methodological basis of this work is introduced since the method proposed is based on the eigensystem analysis of Hermitian matrices.

The eigenvalue equation of a Hermitian matrix H with eigenvector $\mathbf{x}$ and eigenvalue λ is given by Eq.(3.52):

$$H\mathbf{x} = \lambda\mathbf{x} \tag{3.52}$$

Hermitian matrices have the following characteristics:

- All eigenvalues are real (Eq.(3.53)) and can thus be ordered either from $\lambda_{max} = \lambda_1 > \ldots > \lambda_{min} = \lambda_n$, or as in the context of this book by their absolute value.

$$\lambda_k \in \mathbb{R} \qquad \forall k \quad \text{with} \quad \mid \lambda_1 \mid = max_k \mid \lambda_k \mid > \ldots > \mid \lambda_n \mid = min_k \mid \lambda_k \mid \tag{3.53}$$

because $\langle H\mathbf{x} \mid \mathbf{x} \rangle = \langle \lambda\mathbf{x} \mid \mathbf{x} \rangle = \overline{\lambda}\langle \mathbf{x} \mid \mathbf{x} \rangle$ and $\langle \mathbf{x} \mid H\mathbf{x} \rangle = \langle \mathbf{x} \mid \lambda\mathbf{x} \rangle = \lambda\langle \mathbf{x} \mid \mathbf{x} \rangle$ and Eq.(3.20) imply $\langle H\mathbf{x} \mid \mathbf{x} \rangle = \langle \mathbf{x} \mid H\mathbf{x} \rangle$ and thus $\overline{\lambda} = \lambda$ which means by Eq.(3.16) $\lambda \in \mathbb{R}$ (see [Mey00, p. 548], [Kat95, p. 53]).

- The largest absolute eigenvalue is the spectral radius because of Eq.(3.42).

- Eigenvectors belonging to different eigenvalues form an orthogonal system, which can be chosen to be orthonormal

$$\langle \mathbf{x_k} \mid \mathbf{x_l} \rangle = \delta_{kl} \qquad \text{(follows from (3.20))} \tag{3.54}$$

with

$$\delta_{kl} = \begin{cases} 0 & \text{if } k \neq l, \\ 1 & \text{if } k = l \end{cases} \tag{3.55}$$

This also holds true for arbitrary rotation:

$$\begin{aligned} \langle e^{i\phi_k}\mathbf{x}_k \mid e^{i\phi_l}\mathbf{x}_l \rangle &= e^{-i\phi_k} e^{i\phi_l} \langle \mathbf{x}_k \mid \mathbf{x}_l \rangle \\ &= e^{i(\phi_l - \phi_k)} \langle \mathbf{x}_k \mid \mathbf{x}_l \rangle \\ &= e^{i(\phi_l - \phi_k)} \delta_{kl} \end{aligned} \tag{3.56}$$

- They can be represented by a complete spectral decomposition as in Eq.(3.57). The eigenvalues can be interpreted as weights of the corresponding eigenspace.

$$H = \sum_{k=1}^{n} \lambda_k P_k \tag{3.57}$$

with

$$P_k = \mathbf{x}_k \mathbf{x}_k^* = \begin{pmatrix} x_1\overline{x_1} & \dots & x_1\overline{x_n} \\ \dots & \dots & \dots \\ x_n\overline{x_1} & \dots & x_n\overline{x_n} \end{pmatrix} \tag{3.58}$$

representing the orthogonal projectors. Note, that $\sum_{k=1}^{n} P_k = I$, $P_k^* = P_k$, $P_k^2 = P_k$. For more detail see section 3.3.5.

- Any function $f(H)$ of a Hermitian matrix H can also be seen as a function of its eigenvalues $f(\lambda)$. Now let $f(H) = \sum_{p=0}^{\infty} H^p$ be a power series, then it follows that $f(\lambda_i) = \sum_{p=0}^{\infty} \lambda_i^p, \forall i = 1, \dots n$, since $f(H) = f(XDX^{-1})$ with X representing the matrix of all eigenvectors and D a diagonal matrix with $f(\lambda_i)$ as entries. This can be seen when the function is expanded:

$$
\begin{aligned}
f(H) &= \sum_{p=0}^{\infty} H^p \\
&= \sum_{p=0}^{\infty} (\sum_{k=1}^{n} \lambda_k P_k)^p \quad \text{by Eq.(3.57)} \\
&= (\sum_{k=1}^{n} \lambda_k P_k)^0 + (\sum_{k=1}^{n} \lambda_k P_k)^1 + (\sum_{k=1}^{n} \lambda_k P_k)^2 + \ldots \\
&= (\sum_{k=1}^{n} \lambda_k P_k)^0 + (\sum_{k=1}^{n} \lambda_k P_k)^1 + (\sum_{k=1}^{n} \lambda_k P_k) * (\sum_{k=1}^{n} \lambda_k P_k) + \ldots \\
&= (\sum_{k=1}^{n} \lambda_k P_k)^0 + (\sum_{k=1}^{n} \lambda_k P_k)^1 + ((\lambda_1 P_1 * \lambda_1 P_1) \\
&+ (\lambda_1 P_1 * \lambda_2 P_2) + \ldots) + \ldots \\
&= (\sum_{k=1}^{n} \lambda_k P_k)^0 + (\sum_{k=1}^{n} \lambda_k P_k)^1 + (\sum_{k=1}^{n} \lambda_k P_k)^2 + \ldots \quad \text{by } P_k P_l = \delta_{kl} P_k \\
&= \sum_{p=0}^{\infty} \sum_{k=1}^{n} \lambda_k^p P_k \\
&= \sum_{k=1}^{n} f(\lambda_k) P_k
\end{aligned}
\tag{3.59}
$$

It is a well known result that such power series converge under certain conditions which also hold for every adjacency matrix $H \in \mathbb{C}$. [Mey00, p.618]. We now use a special type of power series, the von Neumann series given in Eq.(3.60) and their convergence criteria, since von Neumann series exactly reflect the relationship we need to find the rank index introduced in section 3.2.2.

$$
\begin{aligned}
I + H + H^2 + H^3 + \ldots &= \sum_{p=1}^{\infty} H^p \\
&= (I - H)^{-1} \\
&\Leftrightarrow lim_{p \to \infty} H^p = 0 \\
&\Leftrightarrow \quad |\lambda_{max}| < 1
\end{aligned}
\tag{3.60}
$$

which is equivalent to $\| H \| < 1$. Since $\| H \| = | \lambda_{max} |$ (Eq.(3.42)). This is equivalent to the fact established above that a function of H generates a function of λ. It follows that the corresponding power series for λ converges if $| \lambda_{max} | < 1$. This means that if the von Neumann series converges for H, this is connected to the eigensystem of H in that the power series for λ converges to $(1-\lambda)^{-1} \rightarrow |\lambda| < 1$. Thus the eigensystem of H approximates the eigensystem of the power series and converges in the limit.

- Eq.(3.57) together with Eq.(3.50) yields the result, that the eigenvalues can be used to explain the contained variance of a subspace. The variance σ^2 of $\mathbf{x}$ is defined as $\sigma^2 = \frac{1}{n} \sum_k (x_k - \mu)^2 = \frac{1}{n} \| \mathbf{x} - \mu \mathbf{e} \|^2$ with μ representing the mean and $\mathbf{e}$ the unit vector.

  Proof:

$$
\begin{aligned}
\| H - \sum_{k=1}^{n} \lambda_k P_k \|^2 &= \langle H - \sum_{k=1}^{n} \lambda_k P_k \mid H - \sum_{k=1}^{n} \lambda_k P_k \rangle \quad \text{Eq.(3.35)} \\
&= \langle H \mid H \rangle - \langle H \mid \sum_{k=1}^{n} \lambda_k P_k \rangle - \langle \sum_{k=1}^{n} \lambda_k P_k \mid H \rangle \\
&\quad - \langle H \mid \sum_{k=1}^{n} \lambda_k P_k \rangle \quad \text{Eq.(3.45)} \\
&= \| H \|^2 - 2 \| H \|^2 + \langle \sum_{k=1}^{n} \lambda_k P_k \mid \sum_{k=1}^{n} \lambda_k P_k \rangle \quad \text{Eq.(3.35)} \\
&= - \| H \|^2 + \sum_{i,j} \lambda_i \overline{\lambda_j} \langle P_i \mid P_j \rangle \quad \text{Eqs.(3.53) , (3.57), (3.58)} \\
&= - \| H \|^2 + \sum_{i=1}^{n} \lambda_i^2 = 0 \\
&\Rightarrow \| H \|^2 = \sum_{k=1}^{n} \lambda_k^2
\end{aligned}
\tag{3.61}
$$

  If one sums not over all n but only to an index $m \leq n$ and divides by the total sum of all λ_k^2, the result shows the variance covered by the m first eigenspaces.

- They are well conditioned, which means that a small disturbance E of the Hermitian H matrix only results in a change of the eigensystem up to $\| E \|$. See section 3.3.6 for details.

For matrices of the form discussed in chapters 4 and 6, the following characteristics hold:

Let H be a matrix with $h_{kk} = 0$ (no self reference) then following the fact that $H = UDU^{-1}$ the $\sum_{k=0}^{n} \lambda_k = trace(H) = \sum_{k=0}^{n} h_{kk} = 0$. This leads immediately to the existence of negative eigenvalues.

Of special interest is the matrix B of order $n + m$ with

$$B = \begin{pmatrix} 0_{n\times n} & A \\ A^* & 0_{m\times m} \end{pmatrix} \tag{3.62}$$

with A representing a $n \times m$ matrix. In general, this is the representation of a bipartite graph.

In the special case of n=1 and m=k this matrix represents a directed, weighted star graph with $k+1$ vertices. The spectrum of that system is described as follows:

$$\sigma(B) = \{+\lambda_1, +\lambda_2, \ldots, -\lambda_{m+n-1}, -\lambda_{m+n}\} \tag{3.63}$$

(see [Mey00, p. 555]) with $|\lambda_1| = |\lambda_{m+n}|$, $|\lambda_2| = |\lambda_{m+n-1}|$, etc.

The eigenvalues are by definition of the same absolute value, but being the square roots of the singular values of A they have either sign. For the respective eigenvectors this leads to the fact that they are only determined up to multiples of π.

As an example let H be a 3×3 Hermitian matrix of a star graph with $h_{kk} = 0$ and $h_{kl} = 0$ for $(kl) \in \{(23), (32)\}$. The equations for the eigensystem are then given explicitly following Eq.(3.52) by Eq.(3.64). The phase of the eigenvector components will be calculated by Eq.(3.65).

$$\begin{aligned} 0x_1 + h_{12}x_2 + h_{13}x_3 &= \lambda x_1 \\ \overline{h_{12}}x_1 + 0x_2 + 0x_3 &= \lambda x_2 \\ \overline{h_{13}}x_1 + 0x_2 + 0x_3 &= \lambda x_3 \end{aligned} \tag{3.64}$$

Thus it follows, that the phases for $x_{1,2,3}$ can be expressed as:

$$\begin{aligned} x_3 &= \frac{1}{\lambda}\overline{h_{13}} \\ x_2 &= \frac{1}{\lambda}\overline{h_{12}} \\ x_1 &= \frac{1}{\lambda^2}\sum_{k=1}^{3} \mid h_{1k} \mid^2 = 1 \end{aligned} \tag{3.65}$$

The last equation holds, because the determinant $det(H - \lambda I) = -\lambda^3 + \lambda h_{13}\overline{h_{13}} + \lambda h_{12}\overline{h_{12}} = -\lambda(\lambda^2 - \sum_{k=1}^{3} \mid h_{1k} \mid^2) = 0$. This holds for $\lambda_3 = 0$ and $\lambda^2 = +\sum_{k=1}^{3} \mid h_{1k} \mid^2$ (Eq. 3.34), which is the same as $\lambda_{1,2} = \pm \parallel \mathbf{h}_1 \parallel$ (Eq.3.35).

It can be seen, that in the eigenvector of an unperturbed star, the phase of the original matrix entry is kept but complex conjugated. This is understandable when one looks at the projectors.

3.3.5 Orthogonal Projectors

The fact, that the entries p_{kl} of the projectors P_j in Eq.(3.58) are given by $x_k\overline{x_l}$ with $k, l = 1, \ldots, n$ the index within the eigenvector $\mathbf{x}_j$, it follows from Eqs.(3.17) and (3.19) that

$$\begin{aligned} p_{kl} &= x_k\overline{x_l} \\ &= (Re(x_k)Re(x_l) + Im(x_k)Im(x_l)) + i(Im(x_k)Re(x_l) - Re(x_k)Im(x_l)) \\ &= \langle \mathbf{x}_l \mid \mathbf{x}_k \rangle + i \mid \mathbf{x}_k \times \mathbf{x}_l \mid \end{aligned} \tag{3.66}$$

with $(\mathbf{x}_l \times \mathbf{x}_k)$ the cross product of two vectors. We regard each complex number x_k and x_l as a two component vector $\in \mathbb{R}^2$ in this case with components $x_{k,1} = Re(x_k)$ and $x_{k,2} = Im(x_k)$. The cross product of two vectors is again a vector, that is orthogonal to the plane spanned by the two original vectors and has the length identical to the area of the parallelogram spanned by the two vectors which can be calculated using the determinant of the matrix built by the two row vectors. This leads to the following interpretation of projector P_j in Mat.(3.67) ([Chi98], [BL04]):

- Each entry gives in its real part a measure of the structural similarity or closeness between the communication patterns of two members within this subspace, since the real part is constructed by the scalar product of the two eigenvector components.
- In its imaginary part the projector entry gives a measure of the divergence of behavior, since the imaginary part is the absolute value of the cross product between the eigenvector components.

As an example use the projector P_{λ_1} in Eq.(3.67).

$$P_{\lambda_1} = \begin{pmatrix} 0 & \frac{1}{\lambda}h_{12} & \frac{1}{\lambda}h_{13} & \\ \frac{1}{\lambda}\overline{h_{12}} & 0 & 0 & 0 \\ \frac{1}{\lambda}\overline{h_{13}} & 0 & 0 & 0 \end{pmatrix} \tag{3.67}$$

As will be explained in section 4.3.2 it also yields an additional interpretation in the context of communication pattern analysis.

3.3.6 Perturbation Theory for Hermitian Operators

The behavior under perturbation is well researched for Hermitian operators [Kat95], [DS88] . And since this is a major advantage of the proposed method when thinking of future work in this field, a very short introduction at least for perturbation of eigenvalues is given.

Now assume an unperturbed Hermitian matrix A with eigenvalues $\alpha_1, \ldots,$ α_n, with $\alpha_1 \geq \ldots \geq \alpha_n$ and a Hermitian perturbation matrix E with eigenvalues $\epsilon_1, \ldots, \epsilon_n$, with $\epsilon_1 \geq \ldots \geq \epsilon_n$. For the eigenvalues $\lambda_1, \ldots, \lambda_n$, with $\lambda_1 \geq \ldots \geq \lambda_n$ of the resulting Hermitian matrix $H = A + E$ a Weyl type perturbation bound is given by

$$\alpha_j + \epsilon_1 \geq \lambda_j \geq \alpha_j + \epsilon_n \tag{3.68}$$

See [HJ90, p.181-182], [Kat95, p.61] or [Mey00, p.551-552].

The Bauer-Fike bound in Eq.(3.69) for diagonalizable matrices can be used to give an even better bound for Hermitian perturbations [HJ90, p.367-370]:

$$min_{\alpha_k} \frac{\mid \lambda_k - \alpha_k \mid}{\parallel E \parallel} \leq \kappa(X) \parallel E \parallel \tag{3.69}$$

with $\kappa(X) = \parallel X \parallel \parallel X^{-1} \parallel$ for a matrix X of eigenvectors, where the inverse exists which is the case for the matrix of eigenvectors of a Hermitian matrix. For Hermitian matrices the Bauer-Fike bound in Eq.(3.69) even reduces to $\parallel E \parallel$, since $\kappa(X) = 1$. Since the matrix X is orthogonal ($X^* = X^{-1}$) and $\parallel X \parallel = 1$ due to orthonormality. Thus Hermitian matrices are well conditioned [HJ90, p.528] which has already been mentioned in section 3.3.4.

With these bounds it would be possible to check if and how a matrix H is the result of a perturbation E. This will be of some interest in chapter 4, when the construction and behavior of complex Hermitian adjacency matrices and their respective eigensystems will be discussed. Since a Hermitian matrix H can be represented by a Fourier sum of its subspaces, the addends, ordered by their weights (the corresponding eigenvalues) can be seen as an approximation of a perturbation. The addend with a relative high weight can be seen as the unperturbed matrix, with all other addends as perturbation matrices. This interpretation is highly convinient, when the first one or two subspaces already cover a large part of the variance.

3.4 Eigensystem of real adjacency matrices for non-directional graphs

For real valued adjacency matrices extensive literature about the corresponding eigensystems of graphs can be found in Cvetkovic et al. [CS97]. As discussed therein the eigenspectrum of a graph does not identify the graph uniquely, since cospectrality, which means "having the same eigenspectrum", does not lead to isomorphism, which means "having the same graph structure" in this context. But if, in addition, the eigenspaces are taken into account the uniqueness of the eigensystem can be established. As a reference for later use in chapter 4.4, some results about eigensystems of certain kinds of graphs from Cvetkovic will be presented without proof.

Star graph

Let S be a star graph as in Fig.(3.4) with 4 vertices $v_k, k = 1, 2, 3, 4$. Further let v_1 be the center of that star. Then the normed eigensystem of the real valued adjacency matrix $A = a_{kl}, \quad a_{kl} = 1$ if $e(k, l) \in E$ else $a_{kl} = 0$ has the form as in Tab. 3.3.

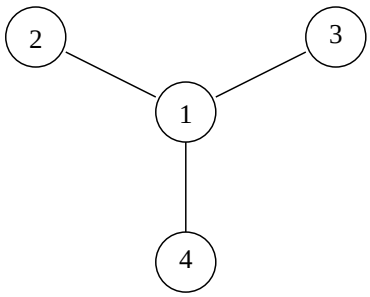

Figure 3.4: Non directional star graph

		$\mathbf{x}_k$			
k	λ_k	$\mathbf{x}_{k,1}$	$\mathbf{x}_{k,2}$	$\mathbf{x}_{k,3}$	$\mathbf{x}_{k,4}$
1	1.73	0.71	0.41	0.41	0.41
2	-1.73	0.71	0.41	0.41	0.41
3	0	0	0.82	0.82	0.82
4	0	0	0.82	0.82	0.82

Table 3.3: Eigensystem of a star graph in Fig.(3.4)

As can be seen, there is one pair of non-zero eigenvalues with the same absolute value but different sign (eigenvalue $\lambda_{1,2} = \pm 1.73$ (Eq.(3.63))). The eigenvectors for the two non zero eigenvalues show, that the vertex v_1 has a higher value than the other vertices, who have equal absolute values. This is intuitive in a star, the center is perceived as the strongest member, while all the others are perceived to be less relevant in comparison but equally relevant amongst themselves. This result qualitatively corresponds to the result from the degree centrality measure in Eq.(3.2), which yields $c_1^o = 1, c_{2,3,4}^o = 1/3$.

Complete Graph

Let C be a complete graph as in Fig.(3.5) again with 4 vertices labeled as above. The eigensystem then is given in Tab. 3.4.

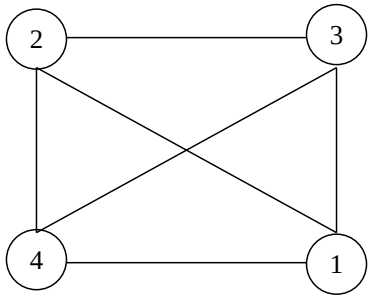

Figure 3.5: Non directional complete graph

k	λ	$\mathbf{x}$			
		$\mathbf{x}_{k,1}$	$\mathbf{x}_{k,2}$	$\mathbf{x}_{k,3}$	$\mathbf{x}_{k,4}$
1	3.00	0.50	0.50	0.50	0.50
2	-1.00	0	0.87	0.87	0.87
3	-1.00	0	0.87	0.87	0.87
4	-1.00	0	0.87	0.87	0.87

Table 3.4: Eigensystem of a complete graph in Fig.(3.5)

This eigensystems shows only one maximal eigenvalue, while all the others have the same absolute value and even the same sign. The eigenvector components of the maximal eigenvalue show that all vertices are of equal relevance.

The star graph and the complete graph are two graphs which represent the two extreme communication patterns for group structures. A group can either be extremely connected, ergo a complete graph, or strongly centered, ergo a star. There exist all kinds of mixtures, and in addition there can also be isolated vertices

within groups. But in the context of this book, all members have at least one connection within the group. This is why isolated vertices need not be discussed here.

As was shown in this chapter, the use of complex Hermitian matrices has many advantages when calculating the eigensystem. These are:

- Real eigenvalues
- Orthogonal eigenvector system $\rightarrow$ orthogonal projectors
- Well conditioned matrices
- Inner product norm
- Fourier sum representation

The relevance of these properties for the purpose of interpreting the structure of email communication will be shown in the next chapter.

Chapter 4

Analysis of General Bidirectional Communication Patterns

This chapter deals in section 4.1 with the coding of bidirectional communication patterns in a weighted adjacency matrix. In section 4.2 it is shown how a complex Hermitian adjacency matrix can be deduced from a weighted directional graph in a social network. Section 4.3 gives an interpretation of the results obtained in chapter 3 in the context of bidirectional communication pattern analysis. Section 4.4 gives some examples of designed synthetic communication matrices and shows how the proposed method can be used to analyze the communication structure hidden in these matrices.

4.1 Communication Behavior

In the following we consider bidirectional communication patterns which can be modeled as a directed and weighted graph $G = \{V, E, A\}$ as described in section 3.1.1. Let v_k and v_l be vertices (members) of the group ($v_k, v_l \in V$). The communication going from v_k to v_l and from v_l to v_k will be transformed into the entry a_{kl} in the matrix A.

Thus the following possibilities for communication between two vertices may arise:

- No self reference: $a_{kk} = 0, \quad \forall k$
- k and l communicate: $a_{kl} \neq 0$
  - k communicates with l on the same level
  - k writes more often to l then vice versa
  - l writes more often to k then vice versa

Coding the communication between vertices k and l is a problem in SNA, as long as $a_{kl} \in \mathbb{R}$, because only one information can be coded in a real number instead of the number of messages sent from k to l and vice versa. It is usually achieved by making a choice of what to code, e.g. only the difference in communication, or the predominant direction, ... and choice implies information loss. A solution to this problem is to regard these two components as a two component vector in a 2 dimensional plane. Thus this real two component vector can be transformed into a complex number, as explained in section 3.3.1. As a consequence $a_{kl} \in \mathbb{C} \quad \forall k, l$. The asymmetry of communication behavior is the characteristic, which has to be dealt with, when trying to find feasible solutions with eigensystem analysis.

4.2 Complex Hermitian Adjacency Matrix

The amount m of outbound communication of a vertex k is translated into the real part of the matrix entry, $m = Re(a_{kl})$, whereas the amount p of inbound communication of vertex k is denoted as the imaginary part, $p = Im(a_{kl})$. Thus the characteristics of complex numbers as described in section 3.3.1 Eq.(3.13) now have the following interpretation:

- The absolute value corresponds to the traffic volume exchanged between two members.
- The phase $\phi(a_{kl})$ represents the relative direction of the communication.

The complex adjacency matrix A has entries as given in Tab.(4.1):

communication behavior	$a_{kl} = m + ip$	$\phi(a_{kl})$
no self reference	$a_{kk} = 0$	arbitrary
$k \to l > l \to k$	$m > p$	$[0, \frac{\pi}{4}[$
$l \to k > k \to l$	$m < p$	$]\frac{\pi}{4}, \frac{\pi}{2}]$
$k \to l = l \to k$	$m = p$	$\frac{\pi}{4}$

Table 4.1: Communication behavior representation

The entries of the complex adjacency matrix A can be completed by following Eq. 4.1:

$$a_{kl} = i\overline{a_{lk}} \tag{4.1}$$

The construction of the matrix A is thus given by Eq. 4.2

$$A = B + iB^t, \quad \text{with} \quad b_{kl} \in \mathbb{R} \tag{4.2}$$

with B representing the weighted real valued adjacency matrix, thus the entries of B reflect the number of messages which go from vertex k to vertex l.

In Fig.(4.1) a sample communication can be seen. The points represent the matrix entries a_{kl} of a sample matrix given in Eq.(4.1). The diagonal line has been drawn to demonstrate the underlying symmetry.

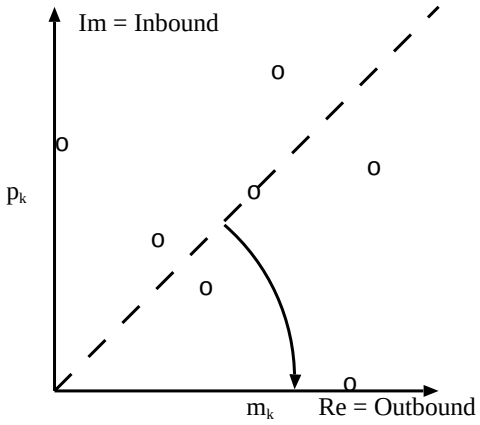

Figure 4.1: Communication behavior before rotation

It can easily be seen as well from Eq.(4.1) as from Fig.(4.1) that A can be transformed into a Hermitian matrix H by rotation. Rotation is achieved by multiplying A following Eq.(3.15). The rotation factor is $e^{-i\frac{\pi}{4}}$ as shown in Eq.(4.3).

$$H = A \cdot e^{-i\frac{\pi}{4}} \tag{4.3}$$

Proof:

1. Let the entry of A be any complex number $a_{kl} = re^{i\phi}$ with absolute value r and phase ϕ.
2. Then by Eq.(4.1) $a_{lk} = i\overline{a_{kl}} = ire^{-i\phi}$
3. $a_{kk} = 0 = h_{kk}$ because of the exclusion of self references
4. After rotation about ψ : $h_{kl} = a_{kl}e^{i\psi} = re^{i\phi}e^{i\psi} = re^{i(\phi+\psi)}$
5. $h_{lk} = a_{lk}e^{i\psi} = ire^{-i\phi}e^{i\psi} = e^{i\frac{\pi}{2}}re^{i(\psi-\phi)}$
6. For Hermitian matrices $h_{kl} = \overline{h_{lk}}$ must hold (Eq.(3.20), therefore, $re^{i(\phi+\psi)} = re^{-i(\frac{\pi}{2}+\psi-\phi)}$.

7. This holds, if $\phi + \psi = -\frac{\pi}{2} - \psi + \phi$.

8. Solving for ψ leads to $2\psi = -\frac{\pi}{2}$. Thus $\psi = -\frac{\pi}{4}$. *qed*

The alternative way given by Chino yields a matrix that is similar to H in Eq.(4.3). The proof is the following:

Let $H_C = \frac{1}{2}(B + B^t) + i\frac{1}{2}(B - B^t)$ by Eq.(3.22) and $H_H = (B + iB^t)e^{-i\frac{\pi}{4}}$ by Eqs.(4.2, 4.3) then:

$$\begin{aligned} H_C &= \frac{1}{2}(B + B^t) + i\frac{1}{2}(B - B^t) \\ &= \frac{1}{2}(B + iB + B^t - iB^t) \\ &= \frac{1}{2}(B(1+i) + B^t(1-i)) \\ &= \frac{\sqrt{2}}{2}(Be^{i\frac{\pi}{4}} + B^t e^{-i\frac{\pi}{4}}) \\ &= \frac{\sqrt{2}}{2}(B + B^t e^{-i\frac{\pi}{2}})e^{i\frac{\pi}{4}}, e^{-i\frac{\pi}{2}} = -i \\ &= \frac{\sqrt{2}}{2}(B - iB^t)e^{i\frac{\pi}{4}} \\ &= \frac{\sqrt{2}}{2}\overline{H_H} \end{aligned} \tag{4.4}$$

with $\overline{H_H}$ representing the complex conjugated matrix of H_H.

This leads to an eigensystem that is complex conjugated and scaled by a constant to the one presented. As will be seen later in section 4.3.2 the interpretation of the orthogonal projectors will be more intuitive and revealing with the matrix given by Eq.(4.3) than with the method proposed by Chino. In addition the comparison with the original adjacency matrix is not easy to achieve, since more than a back rotation is needed in the case of Chino.

Tab.(4.2) shows how the communication behavior patterns of Tab.(4.1) remain visible in the rotated matrix H with entries h_{kl} after the rotation:

1. No self reference: $h_{kk} = 0$

2. More outbound than inbound traffic ($k \to l > l \to k$) leads to a negative sign of the imaginary part $p_r = Im(h_{kl}) < 0$

3. More inbound than outbound traffic ($l \to k > k \to l$) leads to a positive sign $p_r = Im(h_{kl}) > 0$

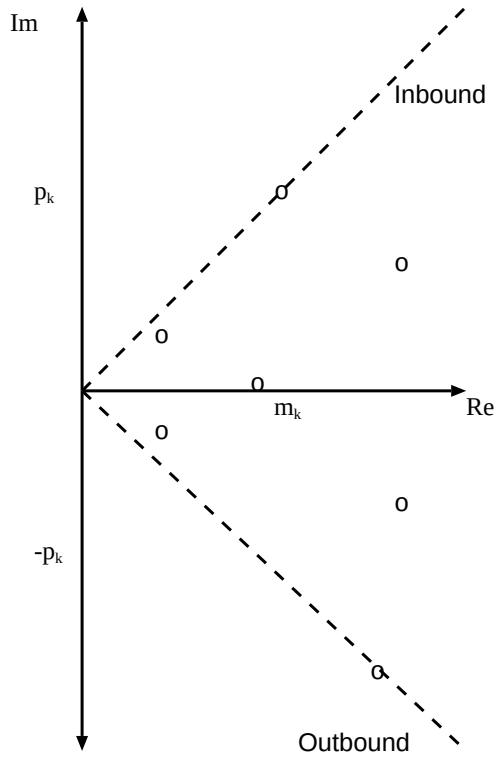

Figure 4.2: Communication behavior after rotation

4. Outbound equals inbound traffic ($k \to l = l \to k$): $p_r = 0$

Fig.(4.2) shows how the data points in Fig.(4.1) behave under rotation. Note that the norm is invariant under rotation. The absolute value - that is the representation of the amount of of communication - does not change.

communication behavior	$a_{kl} = m + ip$	$h_{kl} = m_r + ip_r$
no self reference	$a_{kk} = 0$	$h_{kk} = 0$
$k \to l > l \to k$	$m > p$	$p_r < 0$
$l \to k > k \to l$	$m < p$	$p_r > 0$
$k \to l = l \to k$	$m = p$	$p_r = 0, m_r > 0$

Table 4.2: Communication behavior representation in the matrix H

4.3 Interpretation of the Eigensystem

In this section the interpretation of the components of the eigensystem of the complex Hermitian adjacency matrices introduced in section 4.2 will be discussed. In

the following the solution of the eigensystem $H\mathbf{x} = \lambda\mathbf{x}$ is considered. First, in section 4.3.1 the eigenspectrum will be interpreted in the light of the input data, then, in subsection 4.3.2, the interpretation of eigenvectors and the resulting orthogonal projectors will be explained.

4.3.1 Eigenspectrum

Since the input data consists of inbound and outbound messages, the eigenspectrum reflects the "energy" level, or traffic level within the data set, since

$|\lambda| = \| H \| = \| A \|$

is the spectral radius following Eq.(3.42). Thus λ changes with the number of messages exchanged. λ does not reveal if the number of in- or outbound messages has changed.

The eigenvalue can be interpreted following Eq.(3.57) as the weight of the corresponding eigenspace, thus it is also permissible to see it as the weight of a pattern that serves as a corrective perturbation or pattern on the most prominent eigenspace. If now $\lambda_2 < 0$ and $\lambda_1 > 0$ or vice versa and the anchor corresponding to λ_1 and λ_2 is the same, then the correction that the pattern corresponding to λ_2 brings puts a stronger focus on a characteristic within the communication of the whole group. The sign of the eigenvalue yields information if the communication behavior demonstrated by the subspace is the pattern with the subgroup, or the communication pattern that the subgroup maintains to the rest of the group. For an example see subsection 4.4.3. This could be seen as a kind of filtering function. When the second subspace weighted by its eigenvalue is added to the first, the strongest pattern receives a modulation. The sign of the eigenvalue also yields information.

As was shown in section 3.3.4, the spectrum exhibits a symmetry for undisturbed star graphs. If the star is being perturbed, the symmetry breaks down. This means that if, for example, a group shows the communication behavior of a star graph, additional cross communication takes the role of a perturbation as long as it is small compared to communication in the star. This is analog in the case of a complete graph. In this case for example one sided communication or very little communication between two nodes takes the form of a perturbation.

4.3.2 Eigenvectors and orthogonal projectors

The absolute value of the eigenvector components is the well known eigenvector centrality index (see Bonacich and Lloyd [BL01]). In this context this index can be interpreted as a similarity in communication pattern among the group members. Thus the component with highest absolute value can be interpreted as the highest ranked member within that pattern. This has been defined in section

3.1.1 as the anchor of the subgroup. The phase information of the eigenvector components gives information about the directional similarity compared with the anchor within the subgroup. This means that the phase shows, how the direction of communication of the vertex is similar to the direction of the anchor in that pattern. The anchor can be defined to have a phase of $\phi = 0$, the phase of all other components is a relative information. If for example the eigenvector shows the distribution of absolute values that represent a star like pattern, then the phase gives an indication of the direction of the pattern (inbound or outbound star).

The orthogonal projectors are the bridge between eigenvectors and original adjacency matrix. As has been explained already in section 3.3.5, the real part of the projector consists of the scalar product of the eigenvector components, thus giving an index for similarity. While the imaginary part consists of the absolute amount of the cross product of the eigenvector components, thus giving an index of skewness. Since the projectors are parts of the Fourier sum and thus are part of the original adjacency matrix, it follows that the number of outbound messages in the original matrix is connected to the scalar product of the eigenvector components, while the number of inbound messages is connected to the absolute value of the cross product of the eigenvector components.

4.4 Examples of Eigensystems

After having thus described the construction of the complex Hermitian adjacency matrix, this section will present some examples, which are designed so as to demonstrate how the methods works.

As an introduction to eigensystems of complex Hermitian adjacency matrices the graph patterns used in section.(3.4) will be used. All calculations have been performed with Mathematica [Wol03]. This has the following consequences:

- Eigenvectors are not normalized.
- In Mathematica the eigenvectors have been rotated to result in a phase of 0 for the eigenvector component with the largest absolute value. But this, as explained in section. 3.3.4 Eq.(3.56), does not disturb the orthogonality of the eigenspaces.
- Eigenvalues have been normalized by dividing each eigenvalue with the matrix norm. Thus the largest eigenvalue is equal to $|1|$.

To show how the results, the enhanced methods provides can be interpreted, the analog non-directional graphs will be considered first, and then the asymmetric

version will be discussed. The analogon to a non-directional graph is a bidirectional but equally weighted graph. For validation the results of Cvetkovic [CS97] in the case of star graphs and complete graphs will be used.

Three kinds of graphs will be discussed:

- The star graph (subsection 4.4.1)
- The complete graph (subsection 4.4.2)
- A graph representing two subgroups connected by one link (subsection 4.4.3)

4.4.1 Star Graph

The equivalent of a non-directional star graph in the complex representation is shown in Fig.(4.3). The corresponding complex adjacency matrix A_S is given in Eq.(4.5) and the rotated matrix A_s^{rot} is given in Eq.(4.6).

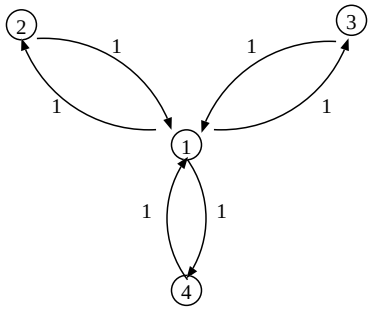

Figure 4.3: Equivalent to non-directional star graph corresponding to Eq.(4.5)

$$A_S = \begin{pmatrix} 0 & 1+i & 1+i & 1+i \\ 1+i & 0 & 0 & 0 \\ 1+i & 0 & 0 & 0 \\ 1+i & 0 & 0 & 0 \end{pmatrix} \tag{4.5}$$

$$A_S^{rot} = H_S = \begin{pmatrix} 0 & 1.41 & 1.41 & 1.41 \\ 1.41 & 0 & 0 & 0 \\ 1.41 & 0 & 0 & 0 \\ 1.41 & 0 & 0 & 0 \end{pmatrix} \tag{4.6}$$

The eigensystem of the rotated matrix $A_S^{rot} = H_S$ is given in Tab.(4.3). Since the rotated matrix has entries $h_{kl} \in \mathbb{R}$ the resulting eigensystem for the non-zero eigenvalues is the same (modulo π) as that in Tab.(3.3), eigenvalues have been

normalized. This eigensystem shows the first two eigenvalues with same absolute value, but with different sign. The corresponding eigenvectors are real in this case and show a phase difference of exactly π (in this case a different sign), apart from the largest absolute eigenvector component. Characteristic for a star graph is the fact that two eigenvalues of the same absolute value but with different sign exist, and that the distribution of the absolute value of the eigenvector components is such that the center of the star has the highest value, while all other members have a lower but equally distributed value.

k	λ_k	$\mathbf{x}_{k,l}$			
		$l=1$	$l=2$	$l=3$	$l=4$
1	-1.0	0.71	-0.41	-0.41	-0.41
2	1.0	0.71	0.41	0.41	0.41
3	0	0	-0.58	-0.21	0.79
4	0	0	-0.58	0.79	-0.21

Table 4.3: Eigensystem for H_S in Eq.(4.6)

The eigensystem in Tab.(4.3) corresponds (modulo π) for the non-zero eigenvalues with the results of Cvetkovic et al. [CS97, p.235].

If the star is perturbed within the star, which means that additional communication takes place between the already connected members of the network, the only effect is a change in the absolute value of the eigenvalues, since by Eq.(3.42) only $\parallel H \parallel$ becomes larger, but no additional members get connected. If the star is subjected to a symmetric perturbation as in Fig.(4.4) between vertices 2 and 3, which means that the matrix entries a_{23} and a_{32} are different from 0 as matrix A_p in Eq.(4.7) shows,

$$A_p = \begin{pmatrix} 0 & 1+i & 1+i & 1+i \\ 1+i & 0 & 1+i & 0 \\ 1+i & 1+i & 0 & 0 \\ 1+i & 0 & 0 & 0 \end{pmatrix} \tag{4.7}$$

the following effects can be observed in the eigensystem given in Tab.(4.4):

- The symmetry for the largest two eigenvalues breaks down according to Eq.(3.69): $\frac{|\lambda_2-\alpha_2|}{\|E\|} = \frac{|-0.68+1.0|}{1.41} = 0.22 \leq 1$, with E being the perturbation matrix with only the entries $e_{23}, e_{32} \neq 0$.

- The eigenvectors loose their symmetry, which means that the eigenvectors of the two largest eigenvalues do not have the same weights anymore as well as the fact that the eigenvector component for vertex k in each eigenvector does not only change the sign, which would mean a phase shift of π (which

is equivalent to a rotation by $180°$ counterclockwise or the ratio between the circumference C of a circle and its diameter d giving $\frac{C}{d} = 3.14\ldots$.

- The distribution of the eigenvector components within each eigenvector looses its star like characteristic. The anchor is still visible, but the behavior of the other vertices changes.

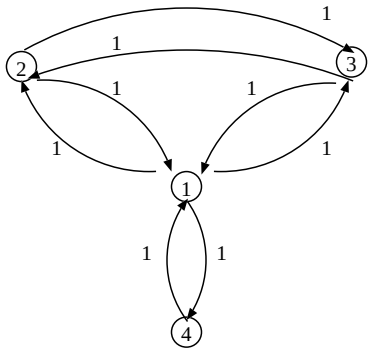

Figure 4.4: Symmetrical perturbation of non-directional star graph represented in Eq.(4.7)

k	λ_k	$\mathbf{x}_{k,l}$			
		$l=1$	$l=2$	$l=3$	$l=4$
1	1.0	0.61	0.52	0.52	0.28
2	-0.68	0.75	-0.3	-0.3	-0.51
3	-0.46	0	-0.71	0.71	0
4	0.14	0.25	-0.37	-0.37	0.82

Table 4.4: Eigensystem for the perturbed star in Eq.(4.7) after rotation in Fig.(4.4)

In addition it can be said, that if one reverses the direction of the edge between two vertices, the eigenvalues are kept, but the eigenvectors become complex conjugated. This can be seen if the star graph is subjected to an asymmetric perturbation as in Fig.(4.5)

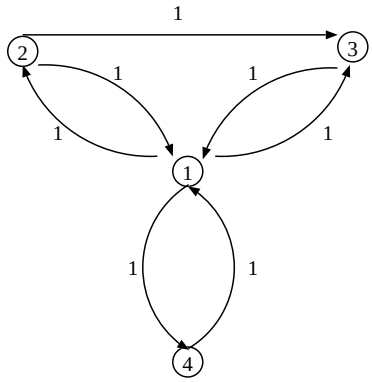

Figure 4.5: Asymmetric perturbation of a non-directional star

The eigensystem of the graph in Fig.(4.5) represented by matrix A_u in Eq.(4.8) is given in Tab.(4.5). In the case of the perturbation in the other direction, the eigensystem behaves as predicted (see Tab.(4.6)).

$$A_u = \begin{pmatrix} 0 & 1+i & 1+i & 1+i \\ 1+i & 0 & 1 & 0 \\ 1+i & i & 0 & 0 \\ 1+i & 0 & 0 & 0 \end{pmatrix} \tag{4.8}$$

		$\mathbf{x}_{k,l}$							
k	λ_k	$\lvert x_{k,1} \rvert$	$\phi(x_{k,1})$	$\lvert x_{k,2} \rvert$	$\phi(x_{k,2})$	$\lvert x_{k,3} \rvert$	$\phi(x_{k,3})$	$\lvert x_{k,4} \rvert$	$\phi(x_{k,4})$
1	1.0	0.65	0	0.48	-0.2	0.48	0.2	0.33	0
2	-0.84	0.71	0	0.40	-2.7	0.40	2.7	0.43	3.1
3	-0.30	0.20	1.4	0.65	2.8	0.65	0	0.34	-1.7
4	0.13	0.20	0	0.43	2.6	0.43	-2.6	0.77	0

Table 4.5: Eigensystem for the perturbed star with asymmetric communication given in Fig.(4.5)

		$\mathbf{x}_{k,l}$							
k	λ_k	$\lvert x_{k,1} \rvert$	$\phi(x_{k,1})$	$\lvert x_{k,2} \rvert$	$\phi(x_{k,2})$	$\lvert x_{k,3} \rvert$	$\phi(x_{k,3})$	$\lvert x_{k,4} \rvert$	$\phi(x_{k,4})$
1	1.0	0.65	0	0.48	0.2	0.48	-0.2	0.33	0
2	-0.84	0.71	0	0.40	2.7	0.40	-2.7	0.43	-3.1
3	-0.30	0.20	-1.4	0.65	-2.8	0.65	0	0.34	1.7
4	0.13	0.20	0	0.43	-2.6	0.43	2.6	0.77	0

Table 4.6: Eigensystem for the perturbed star as in Fig.(4.5) in reversed direction

The eigensystem also indicates the location of the perturbing event. The phase of the eigenvector components $\phi(x_{1,2})$ and $\phi(x_{2,2})$ as well as $\phi(x_{1,3})$ and $\phi(x_{2,3})$ no longer show a phase shift of π as can be seen in Tabs.(4.5, 4.6). This is exactly where the perturbation took place.

The eigenvalues lead to cumulative covered variance as in Tab.(4.7). As can be seen the first two subspaces cover already over 90% of the variance. The eigenprojectors derived from the eigensystem in Tab.(4.5) are given by Eqs.(4.9 – 4.12). The projectors $P_k, k = 1, 2, 3, 4$ are those corresponding to eigenvalues $\lambda_k, k = 1, 2, 3, 4$.

	λ_1	λ_2	λ_3	λ_4
covered variance per eigenvalue	0.55	0.39	0.05	0.01
cumulative covered variance	0.55	0.94	0.99	1.00

Table 4.7: Cumulative covered variance of eigenvalues from Tab.(4.6)

The first two projectors P_1 and P_2 have the following interpretation:

- The anchor is identified by the highest absolute value an identified as vertex 1. $p_{11}^{(1)} = 0.42$ and $p_{11}^{(2)} = 0.50$, where $p_{jl}^{(k)}$ represents the element in row k and column l of matrix P_k.

- P_1 corresponds to the highest absolute valued eigenvalue, thus more traffic is being exchanged in that pattern and P_2 serves as the corrective pattern. If one takes into account that $\lambda_2 < 0$, it can be seen that the second pattern, when added as described by the Fourier sum, has the effect that the diagonal entries of the sum will go towards 0 or below, and that the entries in the first row and first column will be augmented, while the entries in the submatrix $p_{22}^{(1)+(2)} \ldots p_{44}^{(1)+(2)}$ will tend towards 0. This then already comes close to a star like adjacency matrix.

- The pattern in P_1 represents the fact that all members are connected with a slight tendency towards a star. Only P_2 shows a stronger star around vertex 1, since all other matrix entries are lower by half at least. This suggests that P_1 represents the communication within the whole group, while P_2 represents the communication within the star.

$$P_1 = \begin{pmatrix} 0.42 & 0.31 - 0.06i & 0.31 + 0.06i & 0.21 \\ 0.31 + 0.06i & 0.23 & 0.22 + 0.09i & 0.16 + 0.03i \\ 0.31 - 0.06i & 0.22 - 0.09i & 0.23 & 0.16 - 0.03i \\ 0.21 & 0.16 - 0.03i & 0.16 + 0.03i & 0.11 \end{pmatrix} \tag{4.9}$$

$$P_2 = \begin{pmatrix} 0.50 & -0.26 - 0.11i & -0.26 + 0.11i & -0.30 \\ -0.26 + 0.11i & 0.16 & 0.11 - 0.12i & 0.16 - 0.07i \\ -0.26 - 0.11i & 0.11 + 0.12i & 0.16 & 0.16 + 0.07i \\ -0.30 & 0.16 + 0.07i & 0.16 - 0.07i & 0.18 \end{pmatrix} \quad (4.10)$$

P_3 has vertex 3 as anchor, but vertex 2 has the same absolute value, which can be interpreted as a structural similarity between the two. Only the difference in phase shows that compared to vertex 3 that vertex 2 has a slight difference in direction of communication.

$$P_3 = \begin{pmatrix} 0.04 & 0.02 + 0.13i & 0.02 - 0.13i & -0.07 \\ 0.02 - 0.13i & 0.42 & -0.40 - 0.14i & -0.04 + 0.22i \\ 0.02 + 0.13i & -0.40 + 0.14i & 0.42 & -0.04 - 0.22i \\ -0.07 & -0.04 - 0.22i & -0.04 + 0.22i & 0.12 \end{pmatrix} \quad (4.11)$$

In P_4 vertex 4 is the anchor and vertices 2 and 3 again have the same absolute value but different phase.

$$P_4 = \begin{pmatrix} 0.041 & -0.07 + 0.05i & -0.07 - 0.05i & 0.16 \\ -0.07 - 0.05i & 0.18 & 0.07 + 0.17i & -0.28 - 0.18i \\ -0.07 + 0.05i & 0.07 - 0.17i & 0.18 & -0.28 + 0.18i \\ 0.16 & -0.28 + 0.18i & -0.28 - 0.18i & 0.59 \end{pmatrix} \quad (4.12)$$

Now consider a directed and weighted star graph of an asymmetric communication between 5 members or vertices as in Fig.(4.6).

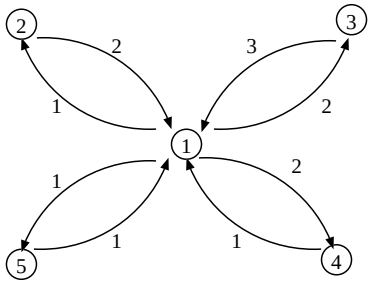

Figure 4.6: Asymmetric star graph

The original complex adjacency matrix A_{S5} corresponding to the graph in Fig.(4.6) is given in Eq.(4.13).

$$A_{S5} = \begin{pmatrix} 0 & 1+2i & 2+3i & 2+i & 1+i \\ 2+i & 0 & 0 & 0 & 0 \\ 3+2i & 0 & 0 & 0 & 0 \\ 1+2i & 0 & 0 & 0 & 0 \\ 1+i & 0 & 0 & 0 & 0 \end{pmatrix} \tag{4.13}$$

After rotation A_{S5} becomes the Hermitian matrix H_{S5}:

$$A_{S5}^{rot} = H_{S5} = \begin{pmatrix} 0 & 2.1+0.7i & 3.5+0.7i & 2.1-0.7i & 1.4 \\ 2.1-0.7i & 0 & 0 & 0 & 0 \\ 3.5-0.7i & 0 & 0 & 0 & 0 \\ 2.1+0.7i & 0 & 0 & 0 & 0 \\ 1.4 & 0 & 0 & 0 & 0 \end{pmatrix} \tag{4.14}$$

The corresponding eigensystem is given in two different representations to make certain aspects more visible. To give a better view of the effect of perturbation on the eigenvalues no normalization has been performed. As can be seen in both Tab.(4.8) and Tab.(4.9) there are two non-zero eigenvalues of the same absolute value ($|\lambda_1| = |\lambda_2| = 5.0$) but with different sign ($\lambda_1 < 0, \lambda_2 > 0$). As was shown in Eq.(3.63) this is indeed the characteristic of the adjacency matrix of a star graph. As can also be seen the eigenvectors belonging to the two eigenvalues are the same in absolute values but differ by π in phase as shown in Eq.(3.65). Note that the entry in the first row (vertex 1) is the center of the star graph and is indicated as such by the eigenvector component of the highest absolute value. This member can thus be described as the most central and prestigious member of the group, ergo the anchor. It can also be seen that the entry in row 3 (member with ID 3) has the second highest absolute eigenvector component, which means that this vertex has a strong similarity in behavior compared to vertex 1.

λ_k	λ_1	λ_2	λ_3	λ_4	λ_5
	-5.0	5.0	0	0	0
$\mathbf{x}_{k,1}$	0.71	0.71	0	0	0
$\mathbf{x}_{k,2}$	-0.3+0.1i	0.30-0.10i	-0.27+0.09i	-0.36+0.27i	0.72
$\mathbf{x}_{k,3}$	-0.5+0.1i	0.50-0.1i	-0.14+0.03i	-0.19+0.11i	-0.64-0.08i
$\mathbf{x}_{k,4}$	-0.3-0.1i	0.30+0.10i	-0.08-0.03i	0.86	0.18+0.13i
$\mathbf{x}_{k,5}$	-0.2	0.20	0.94	-0.08+0.03i	0.13+0.04i

Table 4.8: Eigensystem for H_{S5} in Eq.(4.14) with $z = a + ib$

λ_k	λ_1		λ_2		λ_3		λ_4		λ_5	
	-5.0		5.0		~ 0		0		0	
	$\mid z \mid$	$\phi(z)$	$\mid z \mid$	$\phi(z)$	$\mid z \mid$	$\phi(z)$	$\mid z \mid$	$\phi(z)$	$\mid z \mid$	$\phi(z)$
$\mathbf{x}_{k,1}$	0.71	0	0.71	0	0	undef	0	undef	0	undef
$\mathbf{x}_{k,2}$	0.32	2.82	0.32	-0.32	0.28	2.82	0.45	2.50	0.72	0
$\mathbf{x}_{k,3}$	0.51	2.94	0.51	-0.20	0.14	2.94	0.22	2.62	0.64	-3.02
$\mathbf{x}_{k,4}$	0.32	-2.82	0.32	0.32	0.087	-2.82	0.86	0	0.22	0.64
$\mathbf{x}_{k,5}$	0.20	π	0.20	0	0.94	0	0.09	2.82	0.14	0.32

Table 4.9: Eigensystem for H_{S5} in Eq.(4.14) with $z =\mid z \mid e^{i\phi(z)}$

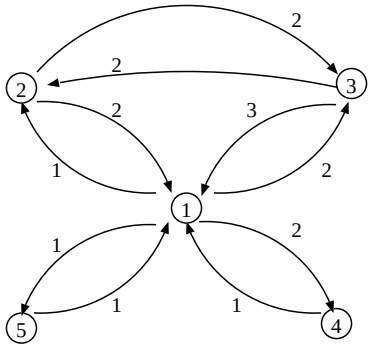

Figure 4.7: Perturbed star graph corresponding to Eq.(4.15)

Now consider a symmetric perturbation of the form given in Fig.(4.7) with the respective matrix A_{S5p} in Eq.(4.15).

$$A_{S5p} = \begin{pmatrix} 0 & 1+2i & 2+3i & 2+i & 1+i \\ 2+i & 0 & 2+2i & 0 & 0 \\ 3+2i & 2+2i & 0 & 0 & 0 \\ 1+2i & 0 & 0 & 0 & 0 \\ 1+i & 0 & 0 & 0 & 0 \end{pmatrix} \tag{4.15}$$

which after rotation becomes the Hermitian matrix H_{S5p} in Eq.(4.16):

$$A^{rot}_{S5p} = H_{S5p} = \begin{pmatrix} 0 & 2.1+0.7i & 3.5+0.7i & 2.1-0.7i & 1.4 \\ 2.1-0.7i & 0 & 2.8 & 0 & 0 \\ 3.5-0.7i & 2.8 & 0 & 0 & 0 \\ 2.1+0.7i & 0 & 0 & 0 & 0 \\ 1.4 & 0 & 0 & 0 & 0 \end{pmatrix} \tag{4.16}$$

λ_k	λ_1	λ_2	λ_3	λ_4	λ_5
	6.2	-4.5	-2.5	0.79	0
$\mathbf{x}_{k,1}$	0.61	0.70	-0.26-0.01i	0.23-0.08i	0
$\mathbf{x}_{k,2}$	0.46-0.13i	0.03+0.07i	0.78	-0.34+0.21i	0
$\mathbf{x}_{k,3}$	0.56-0.13i	-0.57+0.07i	-0.50-0.06i	-0.25+0.17i	0
$\mathbf{x}_{k,4}$	0.21+0.07i	-0.33-0.11i	0.22+0.08i	0.70	-0.51-0.17i
$\mathbf{x}_{k,5}$	0.14	-0.22	0.15	0.42-0.14i	0.85

Table 4.10: Eigensystem for H_{S5p} in Eq.(4.16) with $z = a + ib$

λ_k	λ_1		λ_2		λ_3		λ_4		λ_5	
	6.2		-4.5		-2.5		0.79		0	
	$\mid z \mid$	$\phi(z)$	$\mid z \mid$	$\phi(z)$	$\mid z \mid$	$\phi(z)$	$\mid z \mid$	$\phi(z)$	$\mid z \mid$	$\phi(z)$
	0.61	0	0.70	0	0.27	-3.10	0.25	-0.32	0	undef
	0.48	-0.27	0.073	1.19	0.78	0	0.40	2.60	0	undef
$\mathbf{x}$	0.57	-0.22	0.58	3.02	0.50	-3.03	0.31	2.54	0	undef
	0.22	0.32	0.35	-2.82	0.23	0.37	0.70	0	0.53	-2.82
	0.14	0	0.22	π	0.15	0.04	0.44	-0.32	0.85	0

Table 4.11: Eigensystem for H_{S5p} in Eq.(4.16) with $z = \mid z \mid e^{i\phi(z)}$

The eigensystem belonging to matrix H_{S5p} has the form shown in Tabs.(4.10, 4.11).

As can be seen when comparing Tab.(4.9) and Tab.(4.11) the anchors of the first two eigenspaces did not change, while in the rest of the subspaces the anchors changed. The perturbation thus had effects not in the overall communication pattern, but in the corrective patterns. In Tab.(4.12) the covered variance is shown. As can be seen the first two eigenvalues explain already $\sim 90\%$ of the total variance.

	λ_1	λ_2	λ_3	λ_4	λ_5
covered variance per eigenvalue	0.59	0.31	0.1	0.01	0
cumulative covered variance	0.59	0.89	0.99	1.00	1.00

Table 4.12: Cumulative covered variance of eigenvalues from Tab.(4.6)

The projectors derived from the eigensystem in Tab.(4.10) are given in Eqs.(4.17) - (4.20).

$$P_1^{S5p} = \begin{pmatrix} 0.38 & 0.28+0.08i & 0.34+0.08i & 0.13-0.04i & 0.08 \\ 0.28-0.08i & 0.23 & 0.27-0.01i & 0.09-0.06i & 0.06-0.02i \\ 0.34-0.08i & 0.27+0.01i & 0.33 & 0.12-0.06i & 0.08-0.02i \\ 0.13+0.04i & 0.09+0.06i & 0.12+0.06i & 0.05 & 0.03+0.01i \\ 0.08 & 0.06+0.02i & 0.08+0.02i & 0.03-0.01i & 0.02 \end{pmatrix} \tag{4.17}$$

$$P_2^{S5p} = \begin{pmatrix} 0.49 & 0.02-0.05i & -0.40-0.05i & -0.23+0.08i & -0.16 \\ 0.02+0.05i & 0 & -0.01-0.04i & -0.02-0.02i & -0.01-0.01i \\ -0.40+0.05i & -0.011+0.041i & 0.33 & 0.18-0.09i & 0.13-0.01i \\ -0.23-0.08i & -0.017+0.019i & 0.18+0.09i & 0.12 & 0.07+0.02i \\ -0.16 & -0.01+0.01i & 0.12+0.01i & 0.07-0.02i & 0.05 \end{pmatrix} \tag{4.18}$$

$$P_3^{S5p} = \begin{pmatrix} 0.07 & -0.21-0.01i & 0.13-0.01i & -0.06+0.02i & -0.04 \\ -0.21+0.01i & 0.60 & -0.39+0.04i & 0.17-0.07i & 0.11 \\ 0.13+0.01i & -0.39-0.04i & 0.25 & -0.11+0.03i & -0.07 \\ -0.06-0.02i & 0.17+0.07i & -0.11-0.03i & 0.05 & 0.03+0.01i \\ -0.04 & 0.11 & -0.07 & 0.03-0.01i & 0.02 \end{pmatrix} \tag{4.19}$$

$$P_4^{S5p} = \begin{pmatrix} 0.06 & -0.1-0.02i & -0.07-0.02i & 0.16-0.05i & 0.11 \\ -0.1+0.02i & 0.16 & 0.12+0.01i & -0.24+0.14i & -0.17+0.04i \\ -0.07+0.02i & 0.12-0.01i & 0.1 & -0.18+0.12i & -0.13+0.04i \\ 0.16+0.05i & -0.24-0.14i & -0.18-0.12i & 0.49 & 0.29+0.10i \\ 0.11 & -0.17-0.04i & -0.13-0.04i & 0.29-0.10i & 0.20 \end{pmatrix} \tag{4.20}$$

P_5^{S5p} does not contribute and has been omitted.

The interpretation of the projectors is similar to the interpretation of the projectors for the non-directional star. The star can still be seen, but the effects of the asymmetric bilateral communication and the perturbation are superimposed. Again it can be seen, that P_2^{S5p} is the representative of the star, while in P_1^{S5p} the communication pattern seems to point towards a more equally distributed form. This again has the effect that when both subspaces are weighted and added, the second subspace will enhance the star like pattern.

As predicted by Eq.(3.68) the eigenvalues of matrix H_{S5} is now disturbed. In this intuitive example the consequence of the perturbation can be seen when we view H_{S5p} as the sum of the unperturbed matrix H_{S5} and the Hermitian perturbation matrix F_{S5} of the form

$$F_{S5} = \begin{pmatrix} 0 & 0 & 0 & 0 & 0 \\ 0 & 0 & 2+2i & 0 & 0 \\ 0 & 2+2i & 0 & 0 & 0 \\ 0 & 0 & 0 & 0 & 0 \\ 0 & 0 & 0 & 0 & 0 \end{pmatrix} \tag{4.21}$$

The eigenvalues of matrix F_{S5} after rotation are $\lambda_1^{(F_{S5})} = 2.8, \lambda_2^{(F_{S5})} = -2.8$. Thus the largest eigenvalue of $\lambda_1^{H_{S5p}} = 6.2$ of the perturbed matrix H_{S5p} should be inside the Weyl-type bounds following Eq.(3.68) given by $\lambda_1^{H_{S5}} + \lambda_1^{(F_{S5})} = 5.0 + 2.8 = 7.8 \geq 6.2 \geq 2.2 = 5.0 - 2.8 = \lambda_1^{H_{S5}} + \lambda_2^{(F_{S5})}$ and the smallest eigenvalue $\lambda_2^{H_{S5p}} = -4.5$ should be inside the bound given by $\lambda_2^{H_{S5}} + +\lambda_1^{(F_{S5})} = -5 + 2.8 = -2.2 \geq -4.5 \geq -5 - 2.8 = -7.8 = \lambda_2^{H_{S5}} + +\lambda_2^{(F_{S5})}$. Tab.(4.10) confirms this.

As can be seen, the eigenvalues rise in absolute amount, due to the fact that more traffic volume has occurred within the group. This corresponds to the fact that the norm of the matrix H_{S5p} is greater than the norm of H_{S5}. Since the norm of a Hermitian matrix by Eq.(3.42) defines the spectral radius this means an increase in the largest eigenvalue of H_{S5p}.

Note, that due to the perturbation the symmetry of the eigenvalues in Tab.(4.8) is destroyed. In addition the perturbation leads to a break in symmetry between the eigenvectors. The eigenvector components affected by the perturbation do no longer show the regular phase shift of π anymore. For members with ID 2 and 3 this is visible in Tab.(4.11). However, a perturbed star graph can still be recognized by the fact that there still exists an anchor, which can be identified by the highest absolute value eigenvector component in two eigenvectors at the *same* ID position.

Matrix A_{λ_1} in Eq.(4.22) represents the product $\lambda_1 P_1^{S5p}$. By adding, according to the Fourier sum the product $\lambda_2 P_2^{S5p}$ we get matrix $A_{\sum_{k=1}^{2} \lambda_k P_k}$ in Eq.((4.23).

The remaining partial sum $C_{\sum_{k=3}^{5}\lambda_k P_k}$ only covers about 1% of the variance.

$$A_{\lambda_1} = \begin{pmatrix} 2.31 & 1.74+0.49i & 2.12+0.49i & 0.79-0.26i & 0.53 \\ 1.74-0.49i & 1.42 & 1.70-0.08i & 0.54-0.37i & 0.40-0.11i \\ 2.12-0.49i & 1.70-0.08i & 2.05 & 0.67-0.41i & 0.49-0.11i \\ 0.79+0.26i & 0.54+0.37i & 0.67+0.41i & 0.30 & 0.18+0.06i \\ 0.53 & 0.40+0.11i & 0.49+0.11i & 0.18-0.06i & 0.12 \end{pmatrix} \tag{4.22}$$

$$A_{\sum_{k=1}^{2}\lambda_k} = \begin{pmatrix} 0.1 & 1.7+0.7i & 3.9+0.7i & 1.8-0.6i & 1.2 \\ 1.7-0.7i & 1.4 & 1.7-0.1i & 0.6-0.3i & 0.4 \\ 3.9-0.7i & 1.7-0.1i & 0.6 & -0.1 & -0.1 \\ 1.8+0.6i & 0.6+0.3i & -0.1 & -0.2 & -0.1 \\ 1.2 & 0.4 & -0.1 & -0.1 & -0.1 \end{pmatrix} \tag{4.23}$$

If we now rotate this matrix back by $e^{i\frac{\pi}{4}}$, the matrix $A^{brot}_{\sum_{k=1}^{2}\lambda_k P_k}$ in Eq.(4.24) already looks quite like the original matrix A_2 apart from the entries a_{22}, a_{24}, a_{42}. This matrix could also be written as the original matrix A_{S5} plus the original perturbation matrix F_{S5} plus a matrix C in Eq.(4.25) with the remaining non-zero entries. This C is the back rotated partial sum $C_{\sum_{k=3}^{5}\lambda_k P_k}$.

$$A^{brot}_{\sum_{k=1}^{2}\lambda_k P_k} = \begin{pmatrix} 0 & 1+2i & 2+3i & 2+1i & 1+1i \\ 2+1i & 1+1i & 1+1i & 1 & 0 \\ 3+2i & 1+1i & 0 & 0 & 0 \\ 1+2i & 0+1i & 0 & 0 & 0 \\ 1+1i & 0 & 0 & 0 & 0 \end{pmatrix} \tag{4.24}$$

$$C = \begin{pmatrix} 0 & 0 & 0 & 0 & 0 \\ 0 & -1-1i & 1+1i & -1 & 0 \\ 0 & 1+1i & 0 & 0 & 0 \\ 0 & -1i & 0 & 0 & 0 \\ 0 & 0 & 0 & 0 & 0 \end{pmatrix} \tag{4.25}$$

As a conclusion it can be stated that a star graph like structure can be identified if the eigensystem has the following characteristics:

- Two eigenvalues with different sign, but relatively equal or equal absolute value (in comparison to the other eigenvalues): $\mid \lambda_k \mid \approx \mid \lambda_l \mid, \quad k, l = 1, \ldots, n$ and $k \neq l$.

- The eigenvectors to the above mentioned eigenvalues feature the same anchor: $argmax_j \mid x_{k,j} \mid = argmax_m \mid x_{l,m} \mid$ with $j = m$.
- The distribution of absolute values of eigenvector components shows one high absolute value and the rest is relatively lower. In the case of a clear star, all other absolute values are the same.

If the star is clearly identifiable, it can even be ventured to construct an unperturbed matrix and check for the perturbation, otherwise the alternative way using the Fourier sum as a filter tool should be investigated.

4.4.2 Complete Graph

The spectral behavior of a non-directional complete graph as in Fig.(4.8) and represented by matrix M_{C4} in Eq.(4.26) and its corresponding Hermitian matrix $M_{C4}^{rot} = H_{C4}$ in Eq.(4.27) is characterized by the fact that only one eigenvalue $max_k \mid \lambda_k \mid = \pm\lambda_1$ exists, while all others will be of the same absolute value $\lambda_k < \lambda_1, k \neq 1$. Since the sum of all eigenvalues has to be 0 as explained in section 3.3.4 they also have the opposite sign of the strongest eigenvalue. In addition all eigenvector components of the first eigenvector will have equal absolute value. This holds also when using complex Hermitian matrices (see eigensystem in Tab.(4.13).

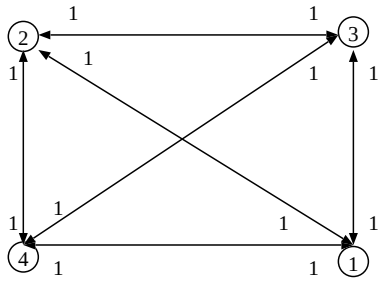

Figure 4.8: Complete symmetric bidirectional graph corresponding to Eq.(4.26)

$$M_{C4} = \begin{pmatrix} 0 & 1+1i & 1+1i & 1+1i \\ 1+1i & 0 & 1+1i & 1+1i \\ 1+1i & 1+1i & 0 & 1+1i \\ 1+1i & 1+1i & 1+1i & 0 \end{pmatrix} \tag{4.26}$$

$$M_{C4}^{rot} = H_{C4} = \begin{pmatrix} 0 & 1.41 & 1.41 & 1.41 \\ 1.41 & 0 & 1.41 & 1.41 \\ 1.41 & 1.41 & 0 & 1.41 \\ 1.41 & 1.41 & 1.41 & 0 \end{pmatrix} \tag{4.27}$$

k	λ_k	$\mathbf{x}_{k,l}$			
		$l=1$	$l=2$	$l=3$	$l=4$
1	1.	0.5	0.5	0.5	0.5
2	-0.33	-0.09	-0.53	-0.20	0.82
3	-0.33	0.04	-0.54	0.79	-0.29
4	-0.33	0.87	-0.29	-0.29	-0.29

Table 4.13: Eigensystem of H_{C4} in Eq.(4.27)

This eigensystem for all eigenvalues and the eigenvector corresponding to the largest eigenvalue correspond to Cvetkovic et al. [CS97, p.235].

Now consider an asymmetric complete graph as in Fig.(4.9). The complex adjacency matrix is given in Eq.(4.28) and the rotated Hermitian matrix $M^{rot}_{C4a} = H_{C4a}$ in Eq.(4.29).

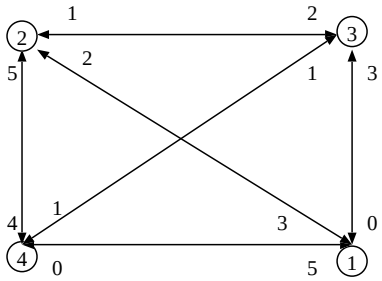

Figure 4.9: Complete directional complex graph

$$M_{C4a} = \begin{pmatrix} 0 & 2+3i & 3 & 5i \\ 3+2i & 0 & 2+1i & 4+5i \\ 3i & 1+2i & 0 & 1+1i \\ 5 & 5+4i & 1+1i & 0 \end{pmatrix} \tag{4.28}$$

$$M^{rot}_{C4a} = H_{C4a} = \begin{pmatrix} 0 & 3.5+0.7i & 2.1-2.1i & 3.5+3.5i \\ 3.5-0.7i & 0 & 2.1-0.7ii & 6.3+0.7i \\ 2.1+2.1i & 2.1+0.7i & 0 & 1.4 \\ 3.5-3.5i & 6.3-0.7i & 1.4 & 0 \end{pmatrix} \tag{4.29}$$

The eigensystem of this graph is given in Tabs.(4.14) and (4.15)

Again the effect of bidirectional asymmetric communication is visible. The eigenvalues loose their strict behavior as do the eigenvectors.

As a conclusion it can be stated that a complete structure can be identified if the eigensystem has the following characteristics:

k	λ_k	$\mathbf{x}_{k,l}$			
		$l=1$	$l=2$	$l=3$	$l=4$
1	1.0	0.44+0.26i	0.55+0.12i	0.21+0.19i	0.58
2	-0.67	-0.12-0.39i	-0.53+0.05i	-0.06+0.19i	0.72
3	-0.37	0.64	-0.36+0.47i	-0.04-0.48i	-0.06-0.08i
4	0.05	-0.06-0.40i	0.04+0.22i	0.80	-0.15+0.34i

Table 4.14: Eigensystem of matrix H_{C4a} in Eq.(4.29)

λ_k	λ_1		λ_2		λ_3		λ_4	
	1.0		-0.67		-0.37		0.05	
	$\mid z \mid$	$\phi(z)$	$\mid z \mid$	$\phi(z)$	$\mid z \mid$	$\phi(z)$	$\mid z \mid$	$\phi(z)$
$\mathbf{x}_{k,1}$	0.51	0.53	0.41	-1.9	0.64	0	0.40	-1.7
$\mathbf{x}_{k,2}$	0.56	0.21	0.53	3.1	0.59	2.2	0.23	1.4
$\mathbf{x}_{k,3}$	0.29	0.75	0.20	1.9	0.48	-1.7	0.80	0
$\mathbf{x}_{k,4}$	0.58	0	0.72	0	0.1	-2.3	0.37	2.0

Table 4.15: Eigensystem for H_{S5p} in Eq.(4.16) with $z = \mid z \mid e^{i\phi(z)}$

- There is only one eigenvalue of relative high absolute value, while all others have the same or almost the same absolute value and are smaller than the largest eigenvalue: $\exists \mid \lambda_{max} \mid >> \mid \lambda_k \mid \quad \forall k \neq max$ and $|\lambda_{max}| = \sum_{max \neq k;k=1}^{n} |\lambda_k|$
- The eigenvector corresponding to the largest eigenvalue shows a distribution of absolute values of eigenvector components that is equally distributed or close to that. All members are of relative equal importance, which is intuitive.

4.4.3 Two subgroups connected by one link

An interesting example that gives more insight into the interpretation of the sign of the eigenvalues can be constructed as follows. Consider a network with two subgroups such that the one subgroup is a star structure while the other is a complete graph. These two subgroups share a link. (see Fig.(4.10)).
The matrix T for this graph is given in Eq.(4.30). The structure of the two subgroups is evident in the matrix T. The eigensystem of the rotated matrix is given in Tab.(4.16). The fact that the second and third eigenvalue share the same anchor points to the fact that a second interpretable characteristic can be seen. The eigenvectors give this interpretation. The subspace corresponding to the negative eigenvalue $\lambda_2 = -0.68$ gives the pattern for the connections in the complete

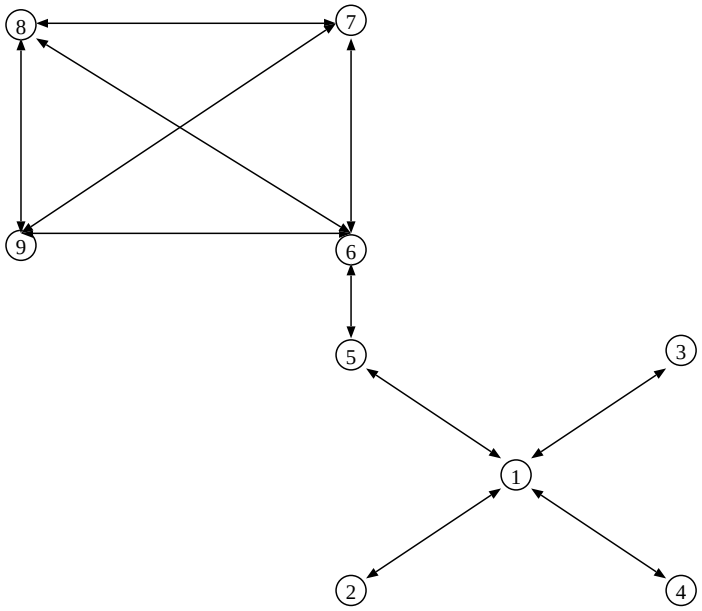

Figure 4.10: A network consisting of two subgroups and symmetric bilateral communication

group, while the subspace corresponding to the positive eigenvalue $\lambda_3 = 0.64$ shows that the two subgroups break apart if vertex 6 is removed.

$$T = \begin{pmatrix} 0 & 1+1i & 1+1i & 1+1i & 1+1i & 0 & 0 & 0 & 0 \\ 1+1i & 0 & 0 & 0 & 0 & 0 & 0 & 0 & 0 \\ 1+1i & 0 & 0 & 0 & 0 & 0 & 0 & 0 & 0 \\ 1+1i & 0 & 0 & 0 & 0 & 0 & 0 & 0 & 0 \\ 1+1i & 0 & 0 & 0 & 0 & 1+1i & 0 & 0 & 0 \\ 0 & 0 & 0 & 0 & 1+1i & 0 & 1+1i & 1+1i & 1+1i \\ 0 & 0 & 0 & 0 & 0 & 1+1i & 0 & 1+1i & 1+1i \\ 0 & 0 & 0 & 0 & 0 & 1+1i & 1+1i & 0 & 1+1i \\ 0 & 0 & 0 & 0 & 0 & 1+1i & 1+1i & 1+1i & 0 \end{pmatrix} \tag{4.30}$$

This behavior also holds for arbitrary matrices of this kind. This follows the observations of Barnett et al. [BR85].

4.5 Conclusion

It can thus be seen from these examples, that the eigensystem of a complex Hermitian adjacency matrix holds all the information, that the real adjacency matrix

k	λ_k	$\mathbf{x}_{k,l}$								
		$l=1$	$l=2$	$l=3$	$l=4$	$l=5$	$l=6$	$l=7$	$l=8$	$l=9$
1	1	0.09	0.03	0.03	0.03	0.2	0.52	0.47	0.47	0.47
2	-0.68	0.64	-0.3	-0.3	-0.3	-0.45	0.32	-0.08	-0.08	-0.08
3	0.64	0.69	0.35	0.35	0.35	0.35	0	-0.12	-0.12	-0.12
4	-0.43	-0.32	0.24	0.24	0.24	-0.3	0.71	-0.21	-0.21	-0.21
5	-0.32	0	0	0	0	0	0	0.76	-0.12	-0.64
6	-0.32	0	0	0	0	0	0	-0.34	0.81	-0.48
7	0.11	-0.09	-0.26	-0.26	-0.26	0.74	0.34	-0.21	-0.21	-0.21
8	0	0	0.72	-0.04	-0.69	0	0	0	0	0
9	0	0	-0.51	0.81	-0.29	0	0	0	0	0

Table 4.16: Eigensystem of the rotated matrix T in Eq.(4.30)

carried and in addition does also provide information of the direction of communication. Informations that can be gained from this analysis are:

- The pattern structure of bidirectional asymmetric communication, which can be represented as a Fourier sum.
- Structural similarity that is represented in the projectors as in real adjacency matrices and directional similarity from the phase information available in complex numbers.
- Pattern homogeneity that is expressed in the eigenvectors corresponding to positive and negative eigenvalues.
- Perturbation theory can be used to explain eigensystem behavior.

The method of eigensystem analysis of complex Hermitian adjacency matrices can thus broaden the set of information that can be gained. The fact that this analysis is performed in Hilbert space is a more general approach then the ones available at the moment. The use of complex numbers allow for the use of bidirectional data without information loss.

Chapter 5

Data sets

In this chapter the data sets used in this work will be shortly described and their characteristics will be introduced. Two well known data sets will be used.

1. The EIES full data set as described in Freeman [FF79]

2. The EIES subset as described in Freeman [Fre97]

These data sets are being used, so that the differences and similarities between the method proposed in chapter 4 and the standard methods become clearly visible. The complete EIES data set is used to show how communication patterns are detected, the subset is used to show how the method yields results that are different from those returned by the standard methods but not implausible.

5.1 EIES data set

This data set is based on research done by L. and S. Freeman in the late 1970s [FF79]. It is thoroughly discussed in [WF94]. It describes the communication behavior of a set of researchers who used an electronic information exchange system (EIES). This research focused on the way CMC influenced the communication behavior within a group of researchers who are geographically apart and share the same interest into a newly developing research field.

This data set gives the opportunity to see that different communication patterns exist in one group with respect to direction, even if the group is not huge. Tab.(5.1) represents the weighted adjacency matrix. In this data set messages from one member to one other member as well as from one member to all other members have been included [Fre04]. For the purposes of this book the entries on the diagonal were set to $g_{kk} = 0$.

	1	2	3	4	5	6	7	8	9	10	11	12	13	14	15	16	17	18	19	20	21	22	23	24	25	26	27	28	29	30	31	32
1	0	488	28	65	20	65	45	346	82	52	177	28	24	49	81	77	77	73	33	31	22	46	31	128	38	89	95	25	388	71	212	185
2	364	0	17	17	15	0	30	20	35	20	22	15	15	15	15	50	25	8	0	15	15	15	15	0	15	15	10	24	89	23	163	39
3	4	5	0	0	0	0	0	5	0	0	0	0	0	0	0	0	0	0	0	0	0	0	0	0	0	0	0	0	0	0	0	0
4	52	30	0	0	0	2	0	32	21	34	9	0	0	0	0	5	4	2	35	0	0	0	0	12	0	0	12	5	20	4	19	33
5	26	4	4	4	0	4	8	4	4	4	4	4	4	4	4	4	4	4	4	0	4	8	4	14	4	0	4	0	4	7	4	4
6	72	23	0	2	0	0	0	16	0	7	15	0	0	0	8	7	6	0	0	0	0	0	0	14	0	0	7	3	34	3	22	0
7	14	0	0	0	0	0	0	0	0	0	0	0	0	0	0	0	0	0	0	0	0	0	0	0	0	0	0	0	0	0	6	0
8	239	82	5	37	3	34	5	0	12	18	164	18	0	0	0	30	53	27	20	4	0	5	4	55	0	9	34	0	146	216	88	288
9	24	25	0	2	0	0	0	8	0	0	15	0	10	0	0	0	5	0	0	0	0	0	0	0	0	0	15	0	10	0	30	44
10	43	15	0	32	0	12	0	14	0	0	25	2	0	0	0	10	10	0	20	15	0	5	20	29	0	4	10	0	47	6	22	19
11	178	36	0	11	0	19	10	172	39	28	0	0	4	0	0	23	15	24	0	0	8	0	0	29	10	11	22	0	46	0	119	34
12	0	5	0	0	0	0	0	5	0	0	0	0	0	0	0	0	0	0	5	0	0	0	0	0	0	0	0	0	53	0	5	9
13	5	0	0	0	0	0	0	0	0	0	5	0	0	0	0	0	0	0	0	0	0	0	0	0	0	0	0	0	0	0	5	0
14	12	0	9	0	0	0	0	0	0	0	0	0	0	0	0	12	0	0	5	0	0	0	0	0	0	0	0	0	35	0	8	0
15	120	0	0	0	0	4	0	0	0	0	0	5	0	0	0	0	0	0	0	0	0	0	0	0	0	0	8	0	58	0	32	0
16	58	25	0	10	0	0	0	20	0	5	10	0	0	5	0	0	10	0	0	0	5	0	0	5	0	0	0	0	35	0	10	0
17	63	18	9	7	0	6	0	36	0	5	9	5	0	5	0	5	0	0	0	5	2	0	0	0	0	0	15	0	10	9	15	9
18	58	8	5	4	0	0	0	4	0	5	18	0	0	0	0	0	0	0	0	0	0	0	0	0	0	0	20	0	8	10	48	0
19	5	5	0	25	0	0	0	10	0	0	0	0	0	5	0	0	0	0	0	0	0	0	5	0	0	0	0	0	0	0	10	0
20	0	0	0	0	0	0	0	0	0	0	0	0	0	0	0	0	0	0	0	0	4	0	0	0	0	0	0	0	4	0	0	0
21	9	0	0	0	0	0	0	0	0	0	3	0	0	0	0	5	0	0	0	0	0	0	0	0	0	0	0	0	5	0	0	0
22	10	0	0	0	0	0	0	0	0	0	0	0	0	0	0	0	0	0	0	0	0	0	0	40	0	0	0	0	15	0	0	5
23	5	5	5	0	0	0	0	0	0	19	0	0	0	0	0	0	0	0	5	0	0	0	0	0	0	0	0	0	14	0	5	0
24	89	17	4	14	14	18	8	41	4	19	31	4	4	9	4	14	4	9	4	4	4	58	4	0	18	14	9	4	156	4	56	10
25	32	5	0	0	0	0	0	0	0	0	0	0	0	15	0	0	0	0	0	0	0	10	0	23	0	0	0	0	0	9	15	0
26	35	5	0	0	0	0	0	0	0	5	0	0	0	0	0	0	0	0	0	0	0	0	0	0	0	0	0	0	10	0	13	0
27	50	28	0	13	0	0	0	19	29	5	8	0	33	0	4	0	10	15	0	0	0	0	0	10	0	0	0	3	32	0	13	33
28	9	6	0	0	0	3	0	0	0	0	0	0	0	0	0	0	0	0	0	0	0	0	0	0	0	0	0	0	0	0	0	6
29	559	132	5	24	21	29	0	155	15	98	69	89	37	76	80	63	15	4	9	18	43	108	29	218	0	15	66	0	0	14	91	126
30	39	21	0	6	3	3	0	140	0	7	0	2	0	0	0	0	9	5	0	0	0	0	0	0	0	0	2	0	18	0	20	8
31	82	125	10	22	10	15	18	70	35	23	114	20	16	15	24	30	28	49	30	5	5	15	8	53	25	8	21	8	65	28	0	67
32	239	99	0	27	3	0	0	268	101	18	35	4	0	0	0	0	7	0	0	0	0	14	0	5	0	0	50	6	71	7	107	0

Table 5.1: Full EIES data set

The plots of in- and out-degree as defined in section 3.2.1 can be seen in Fig.(5.1) and Fig.(5.3). The corresponding plots of strength as given in section 3.2.1 is shown in Fig.(5.2) and Fig.(5.4). These figures show that while the degree distribution does not drop dramatically after the highest degree value, the strength drops sharply. This can be explained by the fact that the member with ID 1, who actually is Linton Freeman, was the system administrator in this experiment. Thus he had to write many messages to all other members [Fre04].

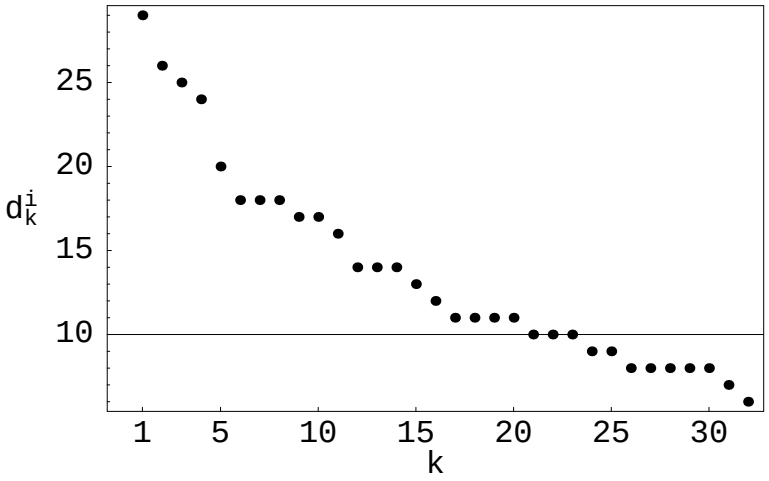

Figure 5.1: EIES: In-degree sorted by amount

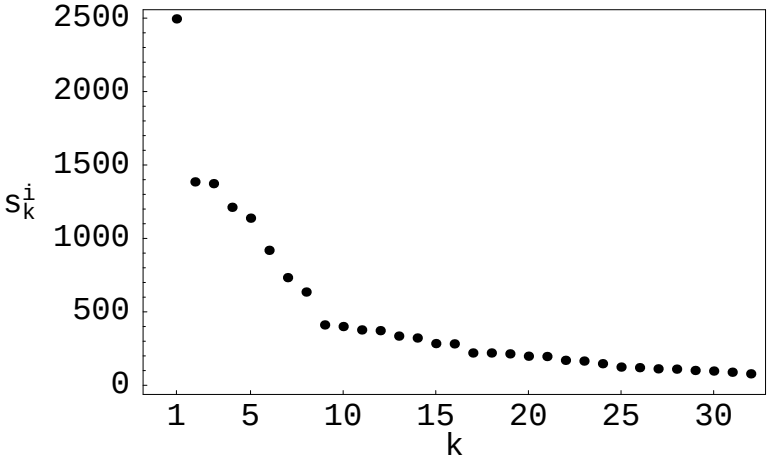

Figure 5.2: EIES: Inbound normalized strength sorted by amount

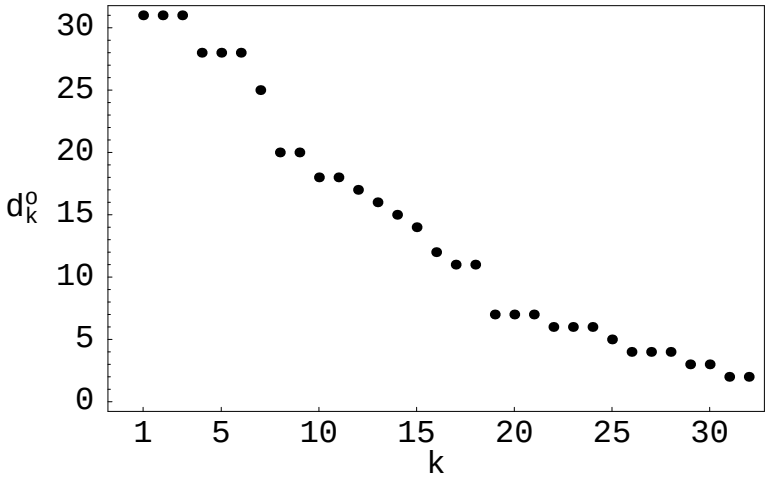

Figure 5.3: EIES: Out-degree sorted by amount

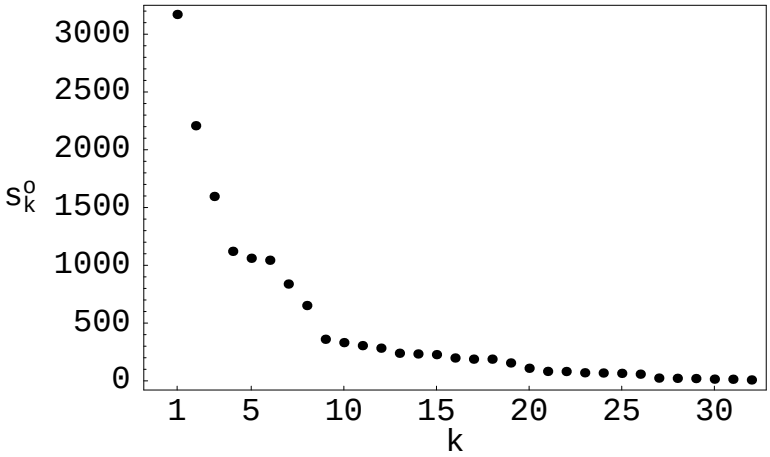

Figure 5.4: EIES: Outbound normalized strength sorted by amount

The standard indices for this data set are:

- Number of authors: 32
- Number of messages: 15034
- Inbound strength distribution : As can be seen in Fig.(5.2) one author (ID 1) clearly has the highest inbound strength as defined in Eq.(3.10). Most of the other members have a strength of below 500. Only 7 authors have a strength in the range of 500 to 1500.
- Outbound strength distribution: As can be seen in Fig.(5.4) the author with ID 1 again clearly stands apart. Most of the other members have a degree of below 500. 5 authors have a strength in the range of 500 to 1200. and 2 authors are in the range of 1500 to 2500.
- Outbound strength/ inbound strength: Tab.(5.2) gives the outbound strength and inbound strength indices normalized with the total amount of messages.
- Centrality: Following Eq.(3.2) is given in Fig.(5.3). In Tab.(5.2) this is also given in comparison to the strength.
- Prestige: Following Eq.(3.9) is given in Fig.(5.1). In Tab.(5.2) this is also given in comparison to the strength.
- Eigenvector centrality calculated as in Freeman [FF79] see Tabs.(7.6), (7.7), (7.8) and (7.9) in the appendix: As can be seen, the eigenvalues come in pairs, thus the two corresponding eigenspaces are used to evaluate the hierarchical structure.

AuthorID	Outbound strength	Inbound strength	Centrality	Prestige
1	0.21	0.17	0.032	0.030
2	0.075	0.081	0.029	0.025
3	0.00093	0.0067	0.003	0.011
4	0.022	0.021	0.019	0.019
5	0.010	0.0059	0.029	0.008
6	0.016	0.014	0.016	0.013
7	0.0013	0.0082	0.001	0.007
8	0.11	0.092	0.026	0.021
9	0.013	0.025	0.011	0.011
10	0.024	0.025	0.021	0.019
11	0.056	0.049	0.021	0.019
12	0.0055	0.013	0.006	0.012
13	0.00100	0.0098	0.003	0.009
14	0.0054	0.013	0.006	0.010
15	0.015	0.015	0.006	0.008
16	0.013	0.022	0.012	0.015
17	0.015	0.019	0.018	0.017
18	0.013	0.015	0.011	0.011
19	0.0043	0.011	0.007	0.011
20	0.00053	0.0065	0.002	0.008
21	0.0015	0.0074	0.004	0.010
22	0.0047	0.019	0.004	0.010
23	0.0039	0.0080	0.007	0.009
24	0.043	0.042	0.032	0.013
25	0.0073	0.0073	0.007	0.006
26	0.0045	0.011	0.005	0.008
27	0.020	0.027	0.017	0.018
28	0.0016	0.0052	0.004	0.008
29	0.15	0.091	0.029	0.026
30	0.019	0.027	0.014	0.014
31	0.069	0.076	0.032	0.027
32	0.071	0.061	0.018	0.018

Table 5.2: Outbound, inbound strength, centrality and prestige of the EIES complete data set

5.2 Subset of EIES data set

The EIES subset is a seven member subset of the total EIES data set (Tab. 5.3, [Fre97]). These seven members are the most prominent in the group. The entries now represent the number of messages that went from one member to the other member [Fre04]. This subset, since it is smaller and thus more open to intuitive investigation, is used to give a comparison between the calculation done by Freeman and the results obtained with the method proposed in chapter 4 [HGS04].

Author	ID	Freeman 1	White 2	Alba 4	Bernard 8	Doreian 11	Mullins 24	Wellman 29
Freeman	1	0	115	17	93	53	33	84
White	2	84	0	4	5	5	0	15
Alba	4	16	10	0	15	3	3	4
Bernard	8	127	22	17	0	57	12	34
Doreian	11	57	9	4	57	0	8	10
Mullins	24	23	4	3	9	8	0	33
Wellman	29	118	24	5	35	15	45	0

Table 5.3: Number of messages exchanged between members in the EIES sub set

The standard indices for this data set are:

- Number of authors: 7
- Number of messages: 1295
- Outbound and inbound strength, centrality and prestige: See Tab.(5.4).
- The most central and prestigious member is Freeman, followed by Bernard (see Tab.(5.4)).
- Eigenvector centrality: Calculated with the dichotomization and subsequent symmetrization see Tab.(5.5). The most central member due to the eigensystem is Wellman. This is only understandable when the preprocessing is taken into account.

In Fig.(5.5) the in-degree is given by author ID. It can be seen that the graph is almost completely connected. This is supported by the out-degree distribution in Fig.(5.7).

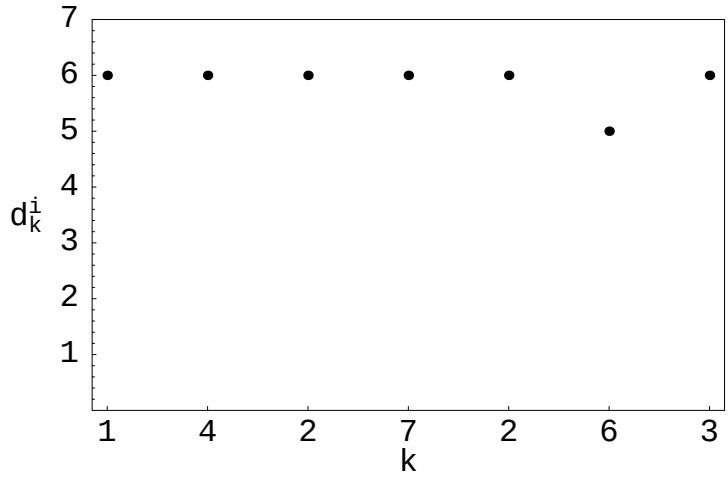

Figure 5.5: EIES subset: In-degree; k: author ID

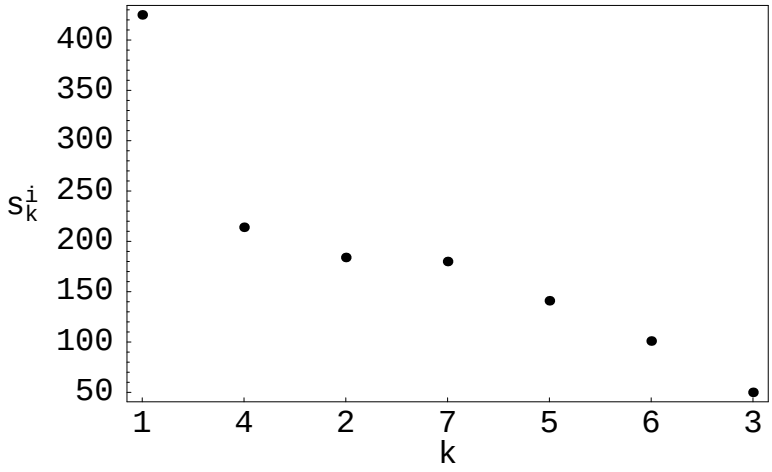

Figure 5.6: EIES subset: Inbound normalized strength sorted by amount; k: author ID

The strength of inbound and outbound traffic in the subset is given in Fig.(5.6) and Fig.(5.8). Clearly now the author with ID 1 (Freeman) is the most active and author with ID 4 (Bernard) comes second, but very close to all others.

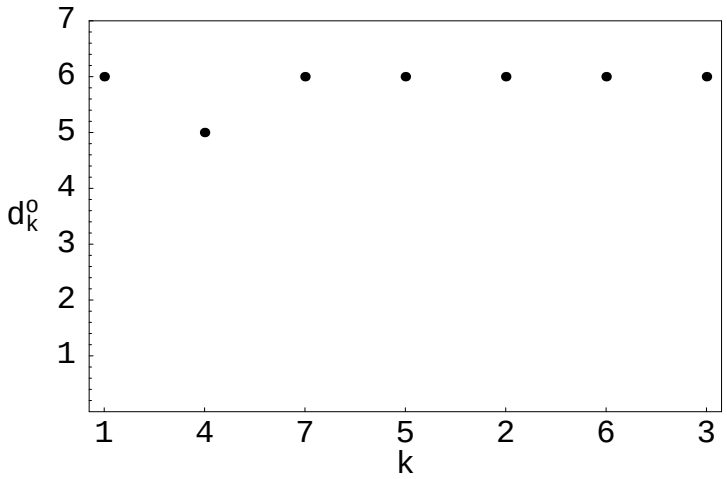

Figure 5.7: EIES subset: Out-degree sorted by amount

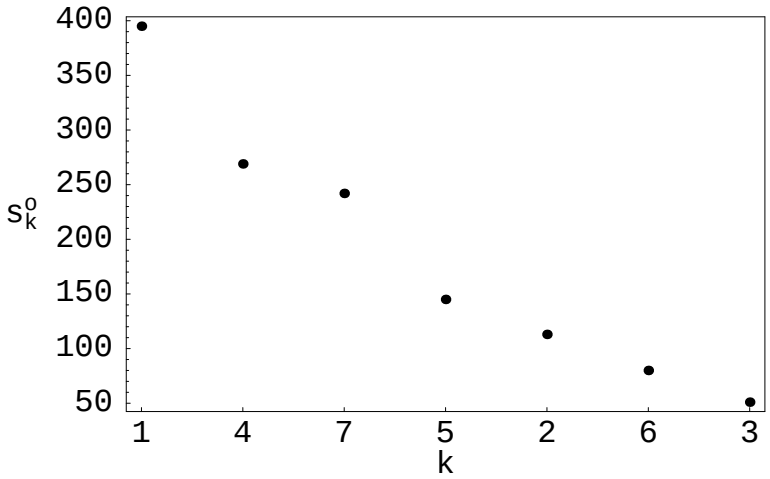

Figure 5.8: EIES subset: Outbound normalized strength sorted by amount

Author	ID	Outbound strength	Inbound strength	Centrality	Prestige
Freeman	1	0.31	0.33	0.24	0.24
White	2	0.087	0.14	0.20	0.24
Alba	4	0.039	0.039	0.24	0.24
Bernard	8	0.21	0.17	0.24	0.24
Doreian	11	0.11	0.11	0.24	0.24
Mullins	24	0.062	0.078	0.24	0.20
Wellman	29	0.19	0.14	0.24	0.24

Table 5.4: Outbound and inbound strength for the EIES subset normalized by the total number of messages, as well as centrality and prestige

These two data sets will be analyzed with the proposed method in chapter 6, and the results obtained will be compared with the standard results and an interpretation will be given.

Author/Eigenvalue	1.0	0.13	0.071	0.071	0.011	0	0
Freeman	0.40	0.25	0.20	0.61	0.47	0	0
White	0	0	0	0	0	0	1.0
Alba	0.16	0.48	-0.47	-0.38	-0.15	0.71	0
Bernard	0.51	0.064	0.47	0.38	-0.71	0	0
Doreian	0.40	0.25	0.27	-0.22	0.47	0	0
Mullins	0.16	0.48	-0.47	-0.38	-0.15	-0.71	0
Wellman	0.60	-0.65	-0.47	-0.38	0.061	0	0

Table 5.5: Eigensystem of the EIES subset as calculated with the method used by Freeman

Chapter 6

Results and Discussion

This chapter will present results obtained with the proposed method. To show the differences between the standard methods and the proposed method the very well described EIES data set of Freeman (see section 5.1) and the subset of that data set described in section 5.2 will be used.

For each data set the following results will be presented and discussed:

- Eigensystem
  - Full data set: 7.2 Tabs.(7.2),(7.3), (7.4) and (7.5)
  - Subset: see section 6.2.1
- Eigenvalue distribution
  - Full data set: see Fig.(6.2)
  - Subset: see Fig.(6.29)
- Cumulative variance covered by eigenvalues
  - Full data set: see Fig.(6.3)
  - Subset: see Fig.(6.30)
- Distribution of the absolute value and phase of eigenvector components
  - Full data set: see Figs.(6.4)-(6.14) and Figs.(6.5)-(6.15)
  - Subset: see Figs.(6.31)-(6.33) and Figs.(6.32)-(6.34)
- Eigenprojector density plots for relevant subspaces (real and imaginary part separately)
  - Full data set: Figs.(6.16)-(6.26) and Figs.(6.17)-(6.27)
  - Subset: Figs.(6.35)-(6.37) and Figs.(6.36)-(6.38)

6.1 EIES Data Set

6.1.1 Eigensystem of the EIES Data Set

The eigensystem of the complete EIES data set (see Tab.(5.1)) obtained with the method described in chapter 4 is given in the appendix in Tabs.(7.2),(7.3), (7.4) and (7.5) . Fig.(6.1) shows the eigenspectrum when sorted by value. For a clearer view of a possible symmetry Fig.(6.2) shows the distribution of the eigenvalues, where the positive eigenvalues with index j and the negative eigenvalues with index f are given. It suggests the broken symmetry of a star graph as discussed in chapter 3.

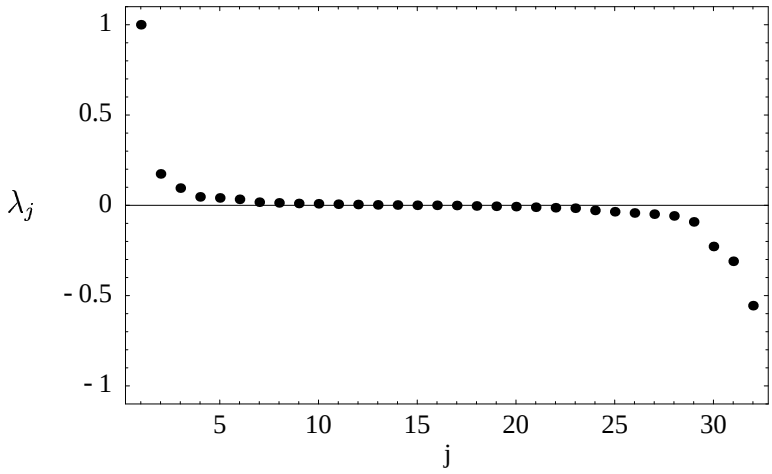

Figure 6.1: Eigenspectrum of the complete EIES data set sorted by value

In addition the first and thus largest eigenvalue covers already 66% of the variance of the data (see Tab.(6.1)). Together with the second eigenvalue they explain 86% of the variance. The first six eigenvalues cover about 98%. For a clearer representation of the cumulative variance see Fig.(6.3).

Thus, to understand the pattern structure with the most message volume it would be sufficient to look at the first two eigenspaces. For a broader view the first six eigenspaces are given and interpreted here. If more detail is necessary, the other subspaces can be taken into account.

As the distribution of the eigenvector components gives a hint about the structure within the pattern, first the distribution of the absolute value of components of the eigenvectors can be seen in Figs.(6.4), (6.6), (6.8), (6.12), (6.10), (6.14) with their respective phase distribution in Figs.(6.5), (6.7), (6.9), (6.13), (6.11), (6.15). The x-axis is denoted by l which is the running index within the eigenvector. This index is not equivalent to the author ID, since the values have been

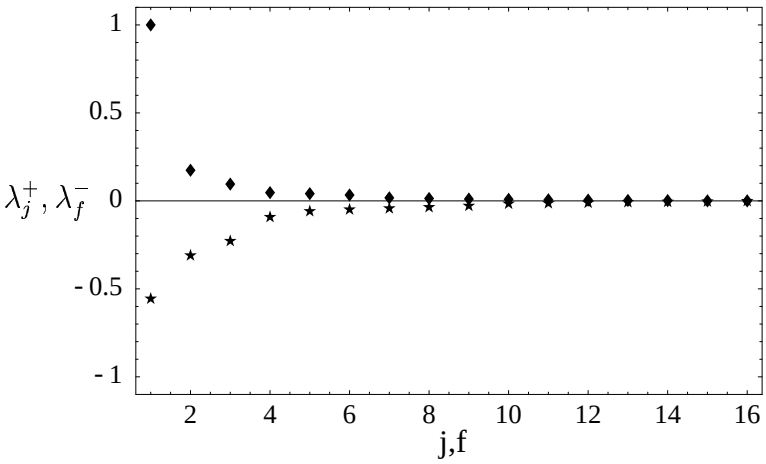

Figure 6.2: Eigenspectrum of the complete EIES data set sorted by absolute value

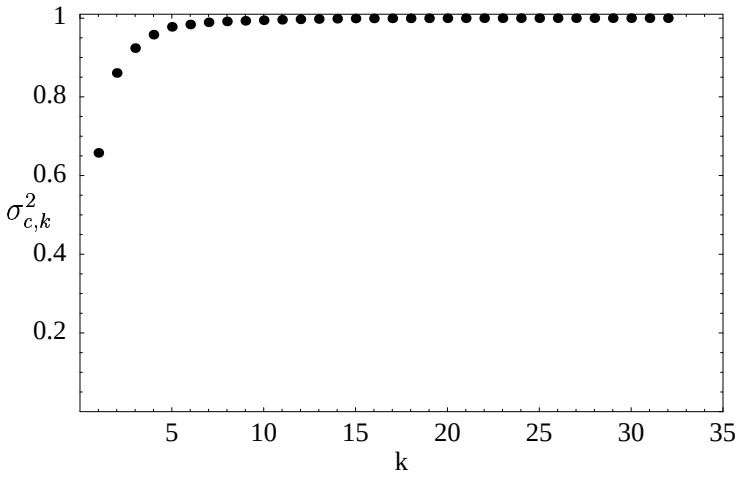

Figure 6.3: Cumulative covered variance by eigenvalues λ_k

k	Covered variance per λ_k	Cumulative covered variance
1	0.66	0.66
2	0.20	0.86
3	0.06	0.92
4	0.03	0.96
5	0.02	0.98
6	0.01	0.98
7-10	< 0.01	0.99
11-32	~ 0	1.0

Table 6.1: Cumulative covered variance of eigenvalues from Tabs.(7.2)-(7.5)

sorted by either absolute value or amount.

First suspace of EIES data set

Let us start with analyzing the subspace corresponding to λ_1 in more detail. As can be seen in Fig.(6.4) the distribution starts of rather low and already the second largest component only has an absolute value of about 0.4. From $k = 10 \ldots 22$ and again for the rest there is almost an equal distribution visible. This points towards a connected graph. The phase distribution, as given in Fig.(6.5), varies between 0 and $\frac{\pi}{4}$, which suggests, that the communication is mostly balanced.

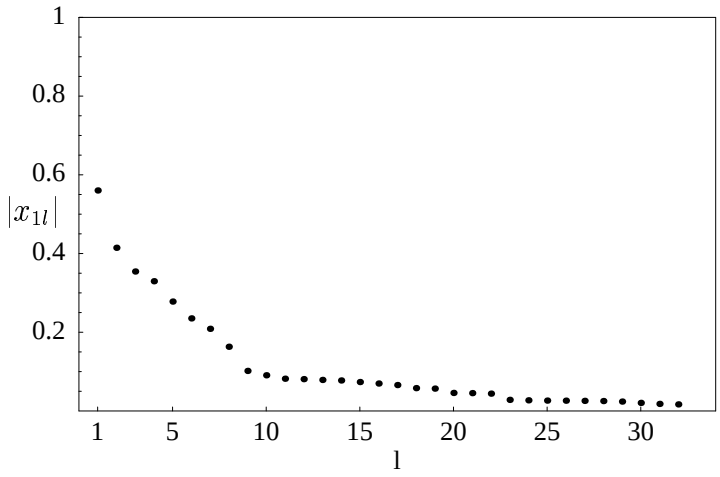

Figure 6.4: Absolute value distribution for the eigenvector corresponding to λ_1

As a representation of the projectors following Eq.(3.66) the real part of the projectors, the pattern similarity of eigenvector components of each eigenvector, and the imaginary part, the absolute value of the cross product of the eigenvector

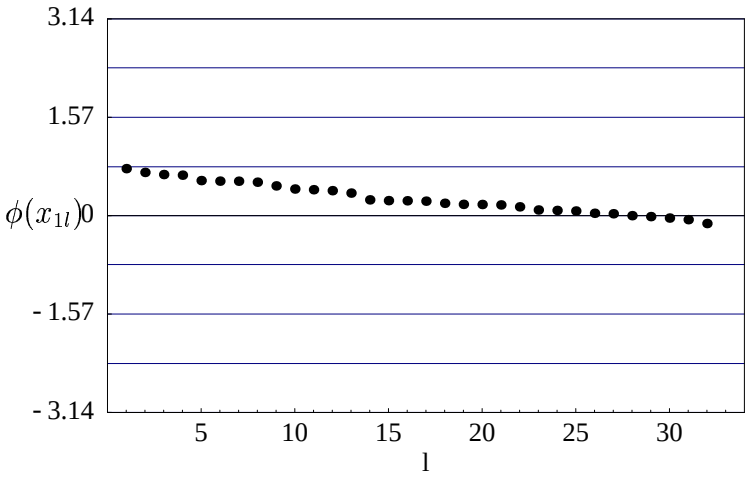

Figure 6.5: Phase distribution of the eigenvector components corresponding to λ_1

components can be visualized in density plots, where the gray level indicates the relative absolute value. The density plot gives the complete matrix of the real, respectively the imaginary part of the projector. The numbers at the bottom and at the left hand side of the plot indicate the author as in the original matrix. This representation is now the link back to the original complex Hermitian adjacency matrix, and thus by back-rotation to the original complex adjacency matrix. The matrix is symmetric for the real part and skew-symmetric for the imaginary part.

Fig.(6.16) shows, that the authors with ID $2, 8, 11, 29, 31$ and 32 have a high pattern similarity to author with ID 1, who is the anchor in this pattern as can be verified by checking against the complete eigensystem, and also amongst each other. This is represented by the bright squares which lie in the bottom row. Since this plot is symmetric, this also holds for the first column. A high brightness stands for a high similarity. Fig.(6.17) in addition shows, that author with ID 29 has a high (first row) skewness compared to author with ID 1, which means he could be viewed as writing more mails to author with ID 1, then he gets back. Whereas authors with IDs 2 and 31 have a low skewness, and are thus more in-bound oriented. Since this plot is skew-symmetric, a bright square in one half of the matrix corresponds to a dark square in the other.

The projector P_{λ_1} of this first subspace weighted by the corresponding eigenvalue and rotated backwards by $e^{i\frac{\Pi}{4}}$ is partly given in Tabs.(6.3) and (6.4). For reason of better clarity only the ten highest ranked members in that eigenvector have been taken. The indices on top and on the left hand side give the author ID.

If this result is now compared to a submatrix of the complex adjacency matrix, which has been extracted from the complex adjacency matrix by using the authors based on the status index within the subspace, this gives a clearer view what the

subpattern is. The submatrix based on the eigenvector centrality given in the first eigenvector is given in Tab.(6.5). As can be seen, the members are connected and the subgraph is complete. This has already been suggested by the projector and the distribution of the absolute values of the eigenvector. Also the direction information given by the projector can be found in this submatrix. The author with ID 1 has more inbound than outbound traffic, while authors with IDs 29 and 8 are more outbound than inbound oriented.

Second subspace of EIES data set

The second subspace already serves as a correction for the first (Fourier sum), in that it almost cancels the diagonal entries, which were present in the first projector, and at the same time shows the second strongest pattern (variance coverage of about 20%) and in this case also describes the behavior of the subgroup consisting of the strongest members in this pattern. Compared to the first subspace, given in Fig.(6.4), Fig.(6.6) shows, that the highest valued component ranks at about 0.7 and the next follows only after a gap of about 0.2. Again after a drop of about 0.2 one more authors stands out, while the rest then drops below 0.1 and out of relevance. This suggests a star pattern with about 3 major centers and a minor one of stars, $k = 1 \ldots 4$. The phase distribution in Fig.(6.7) shows, that the phase ranges from $-\pi \ldots \pi$, which is partly due to corrections for the first subspace. This is probably the case for $\phi \approx \pm\pi$.

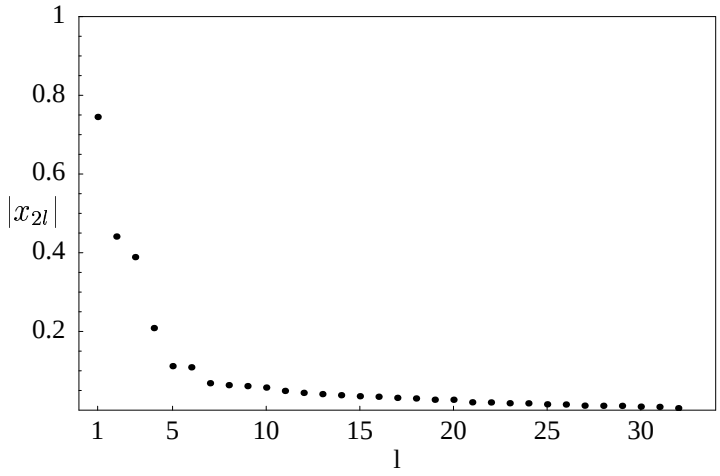

Figure 6.6: Distribution of $|\mathbf{x}_{2l}|$

The real part of the projector given in Fig.(6.18) suggests, that the authors with IDs 2 and 29 again have the strongest structure similarity compared with the anchor, who is the author with ID 1. The pattern in question is a star like

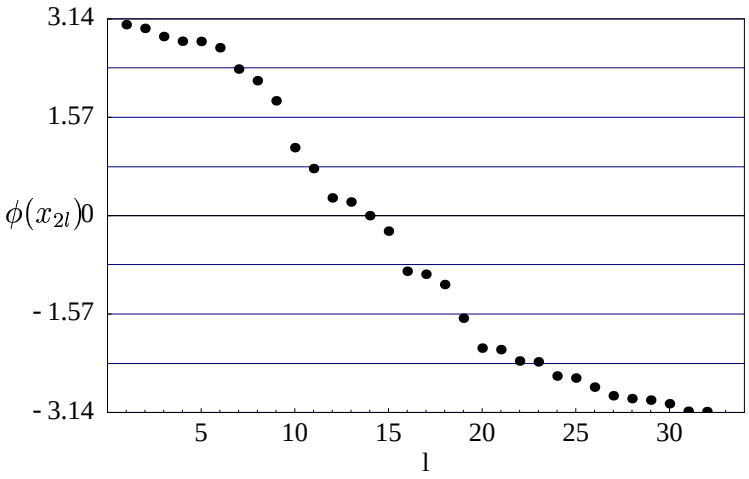

Figure 6.7: Distribution of $\phi(\mathbf{x}_{2l})$

behavior. Fig.(6.19) shows, that the author with ID 8 has a low skewness, which corresponds to a higher outbound behavior towards author 1.

Again the back rotated weighted projector P_{λ_2} is given partly for the second subspace in Tabs.(6.6) and (6.7). As can be seen, this projector corrects the diagonal entries of P_{λ_1} almost completely. In addition it strengthens the position of the anchor (author with ID 1) and the author with ID 29.

The submatrix composed along the second eigenvector is given in Tab.(6.8). This matrix supports the interpretation given already for the corresponding projector P_{λ_2}. A star pattern is clearly visible. The strongest star is around the author with ID 1. The author with ID 29 is also the center of a strong star.

The first two subspaces thus give information about the fact, that while the relevant members are strongly connected amongst themselves and loosely connected with the rest of the group, there are distinct star like patterns for each of the relevant members with the author with ID 1 as the strongest of them.

Third subspace of EIES data set

The distribution of the absolute values of the third eigenvector is given in Fig.(6.8). The anchor has changed, which points toward the fact, that a different group and pattern is described. This time, the author with ID 8 is the anchor. In addition as the anchor of the fifth eigenvector suggests in Tab.(7.2) , there is a star pattern again centered on the author with ID 8. The distribution supports the view, that while there are 4 relevant members, the rest are equally less relevant. The phase distribution in Fig.(6.9) suggests, that there is symmetry, which points towards a $inbound \sim outbound$ pattern with a star pattern, as in subspaces 1 and 3.

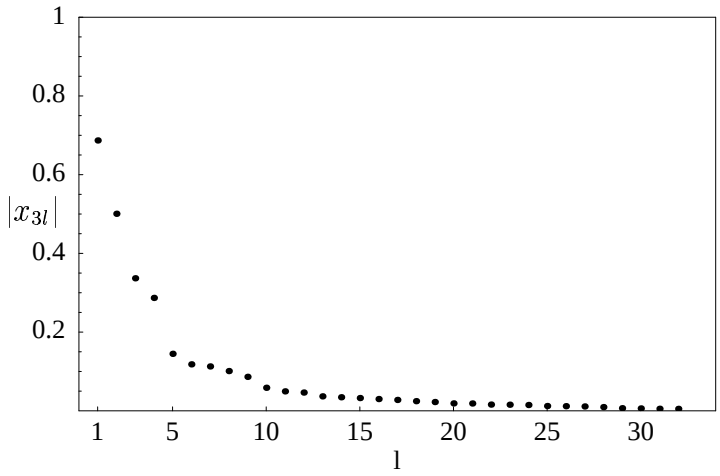

Figure 6.8: Eigenvector component distribution for the 3rd eigenvector

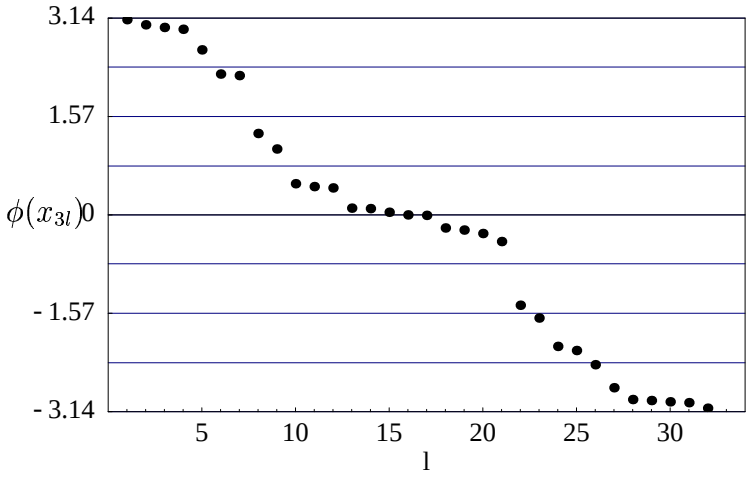

Figure 6.9: Eigenvector component distribution for the 3rd eigenvector

The real part of the projector given in Fig.(6.20) shows the high pattern similarity between the author with ID 8 and the authors with IDs $11, 30$ and 32. While Fig.(6.21) shows a more outbound communication for the authors with IDs 2 and 29 compared to the author with ID 8 and a more inbound communication for the author with ID 30 and 1 compared to the author with ID 8.

The submatrix deduced from the third eigenvector is given in Tab.(6.9). It confirms, that there is a strongly connected group around the anchor with the author with ID 8. For a comparison see the projector P_{λ_3} given in Tabs.(6.10) and (6.11).

Fifth subspace of the EIES data set

The fifth eigenvector again has a similar behavior as the second, suggesting, that this pattern is the complete pattern corresponding to the star pattern found in the third subspace. The distribution is given in Fig.(6.10). The phase distribution in Fig.(6.11) supports that view, in that it is similar to the one of the first eigenvector, if one takes into account, that a phase between $0 \leq \phi \leq \frac{\pi}{4}$ has a similar interpretation as a phase between $-\frac{3}{4}\pi \leq \phi \leq -\pi$. In this case the star pattern of the third eigenspace is stronger then the complete graph pattern of the fifth eigenspace, which is reflected in the absolute value of the respective eigenvalues. The fact, that there lies another eigenvalue and thus another pattern between the two can be explained by the interlacing effect of eigenvalues which occurs if perturbation takes place.

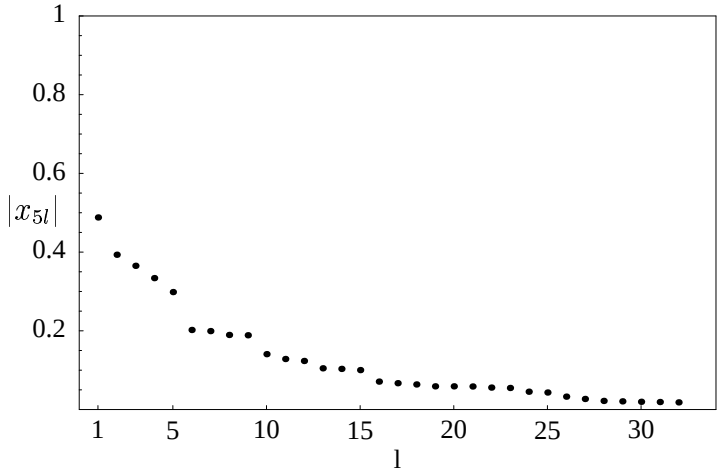

Figure 6.10: Eigenvector component distribution for the 5th eigenvector

The projector in Fig.(6.22) shows the structural similarity within the pattern. Clearly, the authors with IDs $30, 32, 9$ and 11 have a high structural similarity

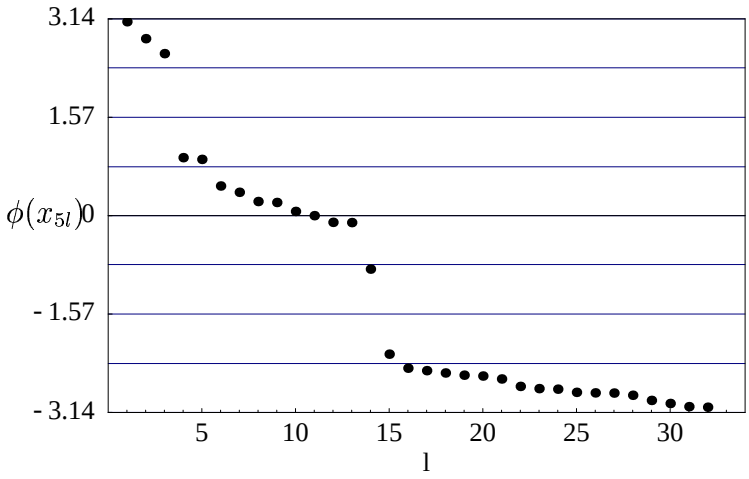

Figure 6.11: Phase distribution for the 5th eigenvector

with author 8. Fig.(6.23) reveals, that authors 30, 9 and 2 have a low skewness, translating into an inbound pattern compared to author 8, while authors 14, 22 and 24 are more outbound in comparison.

The fact, that there are two disturbed star patterns around the author with ID 1 and the author with ID 8, combined with the result that the author with ID 8 also plays a relevant role in the group of the author with ID 1 suggests, that these two star patterns are closely connected. While the first group is more strongly connected with everybody else, while still keeping a star pattern, the second group around the author with ID 8 has a stronger focus on the star pattern than on the complete pattern which might allow the conclusion that the group of the anchor with ID 1 is more "open to the public", while the group around the anchor with ID 8 is more closed.

Fourth subspace of the EIES data set

The distribution in the fourth eigenvector is given in Fig.(6.12). Now the author with ID 29 is the anchor. The other relevant members are those with IDs 2 and 24. It is probable, that again this is a new subpattern and also a new group. The phase distribution in Fig.(6.13) again suggests a strongly connected pattern.

The density plots support the above interpretation. Fig.(6.24) shows, that the authors with IDs 2, 24 and 31 seem to be highly pattern correlated with the author with ID 29. In addition Fig.(6.25) shows, that while the authors with IDs 2 and 24 have a more inbound behavior, the author with ID 31 has a more outbound pattern.

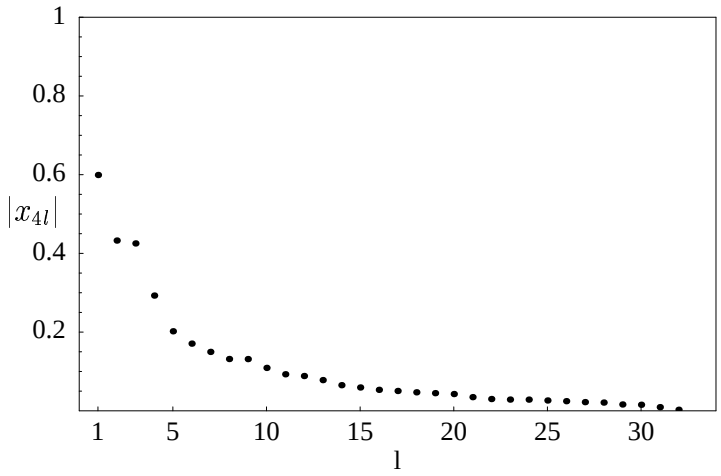

Figure 6.12: Eigenvector component distribution for the 4th eigenvector

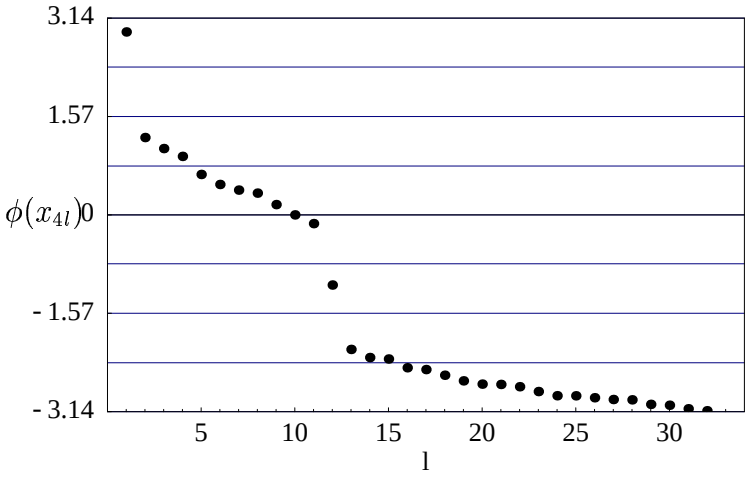

Figure 6.13: Phase distribution for the 4th eigenvector

Sixth subspace of the EIES data set

Fig.(6.14) gives the distribution of the absolute values of the eigenvector components of the sixth eigenvector, while Fig.(6.15) again shows the phase distribution. The anchor of that subspace is the author with ID 2.The author with ID 24 is also close, but overall the relevance of both authors is already not very high with a centrality index of approximately 0.4.

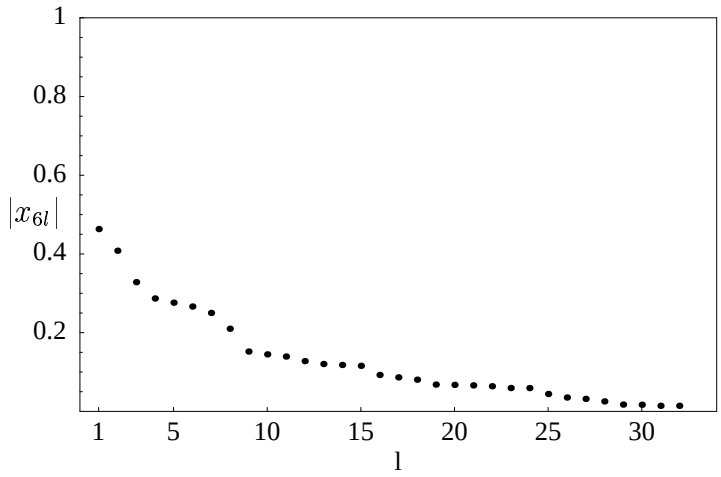

Figure 6.14: Eigenvector component distribution for the 6th eigenvector

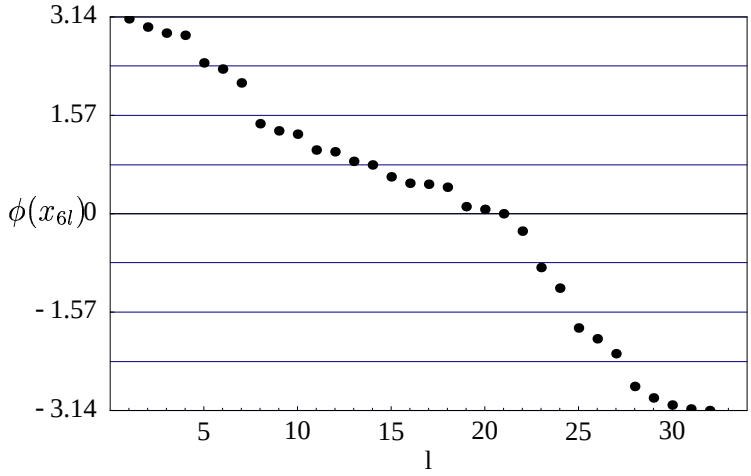

Figure 6.15: Phase distribution for the 6th eigenvector

The projector P_{λ_6} is again given in his real part in Fig.(6.26) and in its imaginary part in Fig.(6.27). The author with ID 2 shows a relative high visibility.

As can be seen, he seems to be more inbound oriented, as in Fig.(6.26) all his relevant partners show a low pattern similarity.

If one now takes a look at the two partial sums of weighted projectors, namely $M_{1,2} = (\sum_{k=1}^{2} \lambda_k P_k) e^{i\frac{\pi}{4}}$ given in Tabs.(7.10), (7.11), (7.12) and (7.13) in the Appendix and $M_{3,6} = (\sum_{k=3}^{6} \lambda_k P_k) e^{i\frac{\pi}{4}}$ given in Tabs.(7.14), (7.15), (7.16) and (7.17)in the Appendix, then it can be seen that $M_{1,2}$ is already a very good approximation of the original matrix when back rotated. $M_{3,6}$ on the other hand shows that once the main bulk of communication has been filtered out, that the author with ID 8, which is Bernard, is actually the central member of the group.

6.1.2 Comparison with dichotomized and symmetrisized eigensystem

If the eigensystem of the full data set is calculated with the method used by Freeman (see Tabs.(7.6) -(7.9) in the Appendix), a comparison given in Tab.(6.2) shows that the anchors of the subpatterns do not match, except for the first eigenspace. $H(\lambda_k)$ and $F(\lambda_k)$ represent the **F**reeman method and the **H**ermitian method. The numbers in brackets correspond to the eigenvalues sorted by absolute value. The author IDs are given from left to right for each eigenvector, going from the anchor to the 10th ranked member in that eigenvector. The effect seen is most probably a result of the dichotomization and thus of information loss.

$H(\lambda_1)$	1	29	8	2	32	31	11	24	30	27
$F(\lambda_1)$	1	31	8	24	5	29	2	11	3	10
$H(\lambda_2)$	1	29	2	8	32	11	15	18	26	31
$F(\lambda_2)$	17	16	12	23	9	22	7	21	20	14
$H(\lambda_3)$	8	32	30	11	29	1	2	9	31	17
$F(\lambda_3)$	5	2	32	30	27	10	19	17	6	25
$H(\lambda_4)$	29	24	2	31	15	32	12	11	14	10
$F(\lambda_4)$	32	2	31	27	4	6	12	24	8	29
$H(\lambda_5)$	8	32	30	29	24	22	11	2	15	14
$F(\lambda_5)$	24	1	27	18	5	13	2	28	20	8
$H(\lambda_6)$	2	24	31	22	29	30	8	9	18	10
$F(\lambda_6)$	11	27	15	10	5	4	32	6	29	25

Table 6.2: Comparison of anchors of the full data set between the method used by Freeman ($F(\lambda_k)$) and the method presented in this book ($H(\lambda_k)$)

	1	29	8	2	32
1	370.81 + 370.81i	237.94 + 306.61i	243.33 + 225.41i	252.20 + 177.74i	181.19 + 186.72i
29	306.61 + 237.94i	203.10 + 203.10i	199.54 + 142.99i	201.64 + 107.16i	150.33 + 120.33i
8	225.41 + 243.33i	142.99 + 199.54i	148.35 + 148.35i	155.11 + 118.43i	110.01 + 122.40i
2	177.74 + 252.20i	107.16 + 201.64i	118.43 + 155.11i	128.36 + 128.36i	86.29 + 126.44i
32	186.72 + 181.19i	120.33 + 150.33i	122.40 + 110.01i	126.44 + 86.29i	91.28 + 91.28i
31	114.67 + 187.96i	66.79 + 148.63i	77.01 + 116.03i	85.35 + 97.45i	55.48 + 94.10i
11	133.87 + 142.30i	85.12 + 116.89i	87.38 + 87.38i	91.90 + 69.06i	65.35 + 71.60i
24	97.75 + 117.32i	60.91 + 95.20i	64.62 + 71.79i	68.45 + 58.20i	47.62 + 58.93i
30	50.12 + 81.04i	29.30 + 64.14i	33.63 + 50.01i	37.19 + 41.95i	24.26 + 40.58i
27	44.02 + 72.56i	25.60 + 57.35i	29.57 + 44.80i	32.80 + 37.64i	21.30 + 36.32i

Table 6.3: Part 1: Back rotated weighted projector based corresponding to the first eigenvalue

	31	11	24	30	27
1	187.96 + 114.67i	142.30 + 133.87i	117.32 + 97.75i	81.04 + 50.12i	72.56 + 44.02i
29	148.63 + 66.79i	116.89 + 85.12i	95.20 + 60.91i	64.14 + 29.30i	57.35 + 25.60i
8	116.03 + 77.01i	87.38 + 87.38i	71.79 + 64.62i	50.01 + 33.63i	44.80 + 29.57i
2	97.45 + 85.35i	69.06 + 91.90i	58.20 + 68.45i	41.95 + 37.19i	37.64 + 32.80i
32	94.10 + 55.48i	71.60 + 65.35i	58.93 + 47.62i	40.58 + 24.26i	36.32 + 21.30i
31	65.37 + 65.37i	44.84 + 68.69i	38.21 + 51.48i	28.29 + 28.29i	25.20 + 25.20i
11	68.69 + 44.84i	51.47 + 51.47i	42.58 + 37.74i	29.61 + 19.59i	26.52 + 17.22i
24	51.48 + 38.21i	37.74 + 42.58i	31.45 + 31.45i	22.18 + 16.67i	19.88 + 14.68i
30	28.29 + 28.29i	19.59 + 29.61i	16.67 + 22.18i	12.24 + 12.24i	10.90 + 10.90i
27	25.20 + 25.20i	17.22 + 26.52i	14.68 + 19.88i	10.90 + 10.90i	9.71 + 9.71i

Table 6.4: Part 2: Back rotated weighted projector based corresponding to the first eigenvalue

	1	29	8	2	32	31	11	24
1	0	388 + 559i	346 + 239i	488 + 364i	185 + 239i	212 + 82i	177 + 178i	128 + 89i
29	559 + 388i	0	155 + 146i	132 + 89i	126 + 71i	91 + 65i	69 + 46i	218 + 156i
8	239 + 346i	146 + 155i	0	82 + 20i	288 + 268i	88 + 70i	164 + 172i	55 + 41i
2	364 + 488i	89 + 132i	20 + 82i	0	39 + 99i	163 + 125i	22 + 36i	17i
32	239 + 185i	71 + 126i	268 + 288i	99 + 39i	0	107 + 67i	35 + 34i	5 + 10i
31	82 + 212i	65 + 91i	70 + 88i	125 + 163i	67 + 107i	0	114 + 119i	53 + 56i
11	178 + 177i	46 + 69i	172 + 164i	36 + 22i	34 + 35i	119 + 114i	0	29 + 31i
24	89 + 128i	156 + 218i	41 + 55i	17	10 + 5i	56 + 53i	31 + 29i	0

Table 6.5: Submatrices based on first eigenvector

	1	29	2	8	32
1	-364.31 - 364.31i	147.15 + 267.28i	144.20 - 3.31i	214.81 + 161.81i	-15.49 + 75.78i
29	267.28 + 147.15i	-127.76 - 127.76i	-81.48 + 25.66i	-148.86 - 56.62i	-3.68 - 45.66i
2	-3.31 + 144.20i	25.66 - 81.48i	-28.56 - 28.56i	-8.78 - 74.78i	18.34 - 11.52i
8	161.81 + 214.81i	-56.62 - 148.86i	-74.78 - 8.78i	-99.26 - 99.26i	13.52 - 38.04i
32	75.78 - 15.49i	-45.66 - 3.68i	-11.52 + 18.34i	-38.04 + 13.52i	-8.21 - 8.21i
11	-37.79 + 12.25i	23.52 - 0.74i	4.83 - 10.02i	18.64 - 9.08i	4.66 + 3.72i
15	68.53 + 31.26i	-33.82 - 29.08i	-19.58 + 7.83i	-37.70 - 11.17i	-1.75 - 11.17i
18	-26.13 + 2.65i	15.30 + 2.80i	4.52 - 5.80i	13.32 - 3.27i	2.49 + 3.05i
26	18.74 - 10.80i	-12.44 + 3.05i	-1.44 + 5.88i	-8.90 + 6.94i	-2.90 - 1.45i
31	-0.76 + 20.57i	3.82 - 11.57i	-4.07 - 4.07i	-1.10 - 10.69i	2.64 - 1.61i

Table 6.6: Part 1: Back rotated weighted projector corresponding to the second eigenvalue

	11	15	18	26	31
1	12.25 - 37.79i	31.26 + 68.53i	2.65 - 26.13i	-10.80 + 18.74i	20.57 - 0.76i
29	-0.74 + 23.52i	-29.08 - 33.82i	2.80 + 15.30i	3.05 - 12.44i	-11.57 + 3.82i
2	-10.02 + 4.83i	7.83 - 19.58i	-5.80 + 4.52i	5.88 - 1.44i	-4.07 - 4.07i
8	-9.08 + 18.64i	-11.17 - 37.70i	-3.27 + 13.32i	6.94 - 8.90i	-10.69 - 1.10i
32	3.72 + 4.66i	-11.17 - 1.75i	3.05 + 2.49i	-1.45 - 2.90i	-1.61 + 2.64i
11	-2.17 - 2.17i	5.80 + 0.25i	-1.70 - 1.10i	0.91 + 1.40i	0.67 - 1.44i
15	0.25 + 5.80i	-7.79 - 7.79i	0.97 + 3.71i	0.52 - 3.12i	-2.78 + 1.16i
18	-1.10 - 1.70i	3.71 + 0.97i	-0.95 - 0.95i	0.39 + 1.03i	0.63 - 0.84i
26	1.40 + 0.91i	-3.12 + 0.52i	1.03 + 0.39i	-0.64 - 0.64i	-0.19 + 0.84i
31	-1.44 + 0.67i	1.16 - 2.78i	-0.84 + 0.63i	0.84 - 0.19i	-0.58 - 0.58i

Table 6.7: Part 2: Back rotated weighted projector corresponding to the second eigenvalue

	1	29	2	8	32	11	15	18	26	31
1	0	388 + 559i	488 + 364i	346 + 239i	185 + 239i	177 + 178i	81 + 120i	73 + 58i	89 + 35i	212 + 82i
29	559 + 388i	0	132 + 89i	155 + 146i	126 + 71i	69 + 46i	80 + 58i	4 + 8i	15 + 10i	91 + 65i
2	364 + 488i	89 + 132i	0	20 + 82i	39 + 99i	22 + 36i	15	8 + 8i	15 + 5i	163 + 125i
8	239 + 346i	146 + 155i	82 + 20i	0	288 + 268i	164 + 172i	0	27 + 4i	9	88+70i
32	239 + 185i	71 + 126i	99 + 39i	268 + 288i	0	35 + 34i	0	0	0	107+67i
11	178 + 177i	46 + 69i	36 + 22i	172 + 164i	34 + 35i	0	0	24 + 18i	11	119+114i
15	120 + 81i	58 + 80i	15i	0	0	0	0	0	0	32+24i
18	58 + 73i	8 + 4i	8 + 8i	4 + 27i	0	18 + 24i	0	0	0	48+49i
26	35 + 89i	10 + 15i	5 + 15i	9i	0	11i	0	0	0	13 + 8i
31	82 + 212i	65 + 91i	125 + 163i	70 + 88i	67 + 107i	114 + 119i	24 + 32i	49 + 48i	8 +13i	0

Table 6.8: Submatrices based on second eigenvector

	8	32	30	11	29	1	2	9	31	17
8	0	288 + 268i	216 + 140i	164 + 172i	146 + 155i	239 + 346i	82 + 20i	12 + 8i	88 + 70i	53 + 36i
32	268 + 288i	0	7 + 8i	35 + 34i	71 + 126i	239 + 185i	99 + 39i	101 + 44i	107 + 67i	7 + 9i
30	140 + 216i	8 + 7i	0	0	18 + 14i	39 + 71i	21 + 23i	0	20 + 28i	9 + 9i
11	172 + 164i	34 + 35i	0	0	46 + 69i	178 + 177i	36 + 22i	39 + 15i	119 + 114i	15 + 9i
29	155 + 146i	126 + 71i	14 + 18i	69 + 46i	0	559 + 388i	132 + 89i	15 + 10i	91 + 65i	15 + 10i
1	346 + 239i	185 + 239i	71 + 39i	177 + 178i	388 + 559i	0	488 + 364i	82 + 24i	212 + 82i	77 + 63i
2	20 + 82i	39 + 99i	23 + 21i	22 + 36i	89 + 132i	364 + 488i	0	35 + 25i	163 + 125i	25 + 18i
9	8 + 12i	44 + 101i	0	15 + 39i	10 + 15i	24 + 82i	25 + 35i	0	30 + 35i	5
31	70 + 88i	67 + 107i	28 + 20i	114 + 119i	65 + 91i	82 + 212i	125 + 163i	35 + 30i	0	28 + 15i
17	36 + 53i	9 + 7i	9 + 9i	9 + 15i	10 + 15i	63 + 77i	18 + 25i	5i	15 + 28i	0

Table 6.9: Submatrices based on third eigenvector

	8	32	30	11	29
8	-5.12 - 5.12i	8.84+ 0.51i	-27.39 + 31.84i	3.83 5.73i	20.55 - 22.69i
32	0.51 + 8.84i	-7.68 -7.68i	51.04 - 6.81i	1.17- 8.37i	-37.32+ 4.01i
30	31.84 - 27.39	-6.81+ 51.04i	-172.74- 172.74i	-34.92 + 19.73i	122.65 +129.07i
11	5.73 + 3.83i	-8.37 + 1.17i	19.73 -34.92i	-4.66 - 4.66i	-15.02+ 25.08i
29	-22.69 + 20.55i	4.01- 37.32i	129.07 + 122.65i	25.08 - 15.02i	-91.76 - 91.76i
1	3.06 -4.30i	0.70 + 6.43i	-26.28 - 15.88i	-3.67+ 3.46i	18.85 +12.06i
2	-11.05 + 13.62i	-0.99 - 21.48i	83.82 + 58.16i	12.89 - 10.70i	-59.99 - 43.93i
9	-2.74 - 0.75i	3.12- 1.55i	-3.15+ 16.21i	2.42+ 1.21i	2.59 - 11.75i
31	-17.91 + 10.15i	8.12- 23.90i	66.69 + 99.46i	18.66 - 6.17i	-46.74 -73.71i
17	1.31 - 0.38i	-0.89+1.41i	-2.76 -7.45i	-1.30 + 0.11i	1.87+ 5.48i

Table 6.10: part 1: Back rotated weighted projector corresponding to the third eigenvalue

	1	2	9	31	17
8	-4.30 + 3.06i	13.62 - 11.05i	-0.75 - 2.74i	10.15- 17.91i	-0.38 + 1.31i
32	6.43 + 0.70i	-21.48 - 0.99i	-1.55 + 3.12i	-23.90 + 8.12i	1.41- 0.89i
30	-15.88 -26.28i	58.16 + 83.82i	16.21- 3.15i	99.46 + 66.69i	-7.45 - 2.76i
11	3.46 -3.67i	-10.70 +12.89i	1.21 +2.42i	-6.17 +18.66i	0.11- 1.30i
29	12.06+18.85i	-43.93 - 59.99i	-11.75 + 2.59i	-73.71 - 46.74i	5.48+ 1.87i
1	-2.73 -2.73i	9.62+ 8.48i	1.88- 0.87i	14.14 +5.14i	-0.99 - 0.11i
2	8.48 + 9.62i	-30.13 - 30.13i	-6.43 + 2.50i	-45.83 -20.02i	3.27+ 0.58i
9	-0.87 + 1.88i	2.50- 6.43i	-0.79 - 0.79i	-0.02 -8.09i	0.13+ 0.52i
31	5.14+ 14.14i	-20.02- 45.83i	-8.09 - 0.02i	-41.51 - 41.51i	3.32+ 2.03i
17	-0.11 - 0.99i	0.58+ 3.27i	0.52 + 0.13i	2.03+ 3.32i	-0.18 - 0.18i

Table 6.11: part 2: Back rotated weighted projector corresponding to the third eigenvalue

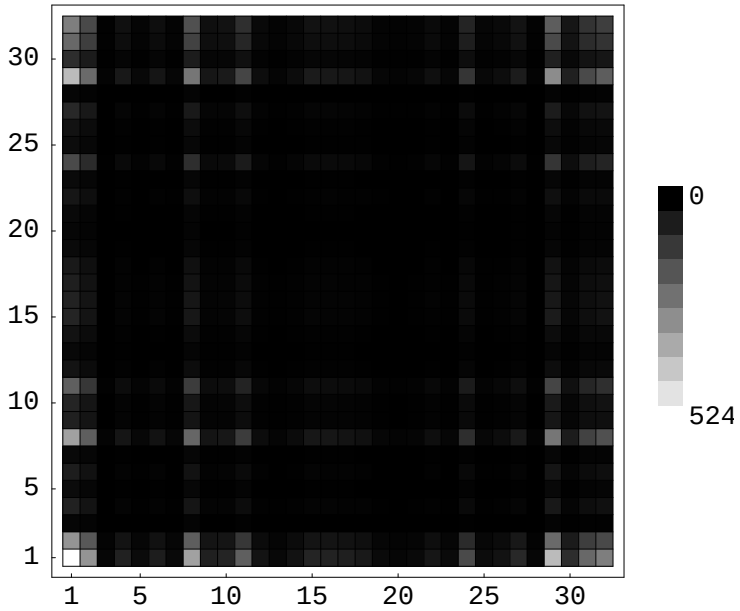

Figure 6.16: Density plot of real part of eigenprojector corresponding to λ_1

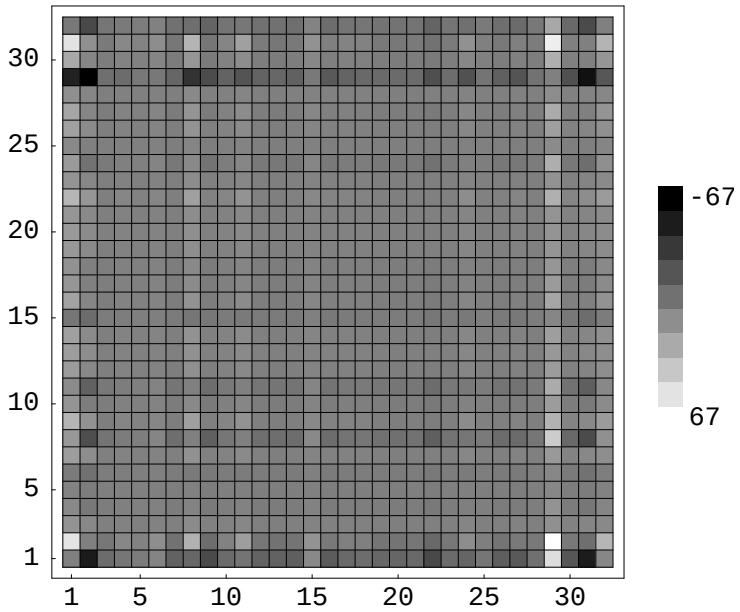

Figure 6.17: Density plot of imaginary part of eigenprojector corresponding to λ_1

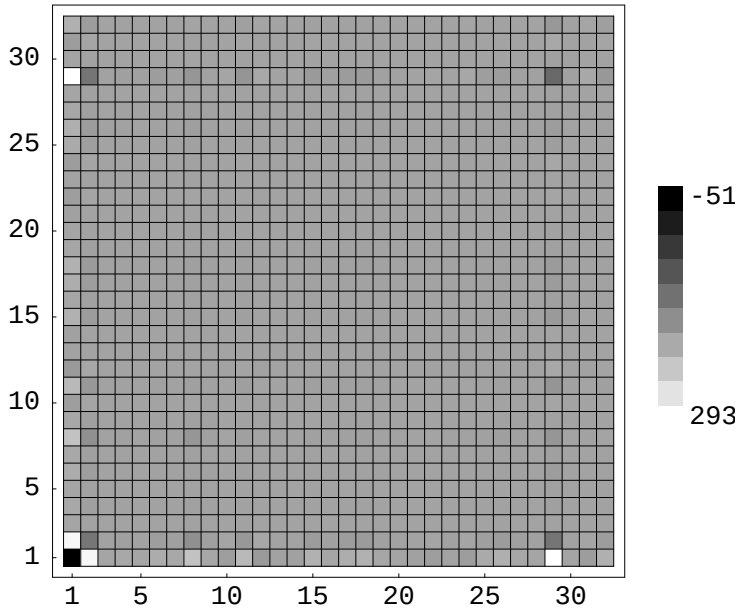

Figure 6.18: Density plot of real part of eigenprojector corresponding to λ_2

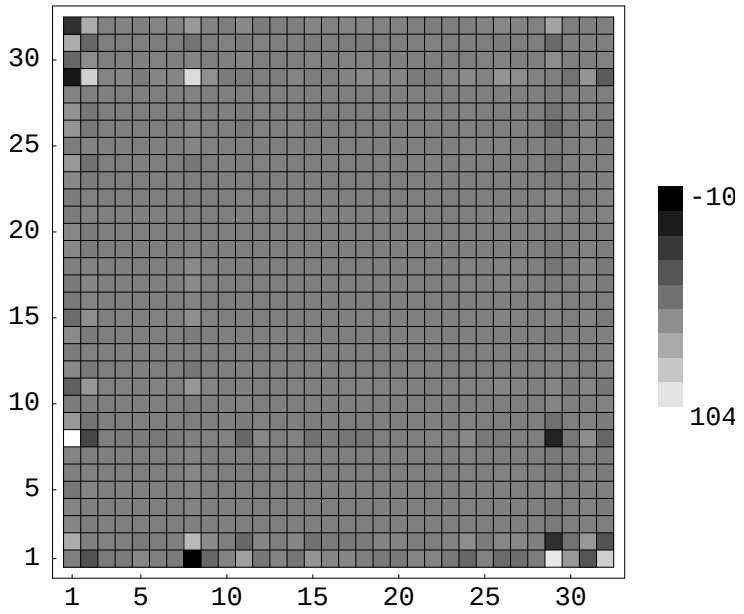

Figure 6.19: Density plot of imaginary part of eigenprojector corresponding to λ_2

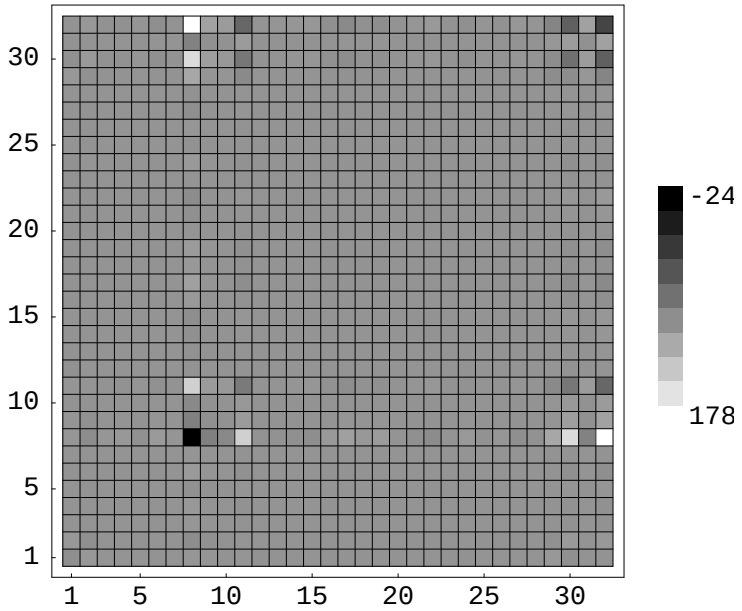

Figure 6.20: Density plot of real part of eigenprojector corresponding to λ_3

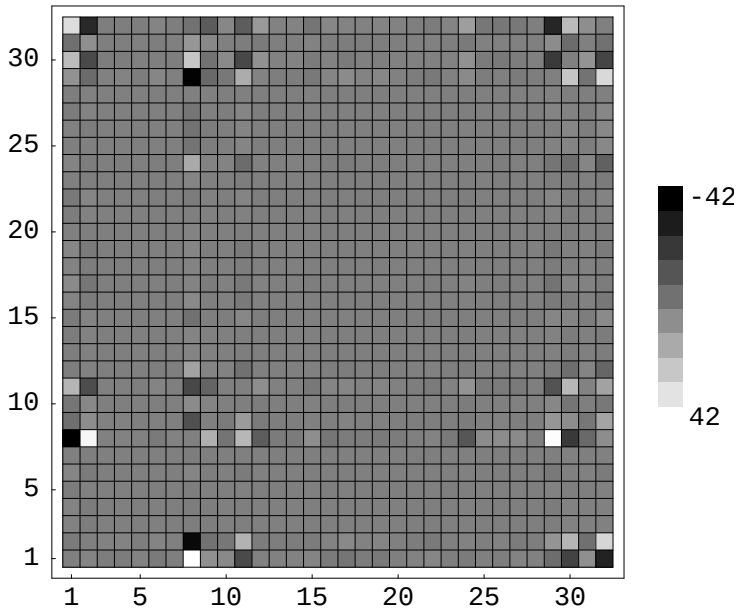

Figure 6.21: Density plot of imaginary part of eigenprojector corresponding to λ_3

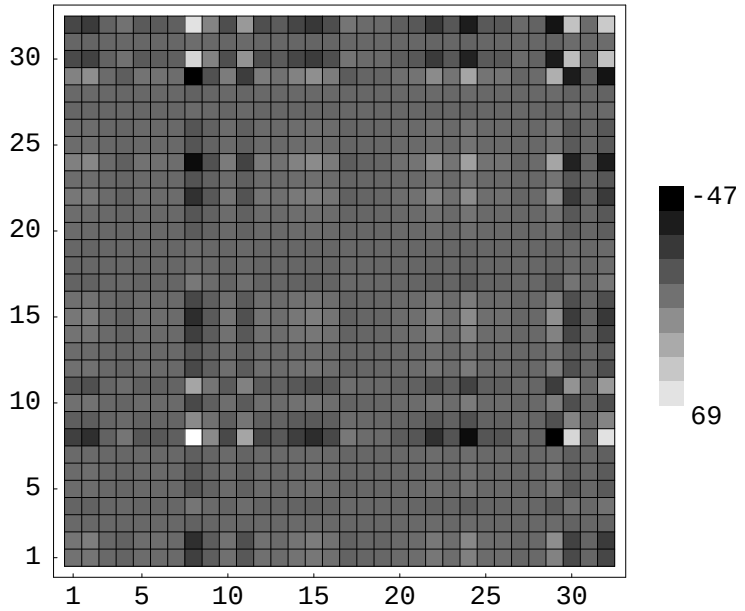

Figure 6.22: Density plot of real part of eigenprojector corresponding to λ_5

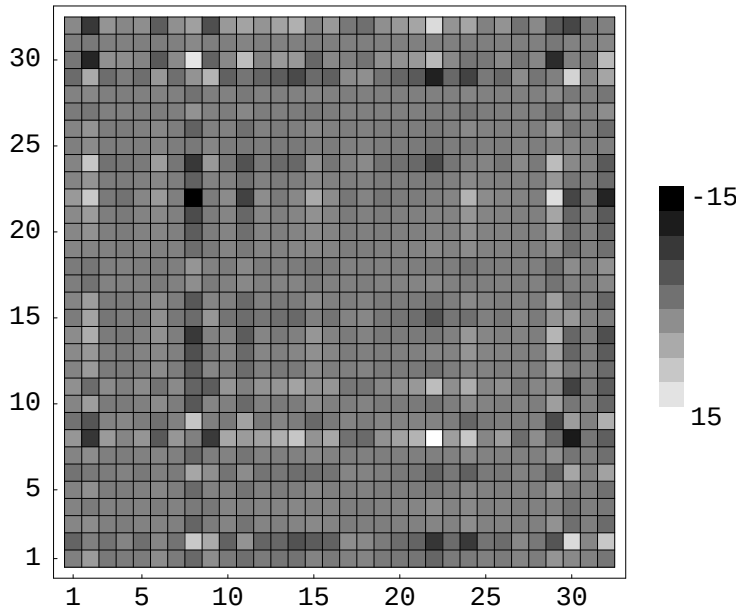

Figure 6.23: Density plot of imaginary part of eigenprojector corresponding to λ_5

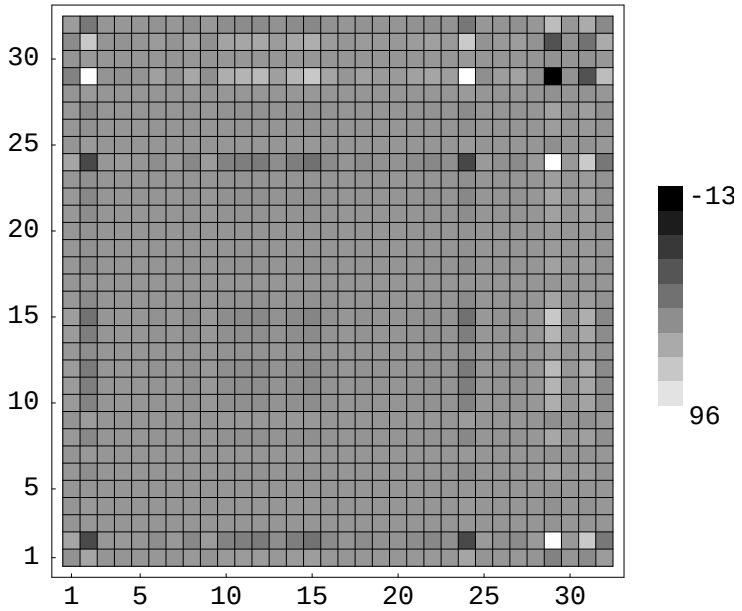

Figure 6.24: Density plot of real part of eigenprojector corresponding to λ_4

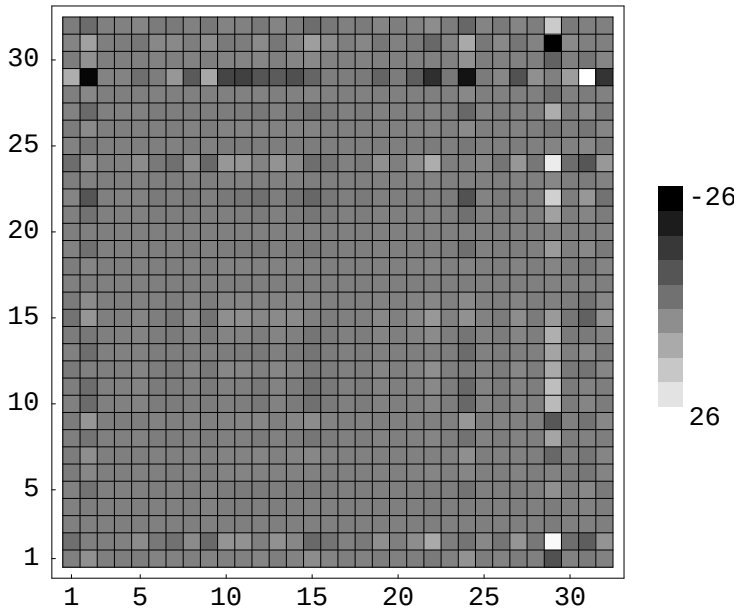

Figure 6.25: Density plot of imaginary part of eigenprojector corresponding to λ_4

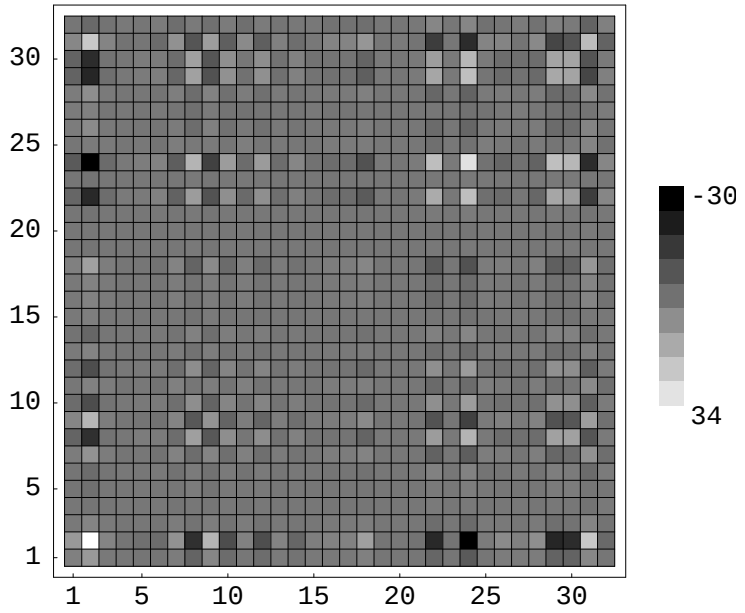

Figure 6.26: Density plot of real part of eigenprojector corresponding to λ_6

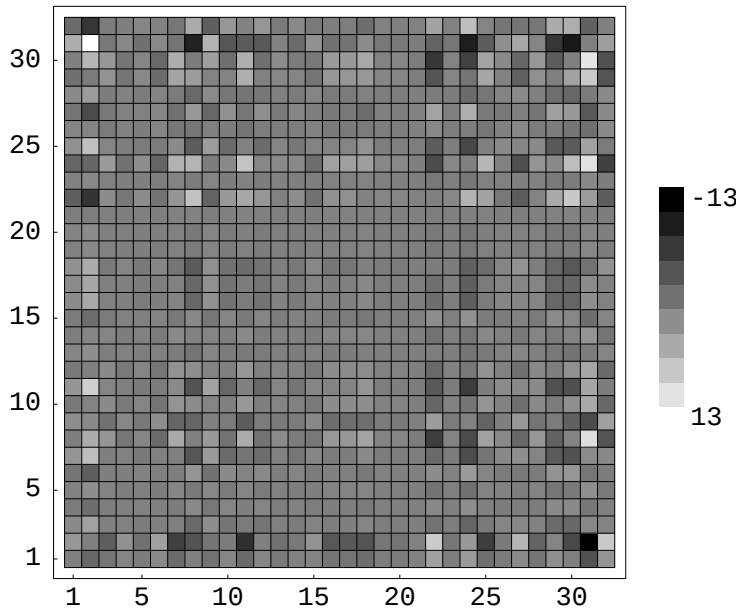

Figure 6.27: Density plot of imaginary part of eigenprojector corresponding to λ_6

6.2 Subset of EIES

The subset of the EIES data set Tab.(5.3) consists of seven prominent members of the original set. For the purpose of showing the advantages of the enhanced method of eigensystem analysis, the results obtained by Freeman and reported in [Fre97] will be used. In this paper Freeman wanted to show a hierarchy of members based on their eigenvector centrality. But to calculate this eigenvector centrality he had to dichotomize the adjacency matrix. This he did, with the effect, that a matrix entry became $a_{kl} = 1$ if the member k wrote more mails to member l then vice versa, and 0 otherwise. Then he had to symmetrize due to the problems described in chapter 2. This now led to the result, that Wellman with ID 29 became the top ranked member.

As can be seen, when the method presented in this book is used, Freeman with ID 1 himself is the most prominent member. Freeman himself stated in his paper, that the dichotomization led to the effect, that the most *garrulous* member became the most prominent, which in his case was Wellman with ID 29. With the method presented here, no dichotomization is necessary and the relevance of the members is solely based on their communication behavior, inbound as well as outbound.

The original adjacency matrix is given in Freeman [Fre97, p.11]. The complex matrix F composed as described in chapter 4 then is given in Eq.(6.1). As can be seen, the graph corresponding to this matrix is complete. Still there are patterns visible.

$$F = \begin{pmatrix} 0 & 115+84i & 17+16i & 93+127i & 53+57i & 33+23i & 84+118i \\ 84+115i & 0 & 4+10i & 5+22i & 5+9i & 4i & 15+24i \\ 16+17i & 10+4i & 0 & 15+17i & 3+4i & 3+3i & 4+5i \\ 127+93i & 22+5i & 17+15i & 0 & 57+57i & 12+9i & 34+35i \\ 57+53i & 9+5i & 4+3i & 57+57i & 0 & 8+8i & 10+15i \\ 23+33i & 4 & 3+3i & 9+12i & 8+8i & 0 & 33+45i \\ 118+84i & 24+15i & 5+4i & 35+34i & 15+10i & 45+33i & 0 \end{pmatrix} \tag{6.1}$$

6.2.1 Eigensystem of the EIES Subset

The eigensystem of the complex Hermitian matrix ($H = Fe^{-i\frac{\pi}{4}}$) is given in Tabs.(6.17) and (6.18).

In Fig.(6.28) all eigenvalues are given sorted by their amount. Again for better visibility of symmetry Fig.(6.29) shows the positive and negative eigenvalues rearranged. It is clearly visible from Fig.(6.29) that a star like structure emerges.

Fig.(6.30) based on Tab.(6.12) shows, that while the largest eigenvalue covers already more than 60% of the variance, the two largest eigenvalues cover about 93%. Only the first two subspaces will be discussed. The diversity of patterns has been discussed in section 6.1.

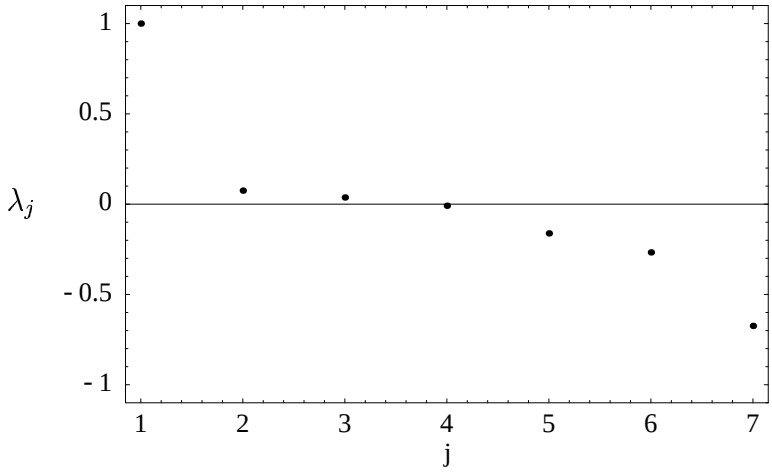

Figure 6.28: Eigenspectrum of the EIES data subset sorted by amount

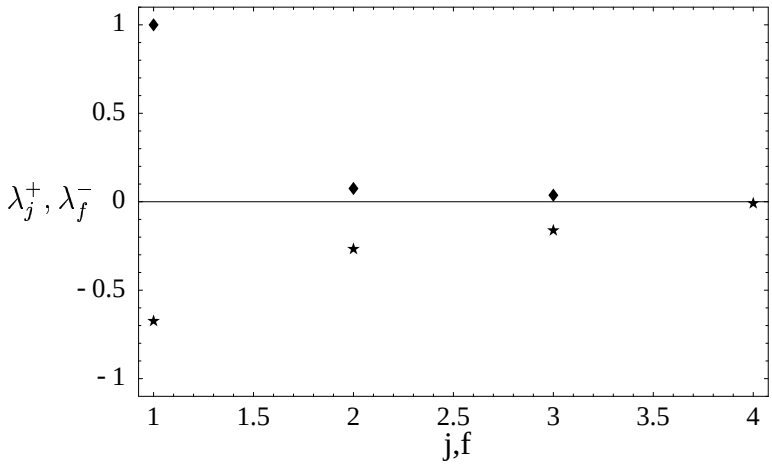

Figure 6.29: Eigenspectrum of the EIES subset sorted by absolute value

The distribution of the eigenvector components within the first and second subspace is given in Figs.(6.31) and (6.33). Together with the phase distribution in Figs.(6.32 and 6.34) the same behavior as in the complete data set can be seen. Namely, that there is a strongly connected pattern visible in the first subspace, whereas the second subspace is predominantly a star like pattern.

k	Covered variance per λ_k	Cumulative covered variance $\frac{\sum_{k=1}^{m} \lambda_k^2}{\sum_{k=1}^{N} \lambda_k^2}$
1	0.64	0.64
2	0.29	0.93
3	0.05	0.98
4	0.02	1.0
5	~ 0	1.0
6	~ 0	1.0
7	~ 0	1.0

Table 6.12: Cumulative covered variance of eigenvalues from Tab.(6.18)

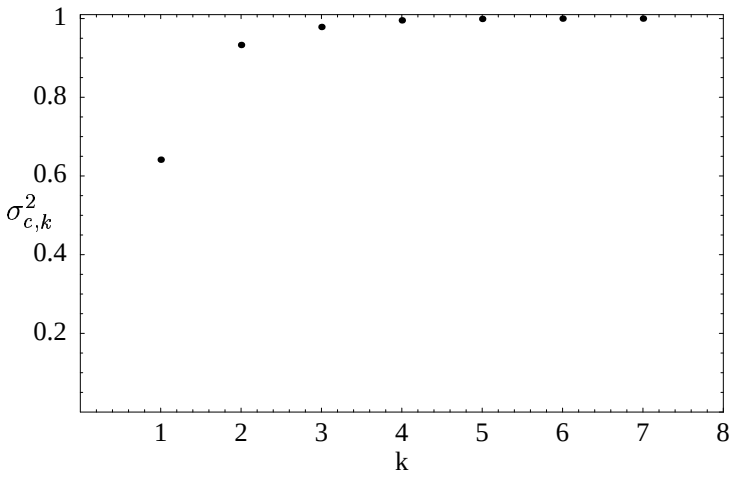

Figure 6.30: Cumulative covered variance given in Tab.(6.12)

The orthogonal projector of the first subspace is again decomposed into the real part, given in Fig.(6.35) and imaginary part, given in Fig.(6.36). As can be seen in Fig.(6.35) the authors with IDs 3 and 6 have a low pattern similarity with the anchor (author with ID 1). On the other hand it can be seen in Fig.(6.36) that the author with ID 1 shares a more inbound oriented pattern with the author with ID 2 and a more outbound relationship to authors with IDs 4 and 7. In addition the author with ID 2 shows a high inbound oriented communication with the authors with IDs 4 and 7.

These results reflect the rearranged matrix given in Tab.(6.13). The second projector given in Figs.(6.37) and (6.38) shows again the author with ID 1 as the anchor of a star with a high pattern similarity with the authors with IDs 2, 4 and 7. This result is supported by the rearranged adjacency matrix in Tab.(6.14) where the inbound character of Freeman (the author with ID 1) is visible and also the strong connection to White (ID 2), Bernard (ID 4) and Wellman (ID 7).

		1	4	7	2	5	6	3
Freeman	1	0	93 + 127i	84 + 118i	115 + 84i	53 + 57i	33 + 23i	17 + 16i
Bernard	4	127 + 93i	0	34 + 35i	22 + 5i	57 + 57i	12 + 9i	17 + 15i
Wellman	7	118 + 84i	35 + 34i	0	24 + 15i	15 + 10i	45 + 33i	5 + 4i
White	2	84 + 115i	5 + 22i	15 + 24i	0	5 + 9i	4i	4 + 10i
Doreian	5	57 + 53i	57 + 57i	10 + 15i	9 + 5i	0	8 + 8i	4 + 3i
Mullins	6	23 + 33i	9 + 12i	33 + 45i	4	8 + 8i	0	3 + 3i
Alba	3	16 + 17i	15 + 17i	4 + 5i	10 + 4i	3 + 4i	3 + 3i	0

Table 6.13: Submatrix based on first eigenvector

		1	2	4	7	5	6	3
Freeman	1	0	115 + 84i	93 + 127i	84 + 118i	53 + 57i	33 + 23i	17 + 16i
White	2	84 + 115i	0	5 + 22i	15 + 24i	5 + 9i	4i	4 + 10i
Bernard	4	127 + 93i	22 + 5i	0	34 + 35i	57 + 57i	12 + 9i	17 + 15i
Wellman	7	118 + 84i	24 + 15i	35 + 34i	0	15 + 10i	45 + 33i	5 + 4i
Doreian	5	57 + 53i	9 + 5i	57 + 57i	10 + 15i	0	8 + 8i	4 + 3i
Mullins	6	23 + 33i	4	9 + 12i	33 + 45i	8 + 8i	0	3 + 3i
Alba	3	16 + 17i	10 + 4i	15 + 17i	4 + 5i	3 + 4i	3 + 3i	0

Table 6.14: Submatrices based on second eigenvector

If the partial sum of the first two subspaces $H_{1,2}$ is taken (Tab.(6.15), multiplied with the eigenvalues and then rotated back, it is clearly visible that compared to the original matrix F in Eq.(6.1) this is already, as predicted a very close match. The remaining partial sum $H_{3,7}$ as given in Tab.(6.16) is decidedly smaller in every entry, and thus serves as a correction for the first partial sum. The main correction is taking place due to the communication of Bernard (ID 4).

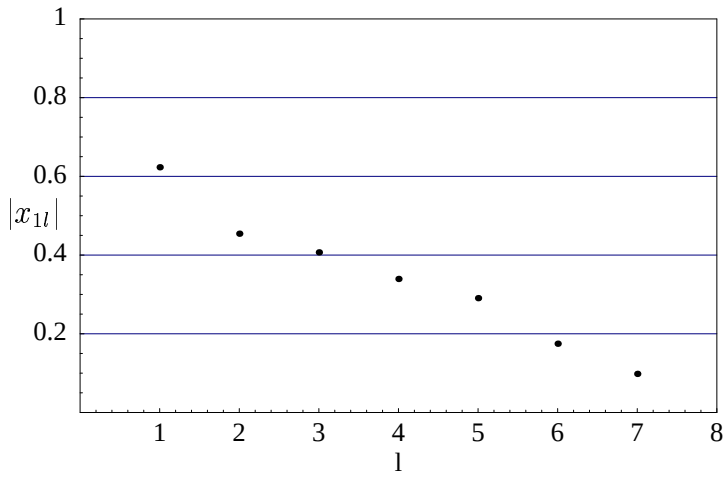

Figure 6.31: Distribution of the absolute value of the eigenvector components for $\mathbf{x}_1$

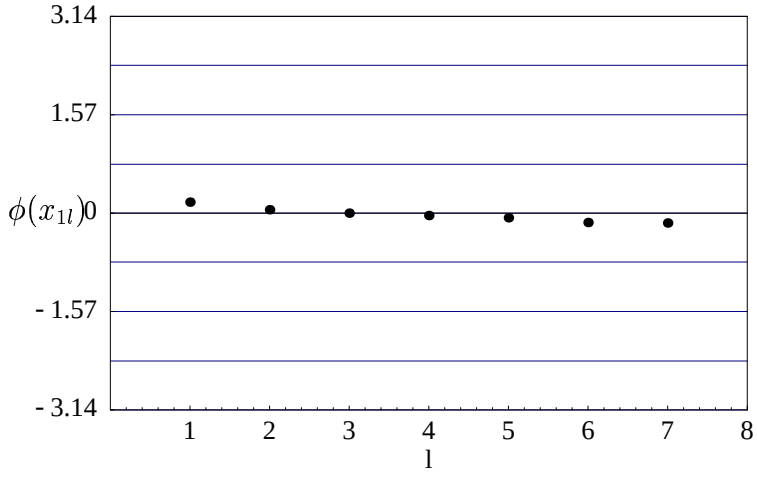

Figure 6.32: Distribution of the phase $\phi(\mathbf{x}_{1l}(\lambda_1))$

	1	2	3	4	5	6	7
1	0.19 + 0.19i	113 + 82i	17 + 15i	100 + 130i	51 + 55i	33 + 22i	80 + 120i
2	82 + 113i	2.9 + 2.9i	4.8 + 9.3i	7 + 17i	12 + 24i	9 + 17i	7 + 14i
3	15 + 17i	9.3 + 4.8i	2.3 + 2.3i	10 + 11i	6.5 + 6.8i	4.4 + 3.7i	8.6 + 9.5i
4	130 + 100i	17 + 7i	11 + 10i	26 + 26i	28 + 26i	20 + 16i	24 + 22i
5	55 + 51i	24 + 12i	6.8 + 6.5i	26 + 28i	19 + 19i	13 + 11i	23 + 25i
6	22 + 33i	17 + 9i	3.7 + 4.4i	16 + 20i	11 + 13i	7.1 + 7.1i	15 + 18i
7	120 + 80i	14 + 7i	9.5 + 8.6i	22 + 24i	25 + 23i	18 + 15i	21 + 21i

Table 6.15: Partial sum $H_{1,2}$

	1	2	3	4	5	6	7
1	-0.19 - 0.19i	2.5 + 2.4i	0.44 + 0.85i	-3.3 - 3.4i	2.0 + 2.5i	0.13 + 0.62i	1.24 - 0.68i
2	2.4 + 2.5i	-2.9 - 2.9i	-0.80 + 0.70i	-1.8 + 5.4i	-7. - 15.i	-9. - 13.i	7.7 + 9.5i
3	0.85 + 0.44i	0.70 - 0.80i	-2.3 - 2.3i	5.4 + 6.5i	-3.5 - 2.8i	-1.4 - 0.6i	-4.6 - 4.5i
4	-3.4 - 3.3i	5.4 - 1.8i	6.5 + 5.4i	-26. - 26.i	29. + 31.i	-7.8 - 7.3i	10. + 13.i
5	2.5 + 2.0i	-15. - 7.i	-2.8 - 3.5i	31. + 29.i	-19. - 19.i	-5.0 - 2.6i	-13. - 10.i
6	0.62 + 0.13i	-13. - 9.i	-0.6 - 1.4i	-7.3 - 7.8i	-2.6 - 5.0i	-7.1 - 7.1i	19. + 27.i
7	-0.68 + 1.24i	9.5 + 7.7i	-4.5 - 4.6i	13. + 10.i	-10. - 13.i	27. + 19.i	-21. - 21.i

Table 6.16: Partial sum $H_{3,7}$

λ_k	1.00	-0.67	-0.27	-0.16	0.07	0.04	-0.01
$\mathbf{x}_{k1}$	0.62	0.76	0.056-0.005i	-0.073-0.021i	0.027-0.0 39i	0.15-0.001i	-0.059-0.026i
$\mathbf{x}_{k2}$	0.33+0.06i	-0.39-0.05i	-0.018-0.057i	0.55+0.07i	0.12-0.16i	0.69	-0.106-0.059i
$\mathbf{x}_{k3}$	0.098-0.008i	-0.011-0.012i	-0.121+0.003i	0.015+0.004i	-0.16+0.03i	0.118-0.037i	0.97
$\mathbf{x}_{k4}$	0.45-0.07i	-0.38+0.06i	0.65	-0.20+0.03i	-0.35+0.15i	-0.18+0.1i	-0.001+0.015i
$\mathbf{x}_{k5}$	0.29-0.02i	-0.079-0.011i	-0.55+0.02i	0.39-0.02i	-0.47+0.25i	-0.32+0.21i	-0.14+0 .02i
$\mathbf{x}_{k6}$	0.17+0.01i	-0.013-0.032i	0.22+0.001i	0.55	0.56	-0.51-0.11i	0.15+0.05i
$\mathbf{x}_{k7}$	0.40-0.06i	-0.33+0.07i	-0.45+0.03i	-0.53+0.13i	0.42-0.11i	-0.16-0.04i	-0.002+0. 014i

Table 6.17: Eigensystem for H with $z = a + ib$

λ_k	1.00		-0.67		-0.27		-0.16		0.07		0.04		-0.01	
	$\mid z \mid$	$\phi(z)$	$\mid z \mid$	$\phi(z)$	$\mid z \mid$	$\phi(z)$	$\mid z \mid$	$\phi(z)$	$\mid z \mid$	$\phi(z)$	$\mid z \mid$	$\phi(z)$	$\mid z \mid$	$\phi(z)$
$\mathbf{x}_{k1}$	0.62	0	0.76	0	0.056	-0.09	0.076	-2.86	0.047	-0.96	0.15	-0.02	0.064	-2.73
$\mathbf{x}_{k2}$	0.34	0.18	0.39	-3.00	0.06	-1.88	0.44	0.15	0.20	-0.92	0.69	0	0.12	-2.63
$\mathbf{x}_{k3}$	0.098	-0.09	0.016	-2.32	0.121	3.12	0.016	0.29	0.16	2.93	0.12	-0.30	0.97	0
$\mathbf{x}_{k4}$	0.45	-0.15	0.38	3.00	0.65	0	0.21	2.99	0.38	2.75	0.20	2.64	0.015	1.67
$\mathbf{x}_{k5}$	0.29	-0.07	0.080	-3.00	0.56	3.10	0.39	-0.04	0.53	2.64	0.38	2.56	0.14	3.0 3
$\mathbf{x}_{k6}$	0.17	0.05	0.034	-1.97	0.22	0.02	0.55	0	0.56	0	0.52	-2.94	0.16	0.34
$\mathbf{x}_{k7}$	0.41	-0.15	0.34	2.93	0.45	3.07	0.55	2.91	0.44	-0.25	0.16	-2.89	0.014	1.7 3

Table 6.18: Eigensystem of H with $z = (\mid z \mid, \phi(z))$

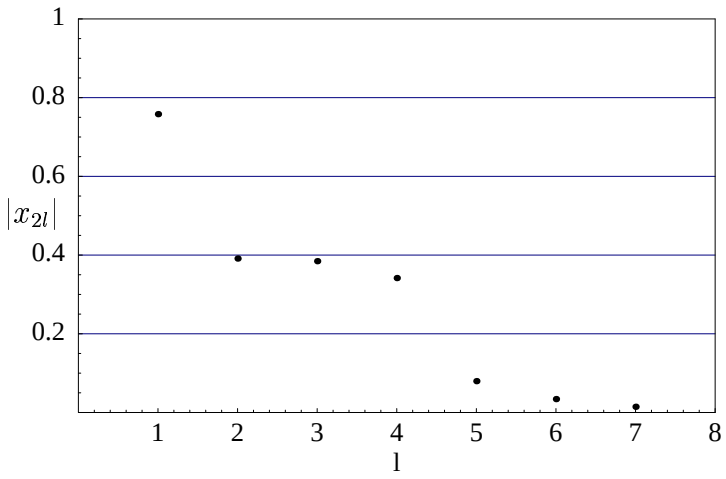

Figure 6.33: Distribution of the absolute value of the eigenvector components for $\mathbf{x}_2$

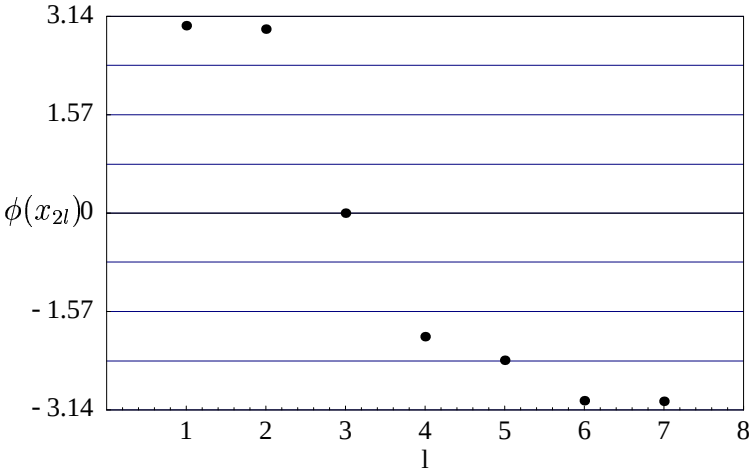

Figure 6.34: Distribution of phase $\phi(\mathbf{x}_{2l}(\lambda_2))$

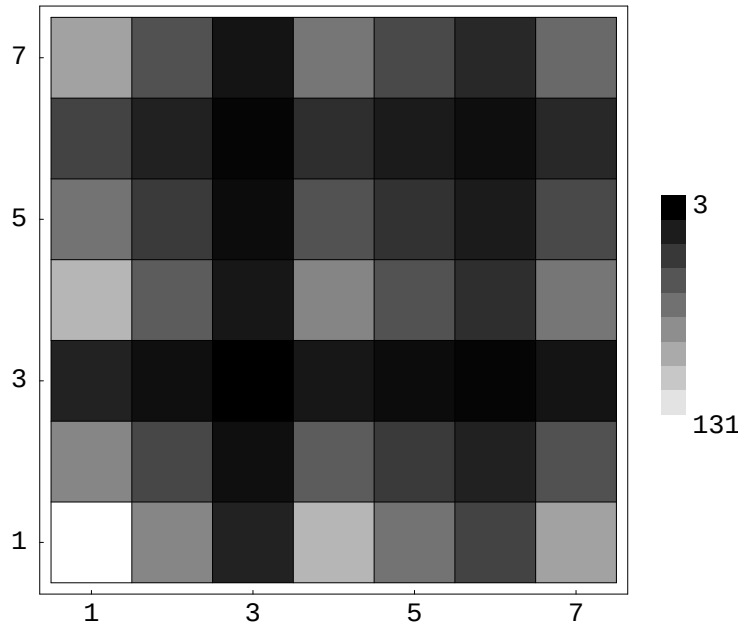

Figure 6.35: Density plot of real part of eigenprojector corresponding to λ_1

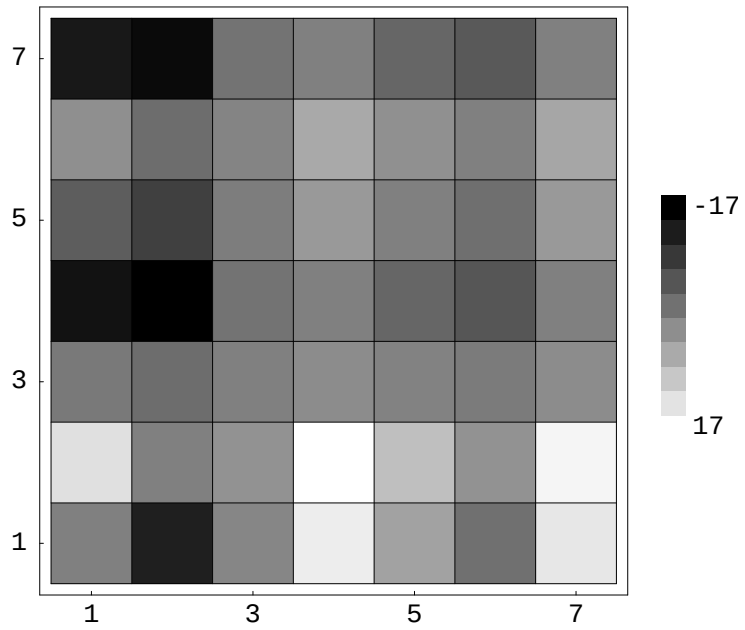

Figure 6.36: Density plot of imaginary part of eigenprojector corresponding to λ_1

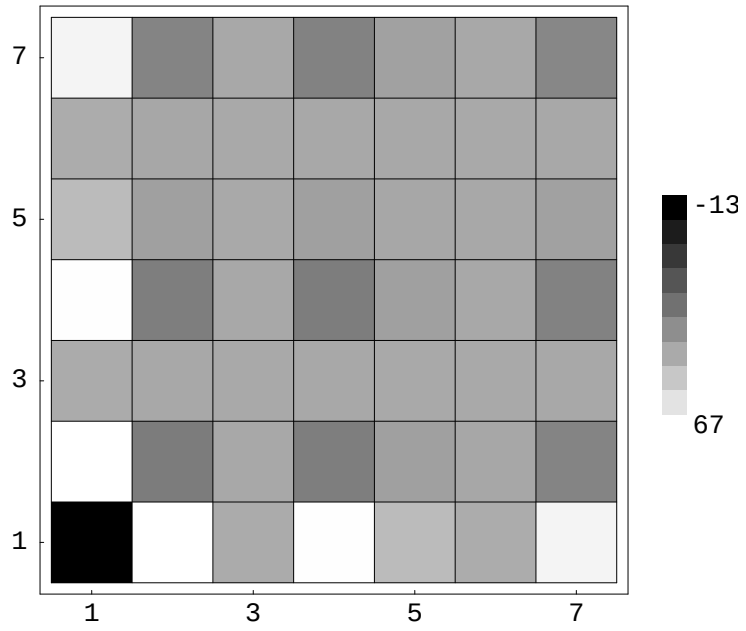

Figure 6.37: Density plot of real part of eigenprojector corresponding to λ_2

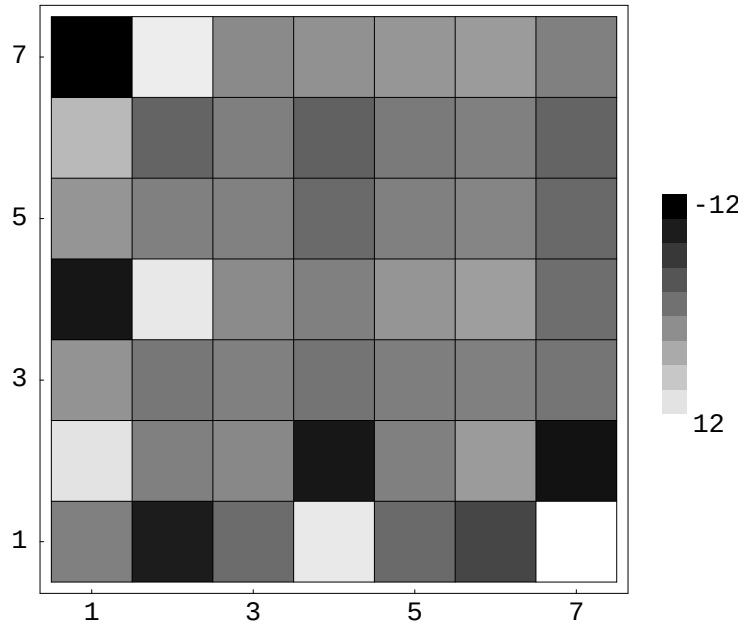

Figure 6.38: Density plot of imaginary part of eigenprojector corresponding to λ_2

6.2.2 Comparison of subset results with dichotomized and symmetrizied eigensystem

Tab.(6.19) shows, that the anchors differ depending on the method used. The representation is again as in Tab.(6.2). While the method used by Freeman still shows the same anchor in the first subspace, he already shows Wellman (ID 7) as the anchor of the second subspace. Freeman in his paper explains that this might be due to the dichotomization. Bernard (ID 4) who seems to be a less active writer but a very important member of the community is clearly visible when the method proposed in this book is used. Not so, when the method used by Freeman is used.

H(λ_1)	1	4	7	2	5	6	3
F(λ_1)	1	3	6	4	5	2	7
H(λ_2)	1	2	4	7	5	6	3
F(λ_2)	7	2	4	5	3	6	1
H(λ_3)	4	5	7	6	3	2	1
F(λ_3)	1	5	2	6	7	3	4
H(λ_4)	6	7	2	5	4	1	3
F(λ_4)	6	5	7	2	4	3	1
H(λ_5)	6	5	7	4	2	3	1
F(λ_5)	6	7	2	3	5	4	1
H(λ_6)	2	6	5	4	7	1	3
F(λ_6)	4	3	5	6	2	7	1
H(λ_7)	3	6	5	2	1	4	7
F(λ_7)	4	3	1	7	2	6	5

Table 6.19: Comparison of anchors for the EIES subset

As could be shown, the method is capable to present a view on the communication patterns based on inbound and outbound traffic within a group. Compared to the standard methods it reveals a clearer picture. In the examples used some insights could be gained into the structure of the respective groups. For the full EIES data set the following results can be stated:

- Since the entries of the adjacency matrix also include messages sent to all other members, thus diluting the person to person communication, it can be stated that the first two subspaces contain a lot of data noise due to these messages “to no one in particular”.
- Freeman (ID 1) is the anchor of the first two subspaces. He is the center of an inbound oriented star and also an important member of a large connected

subgroup. The fact that Freeman was the “administrator” of the communication system makes that plausible.

- Wellman (ID 29) also is a very important member of the group. For one he communicates very extensively (outbound oriented) and also serves as an anchor for subspace three. He also seems to be the connection between the groups around Freeman and Bernard.
- When the next subspaces, especially subspaces 3 and 5 are inspected, they reveal that Bernard (ID 8) is a very important member of the community. He is also the center of a star and an important member of a connected subgroup.

For the subset the following results can be stated:

- The first two subspaces already cover more than 90% of the variance of the data.
- Freeman (ID 1) is again the anchor of a inbound oriented star and also the important member of the almost complete graph.

Chapter 7

Conclusion and Future Applications

SNA provides a rich toolbox to analyze and interpret networks between human actors. The focus of this book is to present a generalized method for one of the tool sets available in SNA, namely the eigenvector centrality. The standard method needs proper data preparation before the results can be interpreted in a useful way. This is due to the fact that neither imaginary eigenvalues have found a good interpretation in social sciences nor have imaginary eigenvectors. Both can be the result of an eigensystem calculated for an asymmetric adjacency matrix. To circumvent these problems data had to be made symmetric, which meant loss of information.

The use of the proposed generalized approach based on the eigensystem analysis of complex Hermitian adjacency matrices obviously solves the problem of having to adjust asymmetric data so as to be fit to be analyzed with standard real valued eigensystem analysis. The suggested solution is based on the fact, that complex numbers can store more information than real numbers and thus no ex ante assumptions or filters have to be applied to the data that might distort the results obtained. In Hilbert space the norm, and thus the distances, is defined by the inner product. There is no need to define similarities or any other construct used in the standard methods when dealing with asymmetric data. This is used when representing inbound and outbound traffic by the real part and the imaginary part of the complex matrix entry. The eigensystems of such matrices allow for more detailed interpretation of the underlying communication patterns as was up to now possible. Since all eigenvalues are real, and depend on the traffic volume, it can easily be assumed, that they can be interpreted as distinct “energy levels” within the group. Since eigenvectors of Hermitian matrices define an orthogonal system it can further be assumed, that the eigenvectors can be viewed as independent with respect to their inherent communication pattern structure. The eigenvector components represent the members of the group. The status or rank of each member is given by the absolute value of the eigenvector component at each energy level.

The phase contains information about the directional similarity of the member with respect of the pattern governed by the anchor. Thus even the anchor of the complete group can be identified. He/She is represented as the highest absolute value eigenvector component belonging to the highest absolute value eigenvalue. In addition the possibility to construct complete subspaces gives the chance to analyze in more detail the substructures of the group.

7.1 Future Applications

7.1.1 Markets

As a motivating example for further applications take a look at forecasting markets, especially forecasting markets like Internet based political stock markets. Each trade can be viewed as a communication between a trader and a share. All transactions are logged in the order book and are thus available. As can easily be seen any such market can be viewed as a bipartite graph, and thus the spectrum will be qualitatively like the one given in Eq.(3.63). The efficiency of markets depend strongly on the information flow within the market. And this again depends on the market structure.

Preliminary experimental results, obtained on a political stock market hosted at the Chair for Information Services and Electronic Markets at the Universität Karlsruhe (TH) (see Tab.(7.1 for results of the election), RMSE (Root Mean Square Error) = $\sqrt{\frac{\sum \Delta^2}{n}}$), suggest that the expected behavior can be made visible. A stock market can be seen as a bipartite graph as in Fig.(7.1). The graph $G = \{E, V_t, V_s\}$ consists of vertices V_t representing the traders in the market and V_s representing the shares.

In %	Result PSM	Result (normalized)	Result Südwest-Presse	Official result
CDU	39,10	39,18	39,27	44,80
SPD	33,00	33,07	31,68	33,30
FDP	8,90	8,92	9,51	8,10
B90/Grüne	9,00	9,02	8,99	7,70
REP	7,20	7,21	7,79	4,40
Sonstige	2,60	2,61	2,76	1,70
Summe	99,80	100,00	100,00	100,00
RMSE	4,356	4,280	4,947	

Table 7.1: Forecasted results vs. actual results of 2001 diet elections in Baden-Württemberg

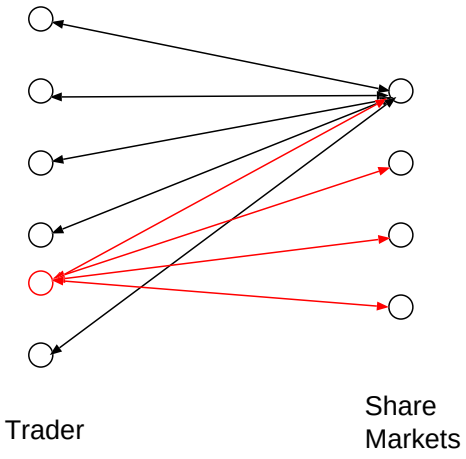

Figure 7.1: Stock market as bipartite- graph

If for example the market is dominated by a monopolist, this could be represented as a star graph like structure, which -as we have seen - can easily be detected with the method. If on the other hand the market is an oligopoly, the representation as a graph would be a connected if not even a complete graph. If it is now taken into account, that transactions, like communication, are recorded as a two-way flow, it is feasible to use the method of Hermitian adjacency matrices to analyze market transactions and thus gain insight into market structure and market efficiency.

It was found that if a share is the anchor of a star, then the traders with the next highest absolute eigenvector components are those that trade heavily in the share. On the other hand, if a trader is the anchor of a star, the share that he/she trades most often in, is identifiable by it´s absolute eigenvector component. The eigenvalues again show the volume, if one uses the exchanged amounts of money as the weights on the edges E. Thus an edge $e \neq 0$ if a trader bought or sold shares. As our market offered also a primary market, where traders could buy portfolios, we also had the opportunity to check for arbitrage traders. This was possible by checking for the eigenvector with the portfolio as anchor or for the index of the portfolio in any eigenvector. The highest ranked trader in that eigenvector could be identified as an arbitrage trader. It is also possible to show, how efficient information is distributed within this market. If the absolute values of the eigenvector components show an uniform distribution , then as was shown in chapter 4 this points towards a complete graph. This leads to the interpretation of equally distributed information within that market. Information efficiency is a prerequisite for market efficiency. This should be further investigated. The eigenspectral analysis over time could also yield some insight into stock market

behavior.

A market, where networking plays an important role has always been the job market. As Arrow and Borzekowski point out in their recent discussion paper ([AB04]) the network effect is more relevant within a group of similar situated workers.

7.1.2 Organization Analysis

Another application area is that of the analysis of organizational behavior. Krackhardt and Hanson [KH93] show in their article how the knowledge about the social networks within a company can help management to use resources better. Ahuja et al. [AGC03] show, that the centrality of a group member, measured in email exchange is a very good predictor of performance of the said member. They also had the already mentioned problem of asymmetric data. If now the analysis of asymmetric data can be achieved, and the status of a member calculated based on asymmetric communication behavior, then the prediction about performance could improve.

7.1.3 Viral Marketing

Viral Marketing, a modern word for "word of mouth" which with the Internet became a *word-of-mouse* (see Helm [Hel00]), has gained wide interest in the past years as a means to use social networks to market new products. Subramani and Rajagopalan [SR03b] for example suggest a framework based on social network considerations to enhance the outcome of viral marketing efforts. As of now viral marketing campaigns are more or less anecdotal in planning and outcome, since the underlying mechanics are not yet well investigated. While the general characteristics of epidemiology are well known, the mechanics that help to "spread" a marketing "virus" are still under investigation. But if one could use the communication within a known scale-free network and analyze it with the appropriate tools (e.g. the one proposed in this work), one might find a way to set up viral marketing campaigns more effectively. Domingos and Richardson [DR01] have already introduced a way to calculate the network value of customers. Network value is in this paper defined as *the expected profit from sales to other customers she may influence to buy, the customers those may influence and so on recursively*. This makes network analysis applicable in Customer Relationship Management (CRM). But to find out who gets influenced to buy by whom is a very difficult task, and Domingos and Richardson model this network as a Markov random field as a good first approximation.

7.2 Outlook

Some interesting questions for further investigation are for example the evolution of such networks, and how they can be analyzed or even predicted with the help of this method. The possibility to apply well known methods of perturbation theory from physics to the Hermitian matrices used here, might bring new insight into the dynamics of group patterns and structures.

Another interesting question would be the comparison with a context based analysis of email traffic. It could well be, that the structure we find through the mere existence of communication might give a clue as to the topics discussed in that substructure. This is already being investigated in the Internet link research community.

As could be shown the proposed method not only yields more insight into asymmetric and thus more generalized communication structures, but also has some potential for further applications in several fields. With the problem of information overflow and the resulting need to structure this information it is safe to predict that these methods will gain ever more relevance.

Appendix

λ_k	1	2	3	4	5	6	7	8
	1.0	-0.56	-0.31	-0.23	0.17	0.095	-0.092	-0.059
$\mathbf{x}_{k1}$	0.56	0.74	-0.009 - 0.118i	0.078 + 0.041i	-0.127 - 0.018i	0.116 - 0.033i	-0.20 + 0.04i	0.011 - 0.039i
$\mathbf{x}_{k2}$	0.32 + 0.06i	-0.39 - 0.05i	0.030 + 0.109i	-0.41 - 0.11i	-0.18 + 0.06i	0.46	-0.095 + 0.103i	-0.12 - 0.24i
$\mathbf{x}_{k3}$	0.014 + 0.011i	-0.0093 - 0.0061i	-0.0116 + 0.0018i	0.0087 + 0.0032i	-0.016 - 0.022i	0.043 + 0.047i	0.016 - 0.020i	-0.014 + 0.049i
$\mathbf{x}_{k4}$	0.073 + 0.005i	-0.026 - 0.006i	-0.019 + 0.002i	0.021 + 0.003i	0.043 - 0.005i	-0.006 - 0.025i	-0.028 - 0.032i	-0.102 + 0.081i
$\mathbf{x}_{k5}$	0.026 + 0.002i	-0.010 + 0.010i	0.0110 + 0.0012i	0.007 - 0.015i	-0.053 - 0.018i	-0.024 + 0.021i	0.009 - 0.023i	-0.046 + 0.008i
$\mathbf{x}_{k6}$	0.066 - 0.002i	-0.044 - 0.001i	-0.030 - 0.005i	-0.043 - 0.002i	-0.050 + 0.031i	-0.037 - 0.047i	0.069 - 0.015i	0.112 + 0.009i
$\mathbf{x}_{k7}$	0.022 + 0.016i	-0.026 - 0.005i	-0.0045 + 0.0025i	0.007 + 0.021i	-0.027 - 0.018i	0.091 + 0.090i	0.021 - 0.006i	0.011 + 0.131i
$\mathbf{x}_{k8}$	0.35 + 0.01i	-0.14 - 0.15i	0.69	-0.071 - 0.033i	0.49	-0.24 + 0.06i	-0.042 - 0.045i	0.121 + 0.030i
$\mathbf{x}_{k9}$	0.071 + 0.030i	-0.018 - 0.029i	0.091 + 0.044i	0.027 + 0.036i	0.110 + 0.056i	0.21 + 0.01i	-0.17 - 0.03i	-0.13 + 0.07i
$\mathbf{x}_{k10}$	0.081 + 0.012i	0.019 + 0.004i	0.048 - 0.010i	-0.096 - 0.052i	-0.098 - 0.032i	-0.14 + 0.004i	0.072 + 0.012i	0.035 + 0.004
$\mathbf{x}_{k11}$	0.21 + 0.006i	-0.102 + 0.038i	-0.28 + 0.05i	-0.119 - 0.056i	0.20 - 0.02i	0.035 + 0.113i	-0.39 - 0.004i	-0.34 + 0.10i
$\mathbf{x}_{k12}$	0.042 + 0.016i	0.040 - 0.010i	0.004 - 0.032i	-0.14 - 0.04i	-0.096 - 0.027i	-0.139 + 0.0001i	0.041 - 0.049i	-0.11 + 0.10i
$\mathbf{x}_{k13}$	0.020 + 0.016i	0.0023 + 0.0044i	0.0086 - 0.0039i	-0.039 - 0.033i	-0.045 - 0.038i	0.039 + 0.020i	0.014 - 0.019i	0.06 + 0.14i
$\mathbf{x}_{k14}$	0.040 + 0.018i	0.009 - 0.012i	0.015 - 0.005i	-0.125 - 0.042i	-0.129 - 0.057i	-0.058 + 0.010i	0.074 + 0.003i	-0.092 + 0.031i
$\mathbf{x}_{k15}$	0.081 - 0.005i	-0.064 + 0.024i	0.024 + 0.013i	-0.20 - 0.02i	-0.19 - 0.02i	0.023 - 0.027i	0.095 - 0.078i	0.005 + 0.131i
$\mathbf{x}_{k16}$	0.076 + 0.020i	-0.016 + 0.008i	-0.023 - 0.009i	-0.059 - 0.001i	-0.100 - 0.032i	0.036 + 0.058i	0.15 - 0.08i	0.04 + 0.21i
$\mathbf{x}_{k17}$	0.069 + 0.012i	-0.048 + 0.007i	-0.058 - 0.003i	-0.0018 - 0.0020i	0.054 + 0.011i	0.036 + 0.055i	0.035 - 0.030i	0.082 + 0.086i
$\mathbf{x}_{k18}$	0.056 + 0.010i	-0.064 - 0.001i	-0.018 - 0.003i	-0.047 - 0.005i	0.014 + 0.017i	0.14 + 0.06i	-0.124 - 0.005i	0.30 + 0.07i
$\mathbf{x}_{k19}$	0.022 + 0.014i	-0.015 - 0.009i	-0.036 - 0.005i	-0.016 - 0.024i	0.013 - 0.014i	-0.007 + 0.012i	-0.086 - 0.038i	0.073 + 0.003i
$\mathbf{x}_{k20}$	0.015 + 0.014i	-0.0059 - 0.0092i	-0.0036 - 0.0034i	-0.015 - 0.003i	-0.036 - 0.028i	0.004 + 0.016i	0.040 + 0.003i	-0.043 + 0.036i
$\mathbf{x}_{k21}$	0.020 + 0.013i	0.0060 + 0.0056i	0.016 + 0.0007i	-0.045 - 0.029i	-0.057 - 0.042i	-0.014 - 0.003i	0.079 + 0.007i	-0.017 + 0.038i
$\mathbf{x}_{k22}$	0.049 + 0.030i	0.019 + 0.006i	0.034 + 0.003i	-0.060 - 0.071i	-0.17 - 0.10i	-0.27 - 0.11i	0.027 - 0.018i	-0.21 + 0.04i
$\mathbf{x}_{k23}$	0.022 + 0.012i	-0.0006 - 0.0089i	-0.0030 - 0.0052i	-0.034 - 0.007i	-0.062 - 0.024i	-0.012 + 0.013i	0.028 - 0.003i	-0.039 + 0.058i
$\mathbf{x}_{k24}$	0.16 + 0.01i	0.024 - 0.029i	-0.026 - 0.038i	-0.42 - 0.10i	-0.29 - 0.06i	-0.41 - 0.04i	0.17 - 0.03i	0.069 - 0.031i
$\mathbf{x}_{k25}$	0.028 + 0.006i	-0.035 + 0.003i	0.0060 + 0.0106i	0.026 - 0.004i	-0.059 - 0.006i	0.012 + 0.092i	-0.071 - 0.011i	0.095 +0.077i
$\mathbf{x}_{k26}$	0.042 + 0.018i	-0.056 - 0.024i	-0.009 + 0.012i	-0.028 + 0.006i	-0.059 - 0.024i	0.067 + 0.008i	0.093 + 0.049i	0.009 + 0.088i
$\mathbf{x}_{k27}$	0.088 + 0.022i	-0.020 - 0.022i	0.020 + 0.009i	-0.051 - 0.041i	0.011 + 0.015i	0.030 - 0.075i	0.092 - 0.017i	-0.27 - 0.06i
$\mathbf{x}_{k28}$	0.014 + 0.009i	-0.0110 - 0.0030i	0.0066 - 0.00005i	0.020 + 0.015i	-0.016 - 0.011i	0.076 + 0.040i	0.008 - 0.025i	-0.038 + 0.096i
$\mathbf{x}_{k29}$	0.41 - 0.05i	-0.42 + 0.12i	-0.09 + 0.12i	0.60	-0.33 + 0.02i	-0.28 - 0.007i	-0.13 + 0.07i	0.062 - 0.036i
$\mathbf{x}_{k30}$	0.099 + 0.023i	-0.008 + 0.030i	-0.33 - 0.07i	0.015 + 0.026i	0.36 + 0.08i	-0.26 + 0.08i	0.025 + 0.052i	-0.32 - 0.04i
$\mathbf{x}_{k31}$	0.23 + 0.06i	0.026 - 0.051i	0.084 - 0.021i	0.27 + 0.11i	0.019 + 0.008i	0.27 + 0.18i	0.70	-0.18 - 0.07i
$\mathbf{x}_{k32}$	0.28 - 0.004i	-0.062 + 0.093i	-0.50 + 0.01i	-0.16 - 0.07i	0.39 + 0.03i	-0.048 - 0.105i	0.29 - 0.003i	0.41

Table 7.2: Full EIES data set eigensystem: λ_1 to λ_8

λ_k	9	10	11	12	13	14	15	16
	-0.049	0.047	-0.042	0.041	-0.036	0.033	-0.028	0.017
$\mathbf{x}_{k1}$	-0.021 + 0.042i	-0.024 + 0.033i	0.0022 - 0.0090i	-0.102 + 0.046i	-0.051 + 0.041i	0.049 - 0.006i	-0.011 - 0.019i	-0.003 - 0.022i
$\mathbf{x}_{k2}$	-0.091 - 0.010i	-0.064 + 0.027i	-0.042 - 0.067i	-0.15 + 0.09i	-0.16 + 0.02i	0.133 + 0.026i	-0.12 - 0.13i	0.14 + 0.04i
$\mathbf{x}_{k3}$	0.051 - 0.001i	-0.044 - 0.031i	-0.016 - 0.006i	-0.074 + 0.041i	0.032 - 0.036i	0.028 + 0.029i	0.065 + 0.078i	-0.020 + 0.074i
$\mathbf{x}_{k4}$	0.010 - 0.040i	0.19 - 0.34i	0.59	0.21 - 0.02i	0.17 - 0.03i	0.37	-0.17 - 0.06i	0.092 + 0.062i
$\mathbf{x}_{k5}$	0.086 + 0.070i	-0.043 + 0.012i	0.0060 - 0.0047i	0.035 - 0.031i	-0.075 + 0.113i	-0.021 + 0.009i	-0.020 + 0.085i	0.12 + 0.13i
$\mathbf{x}_{k6}$	0.14 - 0.06i	-0.110 + 0.011i	0.031 - 0.005i	0.10 + 0.16i	0.099 - 0.031i	-0.032 + 0.037i	0.11 - 0.12i	-0.23 - 0.15i
$\mathbf{x}_{k7}$	0.066 + 0.035i	-0.077 - 0.043i	-0.030 + 0.017i	-0.017 + 0.053i	0.121 + 0.066i	-0.061 + 0.031i	0.087 + 0.079i	0.12 + 0.12i
$\mathbf{x}_{k8}$	0.065 + 0.008i	-0.055 + 0.090i	0.056 + 0.027i	-0.033 + 0.001i	-0.036 + 0.014i	0.035 + 0.018i	0.036 + 0.046i	-0.010 - 0.010i
$\mathbf{x}_{k9}$	-0.17 - 0.02i	0.42	-0.25 - 0.12i	0.03 - 0.18i	0.59	-0.15 - 0.17i	0.058 - 0.076i	0.08 + 0.21i
$\mathbf{x}_{k10}$	0.18 +0.007i	0.06 - 0.25i	-0.51 - 0.16i	0.31 - 0.07i	-0.076 - 0.011i	0.32 + 0.03i	-0.18 - 0.12i	-0.17 - 0.02i
$\mathbf{x}_{k11}$	0.15 - 0.04i	-0.117 - 0.073i	0.100 + 0.045i	0.35	-0.106 - 0.050i	-0.28 + 0.08i	-0.04 + 0.21i	-0.13 - 0.10i
$\mathbf{x}_{k12}$	0.119 + 0.013i	0.024 - 0.0002i	0.032 - 0.020i	-0.17 - 0.04i	0.059 - 0.080i	0.049 - 0.035i	0.024 - 0.005i	-0.103 - 0.004i
$\mathbf{x}_{k13}$	0.0001 + 0.120i	0.13 + 0.09i	0.007 + 0.048i	0.031 - 0.099i	0.035 + 0.108i	-0.008 - 0.18i	-0.23 - 0.24i	-0.20 - 0.17i
$\mathbf{x}_{k14}$	0.135 + 0.039i	-0.039 + 0.012i	0.064 - 0.024i	-0.099 + 0.049i	0.063 - 0.047i	0.047 - 0.016i	-0.112 - 0.047i	0.08 + 0.24i
$\mathbf{x}_{k15}$	0.15 - 0.01i	-0.018 + 0.044i	0.007 + 0.028i	-0.21 + 0.09i	0.17 - 0.10i	-0.010 - 0.034i	-0.017 + 0.065i	-0.29 - 0.06i
$\mathbf{x}_{k16}$	0.123 - 0.021i	-0.123 - 0.049i	-0.081 + 0.069i	-0.06 + 0.18i	0.19 + 0.03i	0.108 + 0.005i	0.28 + 0.05i	-0.029 + 0.047i
$\mathbf{x}_{k17}$	-0.043 + 0.069i	-0.095 -0.040i	-0.028 + 0.094i	-0.07 + 0.16i	0.18 + 0.0001i	0.096 - 0.016i	-0.109 + 0.086i	-0.15 - 0.006i
$\mathbf{x}_{k18}$	0.061 + 0.118i	-0.16 - 0.12i	-0.039 - 0.009i	0.24 + 0.05i	0.24 + 0.13i	-0.30 - 0.006i	-0.021 - 0.061i	-0.21 - 0.11i
$\mathbf{x}_{k19}$	-0.021 + 0.001i	0.13 - 0.22i	-0.34 + 0.07i	0.26 + 0.09i	-0.085 + 0.036i	0.31 + 0.14i	0.23 + 0.15i	0.083 + 0.089i
$\mathbf{x}_{k20}$	0.043 + 0.005i	0.011 - 0.023i	0.053 + 0.107i	-0.034 + 0.021i	0.060 + 0.028i	0.087 + 0.099i	0.037 + 0.117i	-0.048 - 0.037i
$\mathbf{x}_{k21}$	0.054 + 0.030i	-0.030 + 0.010i	0.009 - 0.013i	-0.062 + 0.008i	0.050 - 0.003i	0.0085 + 0.0110i	0.013 - 0.021i	-0.060 - 0.005i
$\mathbf{x}_{k22}$	0.55	0.05 + 0.15i	-0.024 - 0.009i	0.11 - 0.13i	0.038 - 0.005i	-0.17 - 0.01i	-0.06 - 0.24i	0.24 + 0.12i
$\mathbf{x}_{k23}$	0.023 + 0.016i	0.002 - 0.092i	0.23 + 0.07i	0.071 - 0.023i	0.126 + 0.005i	0.22 + 0.06i	0.100 + 0.079i	-0.105 + 0.070i
$\mathbf{x}_{k24}$	-0.52 + 0.09i	0.016 + 0.087i	0.064 + 0.040i	0.25 - 0.08i	0.113 - 0.068i	-0.18 + 0.04i	0.09 + 0.15i	0.104 - 0.018i
$\mathbf{x}_{k25}$	0.15 - 0.002i	-0.054 + 0.038i	-0.027 + 0.013i	0.123 + 0.056i	0.025 + 0.134i	-0.16 + 0.04i	0.15 + 0.01i	0.39
$\mathbf{x}_{k26}$	0.122 + 0.020i	-0.091 - 0.004i	0.032 + 0.003i	-0.052 + 0.032i	0.138 + 0.004i	0.020 + 0.022i	0.127 + 0.006i	0.057 - 0.052i
$\mathbf{x}_{k27}$	0.05 - 0.22i	0.31 - 0.13i	-0.0046 + 0.0125i	-0.072 - 0.097i	-0.23 - 0.17i	-0.16 - 0.23i	0.50	-0.26 - 0.08i
$\mathbf{x}_{k28}$	0.022 + 0.035i	0.022 - 0.010i	-0.041 + 0.0001i	-0.068 + 0.025i	0.077 + 0.011i	0.050 + 0.029i	0.013 + 0.103i	0.097 + 0.085i
$\mathbf{x}_{k29}$	-0.076 + 0.025i	0.063 + 0.032i	-0.015 + 0.021i	-0.093 - 0.009i	0.005 + 0.033i	0.013 - 0.036i	0.014 + 0.027i	-0.059 + 0.007i
$\mathbf{x}_{k30}$	-0.13 - 0.10i	-0.31 + 0.14i	-0.16 - 0.08i	-0.14 + 0.09i	0.29 - 0.13i	0.17 + 0.09i	0.06 - 0.17i	0.026 + 0.008i
$\mathbf{x}_{k31}$	-0.038 - 0.068i	-0.10 - 0.10i	0.018 - 0.036i	0.27 - 0.02i	-0.009 - 0.048i	-0.19 + 0.07i	-0.078 + 0.003i	0.032 + 0.011i
$\mathbf{x}_{k32}$	0.14 + 0.03i	0.26 - 0.01i	0.034 - 0.013i	-0.13 - 0.14i	-0.11 + 0.15i	-0.017 - 0.071i	-0.00113 + 0.00034i	0.112 + 0.071i

Table 7.3: Full EIES data set eigensystem: λ_9 to λ_{16}

λ_k	17	18	19	20	21	22	23	24
	-0.016	0.014	-0.013	-0.011	0.010	0.0086	-0.0071	0.0061
$\mathbf{x}_{k1}$	0.023 - 0.031i	-0.018 - 0.013i	-0.021 - 0.009i	-0.024 + 0.022i	-0.021 - 0.012i	-0.031 - 0.021i	0.0050 - 0.0069i	-0.014 + 0.035i
$\mathbf{x}_{k2}$	0.093 - 0.024i	0.0086 + 0.0013i	-0.023 - 0.034i	-0.122 - 0.027i	-0.066 - 0.018i	0.021 - 0.050i	-0.067 + 0.019i	0.041 - 0.020i
$\mathbf{x}_{k3}$	-0.073 + 0.001i	0.21 + 0.05i	-0.28 - 0.11i	0.34	-0.26 + 0.04i	0.052 + 0.032i	-0.29 + 0.08i	-0.028 - 0.091i
$\mathbf{x}_{k4}$	0.09 + 0.22i	0.048 - 0.059i	-0.22 + 0.08i	-0.047 + 0.026i	-0.042 - 0.029i	-0.16 + 0.08i	-0.010 - 0.030i	-0.002 + 0.051i
$\mathbf{x}_{k5}$	-0.088 + 0.030i	0.11 - 0.19i	-0.011 + 0.028i	-0.15 - 0.08i	-0.16 + 0.02i	0.050 - 0.015i	0.14 - 0.31i	0.50
$\mathbf{x}_{k6}$	0.43	-0.133 + 0.046i	-0.06 - 0.21i	-0.19 - 0.13i	-0.022 - 0.072i	0.0135 - 0.0031i	-0.06 + 0.16i	-0.07 + 0.18i
$\mathbf{x}_{k7}$	-0.049 + 0.055i	0.0001 + 0.032i	-0.053 - 0.010i	0.04 + 0.29i	-0.06 - 0.20i	0.014 - 0.068i	0.04 + 0.15i	0.35 + 0.23i
$\mathbf{x}_{k8}$	-0.018 - 0.017i	-0.0005 - 0.0035i	0.008 + 0.015i	0.053 - 0.013i	0.0098 + 0.0034i	0.0047 + 0.0073i	0.018 + 0.005i	0.00006 - 0.0026i
$\mathbf{x}_{k9}$	0.076 + 0.026i	-0.13 + 0.09i	0.027 - 0.035i	-0.003 - 0.111i	0.050 - 0.017i	0.068 + 0.065i	-0.004 - 0.022i	-0.023 + 0.015i
$\mathbf{x}_{k10}$	-0.21 + 0.32i	-0.127 + 0.001i	-0.16 - 0.02i	0.010 + 0.054i	-0.036 - 0.034i	0.15 - 0.15i	0.060 - 0.023i	-0.066 - 0.017i
$\mathbf{x}_{k11}$	-0.16 - 0.01i	-0.09 + 0.21i	0.085 + 0.062i	0.15 - 0.10i	0.037 + 0.036i	0.043 + 0.064i	0.0072 - 0.0001i	-0.034 - 0.017i
$\mathbf{x}_{k12}$	0.047 + 0.067i	0.079 + 0.050i	-0.098 - 0.004i	-0.16 + 0.04i	0.42	-0.069 + 0.116i	-0.14 + 0.13i	0.27 - 0.18i
$\mathbf{x}_{k13}$	0.050 - 0.128i	0.39	-0.010 + 0.044i	0.31 - 0.05i	-0.18 - 0.06i	0.13 + 0.08i	-0.31 + 0.07i	0.036 + 0.061i
$\mathbf{x}_{k14}$	0.071 + 0.116i	0.26 + 0.07i	0.27 - 0.19i	0.17 + 0.20i	0.08 + 0.34i	-0.01 + 0.25i	0.39	-0.30 - 0.03i
$\mathbf{x}_{k15}$	-0.24 + 0.03i	-0.004 - 0.062i	0.03 + 0.18i	0.13 - 0.08i	0.28 - 0.21i	-0.33 + 0.05i	-0.015 - 0.059i	0.082 + 0.082i
$\mathbf{x}_{k16}$	-0.05 - 0.22i	-0.19 + 0.21i	-0.32 + 0.12i	-0.037 - 0.111i	-0.13 + 0.29i	0.11 + 0.24i	0.15 - 0.13i	-0.0052 + 0.0128i
$\mathbf{x}_{k17}$	-0.15 + 0.05i	0.006 - 0.17i	0.39	-0.19 + 0.21i	-0.19 + 0.15i	0.23 + 0.05i	-0.18 - 0.17i	-0.06 + 0.17i
$\mathbf{x}_{k18}$	0.107 - 0.021i	0.27 - 0.13i	-0.12 - 0.17i	-0.17 + 0.16i	-0.012 + 0.018i	-0.21 - 0.06i	0.18 - 0.15i	-0.02 - 0.17i
$\mathbf{x}_{k19}$	0.17 - 0.33i	0.19 - 0.11i	0.30 + 0.03i	0.095 - 0.048i	0.16 + 0.05i	-0.30 + 0.12i	-0.16 + 0.09i	0.070 - 0.008i
$\mathbf{x}_{k20}$	0.16 - 0.06i	-0.039 - 0.061i	0.002 + 0.089i	0.15 + 0.004i	-0.040 - 0.090i	0.36	-0.022 + 0.020i	-0.033 - 0.102i
$\mathbf{x}_{k21}$	0.0001 + 0.048i	-0.10 + 0.11i	0.080 - 0.056i	-0.029 + 0.064i	-0.034 + 0.112i	0.15 + 0.22i	-0.18 + 0.19i	0.21 + 0.06i
$\mathbf{x}_{k22}$	0.16 - 0.14i	-0.010 - 0.027i	0.19 + 0.03i	-0.069 - 0.094i	-0.15 - 0.10i	0.007 - 0.084i	-0.067 - 0.055i	0.017 - 0.009i
$\mathbf{x}_{k23}$	0.12 - 0.26i	-0.013 - 0.058i	0.17 + 0.05i	-0.050 + 0.085i	0.005 - 0.050i	0.18 - 0.28i	-0.028 - 0.075i	0.005 - 0.047i
$\mathbf{x}_{k24}$	-0.035 + 0.034i	-0.009 - 0.018i	-0.008 + 0.020i	0.044 - 0.012i	-0.097 - 0.043i	0.007 - 0.020i	-0.0031 + 0.0128i	-0.033 - 0.012i
$\mathbf{x}_{k25}$	-0.083 + 0.114i	0.12 - 0.16i	-0.17 + 0.21i	-0.15 + 0.22i	-0.018 + 0.050i	-0.044 + 0.056i	-0.16 + 0.29i	-0.16 + 0.22i
$\mathbf{x}_{k26}$	-0.041 + 0.017i	-0.139 - 0.016i	0.059 + 0.063i	0.067 - 0.007i	-0.04 - 0.22i	-0.05 - 0.21i	0.040 - 0.025i	-0.25 - 0.03i
$\mathbf{x}_{k27}$	0.014 + 0.077i	0.18 - 0.25i	-0.054 + 0.029i	-0.05 + 0.24i	-0.14 + 0.08i	0.049 - 0.035i	0.072 - 0.076i	-0.032 + 0.058i
$\mathbf{x}_{k28}$	-0.15 - 0.04i	0.006 + 0.033i	0.063 + 0.092i	0.22 + 0.13i	-0.07 - 0.15i	-0.011 - 0.123i	0.15 + 0.03i	0.026 + 0.118i
$\mathbf{x}_{k29}$	0.010 + 0.018i	-0.005 + 0.018i	-0.014 - 0.009i	0.039 + 0.019i	0.054 + 0.009i	0.0003 + 0.0139i	0.024 - 0.009i	0.002 - 0.027i
$\mathbf{x}_{k30}$	0.027 + 0.093i	0.24 - 0.18i	-0.038 - 0.052i	-0.048 - 0.073i	-0.039 - 0.040i	-0.021 - 0.110i	-0.001 + 0.071i	0.066 - 0.003i
$\mathbf{x}_{k31}$	-0.042 - 0.008i	0.063 + 0.041i	0.112 + 0.003i	-0.003 - 0.097i	0.094 - 0.022i	-0.032 + 0.033i	-0.071 + 0.042i	0.017 - 0.092i
$\mathbf{x}_{k32}$	0.011 - 0.024i	-0.073 + 0.075i	0.0001 + 0.017i	0.027 + 0.025i	0.050 - 0.024i	0.022 + 0.022i	0.022 - 0.024i	0.000132 - 0.000028i

Table 7.4: Full EIES data set eigensystem: λ_{17} to λ_{24}

λ_k	25	26	27	28	29	30	31	32
	-0.0052	0.0045	-0.0035	0.0025	0.0017	-0.00090	0.00025	0.000074
$\mathbf{x}_{k1}$	-0.0121 + 0.0017i	0.012 + 0.020i	0.0021 + 0.0053i	0.021 - 0.006i	-0.0043 + 0.0064i	-0.018 + 0.005i	-0.016 + 0.014i	0.011 + 0.014i
$\mathbf{x}_{k2}$	-0.016 + 0.048i	0.002 + 0.034i	-0.048 + 0.045i	0.0116 - 0.0032i	-0.010 - 0.022i	0.001 + 0.015i	0.070 - 0.036i	0.0027 - 0.0093i
$\mathbf{x}_{k3}$	0.068 - 0.070i	0.50	-0.074 + 0.104i	-0.117 - 0.068i	0.12 + 0.19i	-0.18 + 0.06i	-0.17 - 0.15i	-0.32 + 0.05i
$\mathbf{x}_{k4}$	-0.058 - 0.005i	-0.13 + 0.13i	-0.013 + 0.035i	-0.031 - 0.016i	-0.001 - 0.047i	-0.110 + 0.014i	-0.041 + 0.008i	-0.050 + 0.064i
$\mathbf{x}_{k5}$	0.48	-0.065 - 0.089i	0.11 - 0.27i	-0.098 + 0.059i	-0.04 + 0.15i	-0.084 + 0.073i	-0.24 + 0.05i	-0.025 + 0.008i
$\mathbf{x}_{k6}$	0.14 - 0.10i	-0.02 + 0.19i	0.13 - 0.10i	-0.16 + 0.28i	0.23 + 0.16i	0.18 - 0.12i	-0.27 - 0.07i	-0.009 - 0.069i
$\mathbf{x}_{k7}$	-0.19 - 0.31i	-0.019 - 0.019i	-0.04 + 0.32i	-0.081 - 0.101i	-0.20 - 0.03i	0.41	-0.20 + 0.04i	0.13 + 0.08i
$\mathbf{x}_{k8}$	-0.0007 - 0.022i	-0.0101 + 0.0010i	-0.0053 + 0.0067i	0.0091 - 0.0007i	-0.009 + 0.015i	0.016 + 0.008i	-0.0025 - 0.0051i	-0.0048 - 0.0039i
$\mathbf{x}_{k9}$	0.068 + 0.044i	0.089 - 0.049i	0.071 - 0.083i	-0.048 + 0.005i	-0.013 + 0.029i	-0.027 - 0.051i	-0.072 - 0.011i	0.050 + 0.025i
$\mathbf{x}_{k10}$	0.008 - 0.030i	0.042 - 0.064i	0.017 - 0.002i	0.028 + 0.015i	-0.010 + 0.031i	0.041 - 0.057i	0.047 + 0.003i	0.060 - 0.053i
$\mathbf{x}_{k11}$	0.004 - 0.061i	-0.039 - 0.071i	0.015 - 0.087i	-0.018 - 0.025i	0.013 + 0.027i	0.078 - 0.067i	-0.027 + 0.034i	-0.033 - 0.022i
$\mathbf{x}_{k12}$	0.13 + 0.18i	0.13 - 0.16i	0.120 - 0.023i	-0.09 - 0.17i	0.06 - 0.20i	0.29 - 0.17i	0.19 + 0.08i	-0.34 - 0.07i
$\mathbf{x}_{k13}$	0.071 + 0.001i	-0.27 - 0.08i	-0.07 - 0.13i	0.05 + 0.16i	-0.17 - 0.09i	0.18 + 0.10i	0.06 + 0.13i	0.04 - 0.14i
$\mathbf{x}_{k14}$	0.15 - 0.20i	0.081 - 0.043i	0.0036 + 0.0062i	0.057 + 0.083i	-0.022 + 0.068i	0.098 - 0.041i	-0.082 + 0.083i	0.062 - 0.113i
$\mathbf{x}_{k15}$	-0.098 - 0.051i	0.13 + 0.07i	-0.091 - 0.102i	-0.036 + 0.108i	0.020 + 0.058i	-0.29 + 0.06i	-0.115 + 0.076i	0.34 - 0.01i
$\mathbf{x}_{k16}$	0.001 + 0.141i	-0.24 + 0.01i	-0.24 + 0.05i	-0.036 + 0.071i	-0.18 - 0.03i	0.003 + 0.053i	0.15 - 0.08i	-0.065 - 0.043i
$\mathbf{x}_{k17}$	-0.25 + 0.16i	0.012 - 0.049i	0.004 - 0.105i	-0.24 - 0.01i	0.11 - 0.19i	-0.07 - 0.19i	-0.13 + 0.13i	-0.18 + 0.11i
$\mathbf{x}_{k18}$	0.008 + 0.055i	0.017 - 0.112i	0.06 + 0.21i	0.08 - 0.15i	0.097 - 0.081i	-0.12 + 0.19i	0.14 - 0.04i	0.009 + 0.029i
$\mathbf{x}_{k19}$	0.020 - 0.003i	-0.09 + 0.12i	0.013 + 0.033i	0.004 - 0.058i	-0.045 + 0.022i	-0.044 + 0.031i	-0.083 + 0.028i	-0.067 + 0.045i
$\mathbf{x}_{k20}$	0.34 + 0.18i	-0.014 + 0.073i	-0.08 + 0.23i	0.18 - 0.36i	0.31 - 0.17i	-0.04 - 0.16i	-0.13 + 0.14i	0.40
$\mathbf{x}_{k21}$	-0.08 - 0.29i	-0.23 - 0.12i	0.47	0.35 - 0.14i	0.046 + 0.048i	-0.37 + 0.03i	0.08 - 0.23i	-0.009 + 0.018i
$\mathbf{x}_{k22}$	-0.18 + 0.10i	0.006 + 0.043i	-0.11 + 0.18i	-0.094 - 0.022i	0.027 - 0.083i	-0.15 + 0.05i	0.045 - 0.076i	-0.05 + 0.14i
$\mathbf{x}_{k23}$	-0.104 + 0.040i	0.29 - 0.36i	0.001 - 0.19i	0.14 + 0.07i	-0.07 + 0.30i	0.19 + 0.07i	0.22 - 0.25i	0.18 - 0.04i
$\mathbf{x}_{k24}$	-0.008 - 0.035i	-0.042 + 0.021i	-0.017 + 0.015i	-0.034 - 0.004i	0.013 - 0.007i	0.012 - 0.010i	-0.015 - 0.015i	-0.052 + 0.037i
$\mathbf{x}_{k25}$	0.038 + 0.110i	0.121 + 0.053i	0.001 - 0.33i	0.063 - 0.037i	0.0049 + 0.0018i	-0.06 - 0.15i	0.117 + 0.005i	0.15 - 0.30i
$\mathbf{x}_{k26}$	0.08 + 0.14i	0.005 + 0.047i	0.21 - 0.06i	0.48	-0.25 - 0.03i	0.057 + 0.124i	-0.25 + 0.30i	-0.39 + 0.05i
$\mathbf{x}_{k27}$	-0.060 + 0.005i	-0.067 + 0.066i	0.047 + 0.036i	0.035 + 0.007i	-0.0031 + 0.0068i	0.008 + 0.013i	-0.0005 + 0.0062i	-0.0037 + 0.0008i
$\mathbf{x}_{k28}$	0.094 + 0.013i	-0.12 + 0.22i	0.20 - 0.01i	-0.07 + 0.25i	0.55	0.13 + 0.22i	0.41	-0.13 + 0.09i
$\mathbf{x}_{k29}$	-0.010 - 0.017i	-0.005 - 0.021i	-0.003 + 0.019i	0.014 - 0.005i	-0.0056 - 0.0023i	0.011 + 0.012i	0.0111 - 0.0029i	-0.011 - 0.011i
$\mathbf{x}_{k30}$	0.021 + 0.012i	-0.066 + 0.069i	-0.056 + 0.035i	0.095 + 0.031i	-0.069 + 0.021i	-0.054 + 0.050i	0.100 - 0.027i	0.084 - 0.030i
$\mathbf{x}_{k31}$	0.0102 + 0.0065i	0.019 - 0.022i	-0.035 - 0.021i	-0.035 + 0.010i	0.016 - 0.041i	0.005 - 0.019i	0.039 - 0.004i	0.017 - 0.011i
$\mathbf{x}_{k32}$	0.0082 - 0.0054i	0.076 - 0.044i	0.023 + 0.006i	-0.017 - 0.0002i	0.026 + 0.009i	-0.006 + 0.034i	-0.015 - 0.0002i	0.029 - 0.001i

Table 7.5: Full EIES data set eigensystem: λ_{25} to λ_{32}

λ_k	1	1	0.3	0.3	0.24	0.24	0.17	0.17
$\mathbf{x}_{k1}$	0.45	0.31	-0.1	-0.024	0.34	0.03	-0.036	0.35
$\mathbf{x}_{k2}$	0.015	-0.1	-0.2	-0.2	-0.011	0.015	-0.22	-0.028
$\mathbf{x}_{k3}$	-0.14	-0.39	0.033	-0.14	0.39	-0.16	0.034	0.091
$\mathbf{x}_{k4}$	-0.019	0.36	-0.034	-0.25	0.05	-0.23	0.06	-0.21
$\mathbf{x}_{k5}$	-0.33	0.18	-0.018	-0.087	0.26	-0.11	-0.086	-0.15
$\mathbf{x}_{k6}$	0.02	0.12	-0.096	0.25	-0.26	-0.2	-0.031	0.046
$\mathbf{x}_{k7}$	0.29	-0.24	0.14	0.0061	0.26	-0.48	-0.11	-0.0021
$\mathbf{x}_{k8}$	-0.057	-0.032	-0.099	-0.0075	-0.14	0.14	0.092	0.47
$\mathbf{x}_{k9}$	0.14	-0.22	-0.12	-0.34	-0.048	0.043	-0.051	-0.15
$\mathbf{x}_{k10}$	-0.036	0.076	0.19	0.53	0.065	-0.2	-0.00097	-0.033
$\mathbf{x}_{k11}$	-0.0061	-0.1	0.018	0.05	-0.36	-0.28	-0.092	0.28
$\mathbf{x}_{k12}$	0.15	0.19	0.19	-0.2	-0.17	0.044	-0.0043	0.00085
$\mathbf{x}_{k13}$	0.19	0.22	0.02	0.016	-0.016	0.034	-0.023	0.056
$\mathbf{x}_{k14}$	-0.0064	-0.072	0.16	-0.3	-0.15	-0.013	-0.037	0.15
$\mathbf{x}_{k15}$	0.17	0.019	0.0078	-0.18	-0.39	-0.3	-0.075	-0.016
$\mathbf{x}_{k16}$	0.23	-0.22	-0.22	0.25	0.15	0.1	0.066	-0.049
$\mathbf{x}_{k17}$	0.004	-0.059	-0.2	0.11	-0.03	0.055	0.036	-0.29
$\mathbf{x}_{k18}$	0.2	-0.081	-0.12	0.026	-0.16	0.43	0.064	-0.1
$\mathbf{x}_{k19}$	-0.13	-0.22	-0.37	0.037	0.026	-0.14	-0.023	-0.028
$\mathbf{x}_{k20}$	0.031	0.058	-0.25	-0.14	-0.14	-0.038	0.26	0.023
$\mathbf{x}_{k21}$	0.0046	0.19	-0.33	-0.073	0.11	-0.27	-0.019	0.27
$\mathbf{x}_{k22}$	-0.042	-0.12	-0.03	0.29	-0.14	0.057	-0.12	-0.02
$\mathbf{x}_{k23}$	0.052	-0.12	0.1	-0.21	0.095	0.17	-0.063	0.14
$\mathbf{x}_{k24}$	0.16	-0.23	0.48	-0.043	-0.024	0.021	0.022	0.076
$\mathbf{x}_{k25}$	-0.072	-0.059	0.18	-0.16	-0.05	-0.022	-0.22	-0.19
$\mathbf{x}_{k26}$	-0.25	0.063	0.037	-0.065	0.08	0.062	0.14	0.24
$\mathbf{x}_{k27}$	0.022	0.0073	-0.097	0.067	0.095	-0.06	0.049	-0.16
$\mathbf{x}_{k28}$	0.29	-0.075	-0.067	-0.08	-0.073	-0.18	-0.048	-0.28
$\mathbf{x}_{k29}$	-0.31	-0.16	-0.12	-0.024	-0.2	-0.036	-0.19	0.2
$\mathbf{x}_{k30}$	0.022	0.25	0.081	0.048	-0.028	-0.021	-0.35	-0.092
$\mathbf{x}_{k31}$	0.13	-0.016	-0.12	0.084	0.14	0.24	-0.68	0.069
$\mathbf{x}_{k32}$	-0.098	0.055	-0.0044	-0.12	0.088	-0.099	-0.22	-0.14

Table 7.6: Full EIES data set eigensystem according to Freeman λ_1 to λ_8

λ_k	0.15	0.15	0.088	0.088	0.067	0.067	0.043	0.043
$\mathbf{x}_{k1}$	-0.012	0.1	0.23	-0.076	-0.065	-0.018	0.056	-0.012
$\mathbf{x}_{k2}$	-0.25	-0.21	0.074	-0.26	-0.18	-0.21	-0.054	-0.26
$\mathbf{x}_{k3}$	-0.15	0.27	-0.15	0.038	0.065	0.055	-0.015	-0.024
$\mathbf{x}_{k4}$	0.18	-0.17	-0.13	-0.21	0.078	-0.027	-0.052	0.011
$\mathbf{x}_{k5}$	0.048	-0.012	-0.14	0.078	0.22	0.092	-0.06	-0.095
$\mathbf{x}_{k6}$	0.027	0.27	-0.53	-0.0069	-0.1	-0.12	-0.31	-0.064
$\mathbf{x}_{k7}$	0.054	-0.0015	0.17	0.12	0.19	0.11	-0.065	-0.042
$\mathbf{x}_{k8}$	0.083	-0.0071	0.14	-0.15	0.00041	-0.047	-0.29	0.013
$\mathbf{x}_{k9}$	-0.18	-0.47	-0.16	0.01	-0.0075	0.0027	-0.069	0.16
$\mathbf{x}_{k10}$	-0.14	-0.52	0.14	-0.0063	0.11	0.13	-0.12	-0.12
$\mathbf{x}_{k11}$	-0.15	-0.047	0.011	0.21	0.066	-0.11	0.27	0.12
$\mathbf{x}_{k12}$	0.19	-0.012	0.056	-0.22	0.2	0.16	0.25	0.24
$\mathbf{x}_{k13}$	-0.2	-0.11	-0.23	0.0076	-0.065	0.14	0.16	-0.44
$\mathbf{x}_{k14}$	-0.15	-0.0087	-0.19	0.044	-0.04	0.41	0.07	-0.17
$\mathbf{x}_{k15}$	-0.1	0.14	0.19	-0.0045	0.25	0.16	-0.23	-0.26
$\mathbf{x}_{k16}$	0.31	-0.21	-0.38	0.13	0.14	-0.16	0.38	0.089
$\mathbf{x}_{k17}$	0.22	0.16	0.31	-0.076	0.028	-0.0049	0.071	-0.5
$\mathbf{x}_{k18}$	-0.017	0.083	0.025	0.34	0.0066	0.39	-0.095	-0.079
$\mathbf{x}_{k19}$	0.22	-0.073	-0.018	-0.19	-0.17	0.31	-0.14	0.0095
$\mathbf{x}_{k20}$	-0.041	-0.15	0.21	0.41	-0.036	-0.3	-0.14	0.095
$\mathbf{x}_{k21}$	0.048	-0.053	-0.11	0.06	-0.39	0.1	0.21	-0.06
$\mathbf{x}_{k22}$	-0.24	0.034	0.026	-0.36	-0.053	0.11	0.17	0.15
$\mathbf{x}_{k23}$	0.29	-0.1	-0.17	-0.017	0.24	-0.21	-0.04	-0.24
$\mathbf{x}_{k24}$	0.45	-0.14	-0.1	0.00077	-0.43	-0.12	-0.076	-0.17
$\mathbf{x}_{k25}$	-0.027	-0.013	0.15	0.081	-0.28	-0.15	0.067	-0.11
$\mathbf{x}_{k26}$	0.15	-0.19	-0.013	0.016	0.086	0.34	-0.19	0.093
$\mathbf{x}_{k27}$	0.089	-0.027	0.09	0.13	-0.19	0.34	0.2	0.077
$\mathbf{x}_{k28}$	0.099	0.18	-0.0031	-0.24	-0.083	0.12	-0.18	0.3
$\mathbf{x}_{k29}$	0.3	-0.027	0.13	-0.17	0.11	0.03	0.3	-0.092
$\mathbf{x}_{k30}$	0.11	0.018	0.0057	0.42	-0.075	0.015	-0.2	0.11
$\mathbf{x}_{k31}$	0.015	-0.057	-0.044	-0.017	0.037	0.034	-0.19	0.11
$\mathbf{x}_{k32}$	-0.12	0.13	0.072	0.22	-0.046	-0.045	0.21	0.079

Table 7.7: Full EIES data set eigensystem according to Freeman λ_9 to λ_{16}

λ_k	0.03	0.03	0.021	0.021	0.012	0.012	0.012	0.012
$\mathbf{x}_{k1}$	0.051	0.046	-0.066	-0.049	-0.061	-0.057	-0.026	0.34
$\mathbf{x}_{k2}$	-0.28	-0.16	-0.17	-0.22	-0.22	-0.24	-0.25	-0.065
$\mathbf{x}_{k3}$	0.19	0.13	-0.24	-0.039	0.017	-0.074	-0.014	-0.1
$\mathbf{x}_{k4}$	-0.069	0.068	-0.18	-0.0065	0.023	-0.016	-0.034	-0.21
$\mathbf{x}_{k5}$	-0.0078	-0.29	0.1	0.16	-0.075	0.086	0.12	0.53
$\mathbf{x}_{k6}$	-0.053	-0.068	-0.021	-0.058	-0.11	-0.092	-0.094	0.13
$\mathbf{x}_{k7}$	-0.19	-0.3	0.021	0.041	0.15	0.036	0.015	-0.15
$\mathbf{x}_{k8}$	-0.079	0.2	0.14	-0.13	-0.016	0.022	-0.023	0.35
$\mathbf{x}_{k9}$	0.31	0.12	-0.016	0.14	-0.085	0.14	0.12	0.31
$\mathbf{x}_{k10}$	-0.083	0.23	-0.066	0.0066	0.13	-0.12	-0.071	0.094
$\mathbf{x}_{k11}$	0.24	-0.32	-0.25	0.044	-0.035	-0.046	-0.068	0.13
$\mathbf{x}_{k12}$	0.0019	-0.12	-0.093	-0.16	0.024	0.16	0.05	-0.003
$\mathbf{x}_{k13}$	0.36	-0.0044	-0.026	0.091	0.24	-0.16	-0.015	-0.078
$\mathbf{x}_{k14}$	-0.55	0.047	-0.18	0.014	0.055	0.19	-0.037	0.15
$\mathbf{x}_{k15}$	0.22	0.2	0.32	-0.028	-0.3	0.065	0.077	-0.15
$\mathbf{x}_{k16}$	-0.19	-0.0091	-0.041	-0.36	0.009	-0.026	-0.032	0.12
$\mathbf{x}_{k17}$	0.15	-0.15	-0.32	-0.017	-0.045	0.28	-0.11	0.18
$\mathbf{x}_{k18}$	-0.036	-0.064	-0.049	-0.0027	0.18	-0.17	-0.017	0.018
$\mathbf{x}_{k19}$	0.083	0.13	0.046	-0.16	0.2	0.21	0.12	-0.035
$\mathbf{x}_{k20}$	-0.13	-0.16	-0.066	0.24	0.069	0.045	-0.14	-0.06
$\mathbf{x}_{k21}$	0.047	-0.023	0.17	0.044	0.13	0.12	0.073	-0.16
$\mathbf{x}_{k22}$	0.0037	-0.21	0.26	0.11	0.13	0.34	-0.33	0.023
$\mathbf{x}_{k23}$	0.02	-0.042	0.36	0.3	0.2	0.0047	-0.42	-0.064
$\mathbf{x}_{k24}$	0.1	0.022	0.004	0.21	-0.13	0.15	-0.16	0.039
$\mathbf{x}_{k25}$	0.013	-0.19	0.39	-0.39	0.27	-0.2	0.24	0.18
$\mathbf{x}_{k26}$	0.31	-0.25	-0.1	-0.33	-0.17	-0.11	-0.4	-0.13
$\mathbf{x}_{k27}$	-0.11	-0.085	0.28	0.24	-0.52	-0.26	-0.12	0.015
$\mathbf{x}_{k28}$	0.071	0.0074	-0.1	0.12	0.29	-0.37	-0.25	0.21
$\mathbf{x}_{k29}$	-0.025	0.19	-0.095	0.27	0.045	-0.41	0.14	0.06
$\mathbf{x}_{k30}$	-0.0071	0.042	-0.069	-0.16	0.14	0.23	-0.15	-0.043
$\mathbf{x}_{k31}$	0.047	-0.091	-0.096	0.11	-0.2	0.099	0.12	-0.19
$\mathbf{x}_{k32}$	0.041	0.46	0.029	-0.14	-0.049	0.13	-0.48	0.13

Table 7.8: Full EIES data set eigensystem according to Freeman λ_{17} to λ_{24}

λ_k	0.004	0.004	0.0028	0.0028	0.0006	0.0006	0.000017	0.000017
$\mathbf{x}_{k1}$	0.04	0.04	0.0035	-0.07	0.33	-0.0077	0.36	-0.017
$\mathbf{x}_{k2}$	-0.13	-0.14	-0.17	-0.13	0.19	-0.18	-0.19	-0.010
$\mathbf{x}_{k3}$	0.16	-0.078	-0.28	0.011	0.14	0.33	-0.04	-0.35
$\mathbf{x}_{k4}$	0.11	0.12	-0.27	0.18	-0.21	-0.026	0.31	-0.45
$\mathbf{x}_{k5}$	-0.12	-0.053	-0.32	0.17	0.12	-0.13	-0.14	0.14
$\mathbf{x}_{k6}$	0.15	-0.063	0.38	0.022	0.19	0.0054	0.0045	-0.23
$\mathbf{x}_{k7}$	0.12	-0.16	0.25	0.048	-0.099	-0.36	0.0027	-0.033
$\mathbf{x}_{k8}$	0.16	0.025	-0.21	0.022	-0.43	0.017	-0.29	-0.20
$\mathbf{x}_{k9}$	0.057	-0.25	0.26	-0.15	-0.075	-0.031	0.11	-0.14
$\mathbf{x}_{k10}$	-0.15	0.058	0.033	0.069	0.17	0.26	-0.1	-0.13
$\mathbf{x}_{k11}$	-0.23	0.4	-0.14	-0.086	-0.1	-0.063	0.08	-0.14
$\mathbf{x}_{k12}$	0.099	-0.07	0.11	0.00046	0.34	0.11	-0.53	-0.21
$\mathbf{x}_{k13}$	0.44	0.068	-0.12	-0.014	-0.11	-0.16	-0.24	0.17
$\mathbf{x}_{k14}$	0.042	0.14	0.082	-0.0055	-0.052	0.25	0.19	0.18
$\mathbf{x}_{k15}$	-0.11	-0.071	-0.17	0.083	0.16	0.11	0.079	0.10
$\mathbf{x}_{k16}$	0.09	-0.035	-0.14	0.063	-0.11	0.055	0.022	0.11
$\mathbf{x}_{k17}$	-0.015	-0.023	0.2	-0.035	-0.2	0.23	-0.00094	-0.095
$\mathbf{x}_{k18}$	-0.25	-0.11	-0.12	0.23	0.097	-0.24	0.034	-0.39
$\mathbf{x}_{k19}$	0.014	0.44	-0.026	-0.21	0.28	-0.27	-0.011	0.029
$\mathbf{x}_{k20}$	0.35	-0.058	-0.059	0.29	0.21	0.25	-0.069	0.11
$\mathbf{x}_{k21}$	-0.42	-0.28	0.077	0.14	-0.13	0.21	-0.17	-0.064
$\mathbf{x}_{k22}$	0.22	-0.23	-0.23	0.1	0.064	-0.0023	0.25	-0.099
$\mathbf{x}_{k23}$	-0.19	0.2	0.083	-0.16	0.12	0.11	0.0054	-0.13
$\mathbf{x}_{k24}$	-0.081	0.018	-0.18	0.14	0.15	-0.073	-0.0069	-0.0030
$\mathbf{x}_{k25}$	0.14	0.15	0.069	0.11	0.021	0.23	0.12	-0.17
$\mathbf{x}_{k26}$	0.021	-0.13	0.15	0.098	-0.04	0.023	0.15	0.22
$\mathbf{x}_{k27}$	0.22	0.16	0.0086	-0.25	-0.096	0.11	-0.1	-0.19
$\mathbf{x}_{k28}$	-0.14	0.012	-0.1	0.037	-0.15	0.21	-0.093	0.29
$\mathbf{x}_{k29}$	0.14	-0.21	0.14	0.21	0.13	-0.092	0.16	0.028
$\mathbf{x}_{k30}$	0.052	-0.21	-0.26	-0.54	-0.05	0.072	-0.015	-0.014
$\mathbf{x}_{k31}$	0.058	0.24	0.055	0.34	-0.094	0.18	-0.079	0.036
$\mathbf{x}_{k32}$	0.019	0.15	0.18	0.34	-0.021	-0.24	-0.14	-0.017

Table 7.9: Full EIES data set eigensystem according to Freeman λ_{25} to λ_{32}

	1	2	3	4	5	6	7	8
1	6.5 + 6.5i	470 + 340i	24. + 4.i	68. + 55.i	19. + 26.i	64. + 66.i	40. + 14.i	390 + 220i
2	340 + 470i	29. + 29.i	5.7 + 1.6i	18. + 25.i	10.1 + 5.9i	10. + 18.i	7.0 - 1.8i	40 + 150i
3	4. + 24.i	1.6 + 5.7i	0.30 + 0.30i	0.3 + 1.9i	0.25 + 0.65i	0.08 + 1.5i	0.47 + 0.32i	0.1 + 9.4i
4	55. + 68.i	25. + 18.i	1.9 + 0.3i	5.9 + 5.9i	2.4 + 1.9i	4.4 + 5.4i	2.8 + 0.2i	25. + 31.i
5	26. + 19.i	5.9 + 10.1i	0.65 + 0.25i	1.9 + 2.4i	0.67 + 0.67i	1.2 + 2.3i	0.81 + 0.34i	9. + 13.i
6	66. + 64.i	18. + 10.i	1.5 + 0.08i	5.4 + 4.4i	2.3 + 1.2i	3.9 + 3.9i	2.1 - 0.3i	21. + 25.i
7	14. + 40.i	-1.8 + 7.0i	0.32 + 0.47i	0.2 + 2.8i	0.34 + 0.81i	-0.3 + 2.1i	0.40 + 0.40i	-2. + 15.i
8	220 + 390i	150 + 40i	9.4 + 0.1i	31. + 25.i	13. + 9.i	25. + 21.i	15. - 2.i	120 + 120i
9	22. + 90.i	24. + 24.i	1.9 + 0.8i	4.3 + 7.7i	1.9 + 2.8i	3.2 + 6.7i	3.0 + 1.0i	15. + 36.i
10	39. + 50.i	37. + 36.i	2.6 + 0.7i	7.0 + 7.9i	2.3 + 2.9i	5.6 + 8.1i	3.9 + 1.4i	34. + 38.i
11	200 + 170i	54. + 58.i	5.1 + 1.2i	16. + 17.i	6.3 + 4.7i	11. + 16.i	6.7 + 1.0i	68. + 95.i
12	-7. + 24.i	28. + 26.i	1.6 + 0.6i	3.6 + 5.2i	1.1 + 2.3i	3.3 + 5.4i	2.7 + 1.3i	20. + 22.i
13	3. + 21.i	3. + 15.i	0.54 + 0.61i	0.5 + 3.2i	0.14 + 1.13i	0.1 + 3.0i	0.77 + 0.98i	2. + 16.i
14	4. + 40.i	17. + 19.i	1.24 + 0.59i	2.6 + 4.8i	1.0 + 1.9i	2.1 + 4.5i	2.0 + 0.9i	12. + 22.i
15	100. + 70.i	14. + 16.i	1.7 + 0.3i	6.3 + 5.7i	2.5 + 1.2i	3.9 + 5.0i	2.0 - 0.1i	25. + 35.i
16	49. + 67.i	22. + 32.i	2.0 + 0.9i	5.1 + 7.9i	1.9 + 2.6i	3.4 + 7.4i	2.9 + 1.3i	22. + 41.i
17	65. + 74.i	12. + 19.i	1.5 + 0.6i	4.3 + 6.2i	1.9 + 1.7i	2.5 + 5.3i	1.9 + 0.5i	15. + 35.i
18	61. + 75.i	4.0 + 8.1i	0.99 + 0.38i	3.1 + 4.6i	1.6 + 1.1i	1.5 + 3.4i	1.15 - 0.08i	8. + 27.i
19	9. + 36.i	3.4 + 7.4i	0.48 + 0.37i	0.8 + 2.7i	0.49 + 0.90i	0.4 + 2.1i	0.74 + 0.37i	1.2 + 13.3i
20	-1. + 27.i	2.6 + 7.1i	0.35 + 0.37i	0.3 + 2.2i	0.23 + 0.81i	0.08 + 1.8i	0.59 + 0.45i	-0.3 + 10.4i
21	5. + 16.i	6. + 15.i	0.60 + 0.53i	0.9 + 3.0i	0.24 + 1.07i	0.5 + 2.9i	0.87 + 0.89i	5. + 15.i
22	6. + 41.i	17. + 35.i	1.5 + 1.2i	2.5 + 7.2i	0.7 + 2.7i	1.7 + 7.0i	2.3 + 2.0i	13. + 34.i
23	3. + 27.i	8.2 + 9.6i	0.64 + 0.34i	1.3 + 2.7i	0.54 + 1.01i	1.0 + 2.4i	1.04 + 0.47i	4.9 + 12.3i
24	72. + 120.i	82. + 55.i	5.1 + 0.8i	15. + 14.i	5.4 + 5.4i	12. + 14.i	8.1 + 1.4i	69. + 66.i
25	33. + 38.i	-0.2 + 4.6i	0.44 + 0.23i	1.4 + 2.3i	0.73 + 0.49i	0.5 + 1.7i	0.44 + 0.01i	3. + 14.i
26	31. + 79.i	2.1 + 2.5i	0.66 + 0.35i	1.6 + 3.8i	1.2 + 1.1i	0.7 + 2.5i	0.94 - 0.17i	0.2 + 20.i
27	43. + 93.i	32. + 27.i	2.4 + 0.7i	6.3 + 8.3i	2.6 + 2.9i	4.9 + 7.5i	3.7 + 0.8i	26. + 41.i
28	8. + 22.i	1.3 + 5.1i	0.29 + 0.26i	0.5 + 1.7i	0.28 + 0.54i	0.15 + 1.40i	0.41 + 0.26i	0.7 + 9.0i
29	570 + 390i	53. + 51.i	7.9 + 0.4i	32. + 25.i	14. + 4.i	19. + 21.i	8.4 - 3.0i	120 + 170i
30	69. + 70.i	28. + 49.i	2.7 + 1.4i	6.8 + 10.6i	2.2 + 3.5i	4.4 + 10.4i	3.7 + 2.2i	32. + 56.i
31	80 + 200i	104. + 88.i	7.0 + 2.1i	18. + 23.i	6.7 + 8.7i	15. + 22.i	11.1 + 3.2i	82. + 106.i
32	260 + 170i	88. + 100.i	7.5 + 1.8i	24. + 23.i	8.2 + 6.9i	17. + 23.i	9.9 + 2.6i	110 + 130i

Table 7.10: Part 1 of partial sum $M_{1,2}$ of the first two weighted projectors of the full EIES data set

	9	10	11	12	13	14	15	16
1	90. + 22.i	50. + 39.i	170 + 200i	24. - 7.i	21. + 3.i	40. + 4.i	70. + 100.i	67. + 49.i
2	24. + 24.i	36. + 37.i	58. + 54.i	26. + 28.i	15. + 3.i	19. + 17.i	16. + 14.i	32. + 22.i
3	0.8 + 1.9i	0.7 + 2.6i	1.2 + 5.1i	0.6 + 1.6i	0.61 + 0.54i	0.59 + 1.24i	0.3 + 1.7i	0.9 + 2.0i
4	7.7 + 4.3i	7.9 + 7.0i	17. + 16.i	5.2 + 3.6i	3.2 + 0.5i	4.8 + 2.6i	5.7 + 6.3i	7.9 + 5.1i
5	2.8 + 1.9i	2.9 + 2.3i	4.7 + 6.3i	2.3 + 1.1i	1.13 + 0.14i	1.9 + 1.0i	1.2 + 2.5i	2.6 + 1.9i
6	6.7 + 3.2i	8.1 + 5.6i	16. + 11.i	5.4 + 3.3i	3.0 + 0.1i	4.5 + 2.1i	5.0 + 3.9i	7.4 + 3.4i
7	1.0 + 3.0i	1.4 + 3.9i	1.0 + 6.7i	1.3 + 2.7i	0.98 + 0.77i	0.9 + 2.0i	-0.1 + 2.0i	1.3 + 2.9i
8	36. + 15.i	38. + 34.i	95. + 68.i	22. + 20.i	16. + 2.i	22. + 12.i	35. + 25.i	41. + 22.i
9	6.3 + 6.3i	5.3 + 9.8i	13. + 22.i	3.4 + 5.4i	3.0 + 1.7i	3.7 + 4.1i	4.6 + 8.1i	6.4 + 7.8i
10	9.8 + 5.3i	7.7 + 7.7i	18. + 24.i	5.0 + 2.6i	3.3 + 0.8i	5.4 + 2.6i	6.3 + 10.5i	8.5 + 7.1i
11	22. + 13.i	24. + 18.i	44. + 44.i	17. + 10.i	9.3 + 0.8i	15. + 7.i	13. + 17.i	22. + 13.i
12	5.4 + 3.4i	2.6 + 5.0i	10. + 17.i	1.3 + 1.3i	1.6 + 1.0i	2.5 + 1.6i	3.8 + 7.8i	4.1 + 5.2i
13	1.7 + 3.0i	0.8 + 3.3i	0.8 + 9.3i	1.0 + 1.6i	0.76 + 0.76i	1.0 + 1.6i	-0.1 + 3.7i	1.1 + 3.2i
14	4.1 + 3.7i	2.6 + 5.4i	7. + 15.i	1.6 + 2.5i	1.6 + 1.0i	2.1 + 2.1i	2.7 + 5.9i	3.6 + 4.8i
15	8.1 + 4.6i	10.5 + 6.3i	17. + 13.i	7.8 + 3.8i	3.7 - 0.1i	5.9 + 2.7i	4.7 + 4.7i	8.8 + 4.0i
16	7.8 + 6.4i	7.1 + 8.5i	13. + 22.i	5.2 + 4.1i	3.2 + 1.1i	4.8 + 3.6i	4.0 + 8.8i	7.1 + 7.1i
17	6.2 + 5.4i	7.3 + 7.4i	12. + 15.i	5.5 + 4.4i	3.1 + 0.7i	4.4 + 3.3i	3.2 + 5.5i	6.6 + 5.3i
18	4.2 + 4.4i	6.2 + 6.4i	9.2 + 10.1i	4.7 + 4.5i	2.6 + 0.6i	3.4 + 3.0i	2.3 + 2.9i	5.3 + 3.9i
19	1.5 + 2.6i	1.5 + 3.6i	2.6 + 7.1i	1.1 + 2.3i	0.98 + 0.70i	1.0 + 1.7i	0.7 + 2.4i	1.7 + 2.8i
20	0.9 + 2.2i	0.5 + 3.0i	1.1 + 6.2i	0.4 + 1.8i	0.62 + 0.69i	0.5 + 1.4i	0.3 + 2.2i	0.9 + 2.5i
21	2.0 + 2.6i	1.1 + 2.9i	1.8 + 8.8i	1.1 + 1.2i	0.78 + 0.61i	1.2 + 1.3i	0.4 + 3.7i	1.4 + 2.9i
22	5.1 + 6.1i	2.7 + 7.1i	6. + 22.i	2.3 + 2.9i	1.9 + 1.5i	2.7 + 3.1i	1.5 + 9.0i	3.6 + 7.1i
23	2.0 + 2.2i	1.4 + 3.2i	3.7 + 7.9i	0.9 + 1.7i	0.92 + 0.62i	1.1 + 1.4i	1.3 + 3.0i	1.9 + 2.8i
24	19. + 9.i	16. + 15.i	41. + 44.i	9.3 + 5.9i	6.8 + 1.5i	10.5 + 4.8i	15. + 18.i	18. + 13.i
25	2.0 + 2.4i	3.1 + 3.2i	3.9 + 4.9i	2.5 + 2.3i	1.31 + 0.29i	1.7 + 1.6i	0.8 + 1.3i	2.5 + 2.0i
26	2.3 + 3.9i	3.7 + 6.4i	6.1 + 8.5i	2.6 + 4.9i	2.0 + 1.0i	1.9 + 3.1i	1.8 + 2.0i	3.6 + 3.9i
27	8.7 + 6.4i	8.0 + 10.1i	18. + 24.i	5.1 + 5.3i	3.8 + 1.3i	5.2 + 4.0i	6.4 + 9.1i	8.7 + 8.0i
28	0.9 + 1.7i	1.0 + 2.3i	1.4 + 4.5i	0.8 + 1.5i	0.63 + 0.42i	0.71 + 1.10i	0.3 + 1.5i	1.1 + 1.7i
29	40. + 21.i	57. + 30.i	88. + 51.i	42. + 21.i	19. - 2.i	30. + 13.i	24. + 16.i	46. + 16.i
30	10.7 + 8.6i	9.3 + 10.3i	16. + 30.i	7.2 + 4.4i	4.1 + 1.3i	6.6 + 4.3i	4.5 + 12.5i	9.2 + 9.3i
31	25. + 16.i	20. + 25.i	51. + 69.i	12. + 11.i	9.5 + 3.6i	14. + 9.i	18. + 28.i	23. + 22.i
32	32. + 16.i	33. + 22.i	60. + 64.i	24. + 9.i	12.0 + 0.5i	20. + 8.i	18. + 27.i	30. + 18.i

Table 7.11: Part 2 of partial sum $M_{1,2}$ of the first two weighted projectors of the full EIES data set

	17	18	19	20	21	22	23	24
1	74. + 65.i	75. + 61.i	36. + 9.i	27. - 1.i	16. + 5.i	41. + 6.i	27. + 3.i	120. + 72.i
2	19. + 12.i	8.1 + 4.0i	7.4 + 3.4i	7.1 + 2.6i	15. + 6.i	35. + 17.i	9.6 + 8.2i	55. + 82.i
3	0.6 + 1.5i	0.38 + 0.99i	0.37 + 0.48i	0.37 + 0.35i	0.53 + 0.60i	1.2 + 1.5i	0.34 + 0.64i	0.8 + 5.1i
4	6.2 + 4.3i	4.6 + 3.1i	2.7 + 0.8i	2.2 + 0.3i	3.0 + 0.9i	7.2 + 2.5i	2.7 + 1.3i	14. + 15.i
5	1.7 + 1.9i	1.1 + 1.6i	0.90 + 0.49i	0.81 + 0.23i	1.07 + 0.24i	2.7 + 0.7i	1.01 + 0.54i	5.4 + 5.4i
6	5.3 + 2.5i	3.4 + 1.5i	2.1 + 0.4i	1.8 + 0.08i	2.9 + 0.5i	7.0 + 1.7i	2.4 + 1.0i	14. + 12.i
7	0.5 + 1.9i	-0.08 + 1.15i	0.37 + 0.74i	0.45 + 0.59i	0.89 + 0.87i	2.0 + 2.3i	0.47 + 1.04i	1.4 + 8.1i
8	35. + 15.i	27. + 8.i	13.3 + 1.2i	10.4 - 0.3i	15. + 5.i	34. + 13.i	12.3 + 4.9i	66. + 69.i
9	5.4 + 6.2i	4.4 + 4.2i	2.6 + 1.5i	2.2 + 0.9i	2.6 + 2.0i	6.1 + 5.1i	2.2 + 2.0i	9. + 19.i
10	7.4 + 7.3i	6.4 + 6.2i	3.6 + 1.5i	3.0 + 0.5i	2.9 + 1.1i	7.1 + 2.7i	3.2 + 1.4i	15. + 16.i
11	15. + 12.i	10.1 + 9.2i	7.1 + 2.6i	6.2 + 1.1i	8.8 + 1.8i	22. + 6.i	7.9 + 3.7i	44. + 41.i
12	4.4 + 5.5i	4.5 + 4.7i	2.3 + 1.1i	1.8 + 0.4i	1.2 + 1.1i	2.9 + 2.3i	1.7 + 0.9i	5.9 + 9.3i
13	0.7 + 3.1i	0.6 + 2.6i	0.70 + 0.98i	0.69 + 0.62i	0.61 + 0.78i	1.5 + 1.9i	0.62 + 0.92i	1.5 + 6.8i
14	3.3 + 4.4i	3.0 + 3.4i	1.7 + 1.0i	1.4 + 0.5i	1.3 + 1.2i	3.1 + 2.7i	1.4 + 1.1i	4.8 + 10.5i
15	5.5 + 3.2i	2.9 + 2.3i	2.4 + 0.7i	2.2 + 0.3i	3.7 + 0.4i	9.0 + 1.5i	3.0 + 1.3i	18. + 15.i
16	5.3 + 6.6i	3.9 + 5.3i	2.8 + 1.7i	2.5 + 0.9i	2.9 + 1.4i	7.1 + 3.6i	2.8 + 1.9i	13. + 18.i
17	4.2 + 4.2i	2.3 + 3.0i	2.0 + 1.2i	1.9 + 0.7i	2.9 + 1.0i	7.0 + 3.0i	2.3 + 1.7i	12. + 16.i
18	3.0 + 2.3i	1.2 + 1.2i	1.3 + 0.8i	1.27 + 0.55i	2.6 + 0.9i	6.1 + 2.8i	1.7 + 1.5i	10. + 14.i
19	1.2 + 2.0i	0.8 + 1.3i	0.62 + 0.62i	0.58 + 0.44i	0.86 + 0.82i	2.0 + 2.1i	0.58 + 0.87i	1.9 + 7.3i
20	0.7 + 1.9i	0.55 + 1.27i	0.44 + 0.58i	0.42 + 0.42i	0.50 + 0.75i	1.1 + 1.9i	0.33 + 0.73i	0.4 + 5.7i
21	1.0 + 2.9i	0.9 + 2.6i	0.82 + 0.86i	0.75 + 0.50i	0.63 + 0.63i	1.6 + 1.5i	0.72 + 0.77i	2.2 + 6.0i
22	3.0 + 7.0i	2.8 + 6.1i	2.1 + 2.0i	1.9 + 1.1i	1.5 + 1.6i	3.7 + 3.7i	1.7 + 1.8i	5. + 14.i
23	1.7 + 2.3i	1.5 + 1.7i	0.87 + 0.58i	0.73 + 0.33i	0.77 + 0.72i	1.8 + 1.7i	0.70 + 0.70i	2.4 + 6.3i
24	16. + 12.i	14. + 10.i	7.3 + 1.9i	5.7 + 0.4i	6.0 + 2.2i	14. + 5.i	6.3 + 2.4i	30. + 30.i
25	1.2 + 1.2i	0.23 + 0.62i	0.56 + 0.44i	0.60 + 0.33i	1.30 + 0.45i	3.1 + 1.4i	0.84 + 0.79i	4.8 + 7.2i
26	2.2 + 1.8i	0.89 + 0.38i	0.81 + 0.62i	0.81 + 0.57i	1.9 + 1.3i	4.2 + 3.6i	1.0 + 1.4i	4.5 + 13.1i
27	7.3 + 6.6i	5.8 + 4.7i	3.3 + 1.4i	2.7 + 0.7i	3.4 + 1.8i	8.0 + 4.6i	3.0 + 2.0i	14. + 21.i
28	0.6 + 1.3i	0.32 + 0.86i	0.36 + 0.43i	0.37 + 0.30i	0.57 + 0.49i	1.3 + 1.3i	0.38 + 0.57i	1.4 + 4.7i
29	27. + 10.i	11.9 + 6.0i	11.0 + 2.3i	10.2 + 0.9i	20. + 0.8i	48. + 6.i	15. + 6.i	98. + 76.i
30	6.6 + 9.3i	4.9 + 8.1i	3.8 + 2.5i	3.4 + 1.2i	3.7 + 1.6i	9.2 + 4.0i	3.8 + 2.4i	18. + 23.i
31	21. + 20.i	18. + 16.i	9.8 + 4.0i	7.9 + 1.6i	8.2 + 4.6i	19. + 11.i	8.3 + 4.7i	37. + 50.i
32	22. + 18.i	15. + 16.i	10.6 + 3.9i	9.1 + 1.2i	11.3 + 1.6i	28. + 5.i	11.3 + 4.3i	62. + 50.i

Table 7.12: Part 3 of partial sum $M_{1,2}$ of the first two weighted projectors of the full EIES data set

	25	26	27	28	29	30	31	32
1	38. + 33.i	79. + 31.i	93. + 43.i	22. + 8.i	390 + 570i	70. + 69.i	200 + 80i	170 + 260i
2	4.6 - 0.2i	2.5 + 2.1i	27. + 32.i	5.1 + 1.3i	51. + 53.i	49. + 28.i	88. + 104.i	100. + 88.i
3	0.23 + 0.44i	0.35 + 0.66i	0.7 + 2.4i	0.26 + 0.29i	0.4 + 7.9i	1.4 + 2.7i	2.1 + 7.0i	1.8 + 7.5i
4	2.3 + 1.4i	3.8 + 1.6i	8.3 + 6.3i	1.7 + 0.5i	25. + 32.i	10.6 + 6.8i	23. + 18.i	23. + 24.i
5	0.49 + 0.73i	1.1 + 1.2i	2.9 + 2.6i	0.54 + 0.28i	4. + 14.i	3.5 + 2.2i	8.7 + 6.7i	6.9 + 8.2i
6	1.7 + 0.5i	2.5 + 0.7i	7.5 + 4.9i	1.40 + 0.15i	21. + 19.i	10.4 + 4.4i	22. + 15.i	23. + 17.i
7	0.01 + 0.44i	-0.17 + 0.94i	0.8 + 3.7i	0.26 + 0.41i	-3.0 + 8.4i	2.2 + 3.7i	3.2 + 11.1i	2.6 + 9.9i
8	14. + 3.i	20. - 0.2i	41. + 26.i	9.0 + 0.7i	170 + 120i	56. + 32.i	106. + 82.i	130 + 110i
9	2.4 + 2.0i	3.9 + 2.3i	6.4 + 8.7i	1.7 + 0.9i	21. + 40.i	8.6 + 10.7i	16. + 25.i	16. + 32.i
10	3.2 + 3.1i	6.4 + 3.7i	10.1 + 8.0i	2.3 + 1.0i	30. + 57.i	10.3 + 9.3i	25. + 20.i	22. + 33.i
11	4.9 + 3.9i	8.5 + 6.1i	24. + 18.i	4.5 + 1.4i	51. + 88.i	30. + 16.i	69. + 51.i	64. + 60.i
12	2.3 + 2.5i	4.9 + 2.6i	5.3 + 5.1i	1.5 + 0.8i	21. + 42.i	4.4 + 7.2i	11. + 12.i	9. + 24.i
13	0.29 + 1.31i	1.0 + 2.0i	1.3 + 3.8i	0.42 + 0.63i	-2. + 19.i	1.3 + 4.1i	3.6 + 9.5i	0.5 + 12.0i
14	1.6 + 1.7i	3.1 + 1.9i	4.0 + 5.2i	1.10 + 0.71i	13. + 30.i	4.3 + 6.6i	9. + 14.i	8. + 20.i
15	1.3 + 0.8i	2.0 + 1.8i	9.1 + 6.4i	1.5 + 0.3i	16. + 24.i	12.5 + 4.5i	28. + 18.i	27. + 18.i
16	2.0 + 2.5i	3.9 + 3.6i	8.0 + 8.7i	1.7 + 1.1i	16. + 46.i	9.3 + 9.2i	22. + 23.i	18. + 30.i
17	1.2 + 1.2i	1.8 + 2.2i	6.6 + 7.3i	1.3 + 0.6i	10. + 27.i	9.3 + 6.6i	20. + 21.i	18. + 22.i
18	0.62 + 0.23i	0.38 + 0.89i	4.7 + 5.8i	0.86 + 0.32i	6.0 + 11.9i	8.1 + 4.9i	16. + 18.i	16. + 15.i
19	0.44 + 0.56i	0.62 + 0.81i	1.4 + 3.3i	0.43 + 0.36i	2.3 + 11.0i	2.5 + 3.8i	4.0 + 9.8i	3.9 + 10.6i
20	0.33 + 0.60i	0.57 + 0.81i	0.7 + 2.7i	0.30 + 0.37i	0.9 + 10.2i	1.2 + 3.4i	1.6 + 7.9i	1.2 + 9.1i
21	0.45 + 1.30i	1.3 + 1.9i	1.8 + 3.4i	0.49 + 0.57i	0.8 + 20.i	1.6 + 3.7i	4.6 + 8.2i	1.6 + 11.3i
22	1.4 + 3.1i	3.6 + 4.2i	4.6 + 8.0i	1.3 + 1.3i	6. + 48.i	4.0 + 9.2i	11. + 19.i	5. + 28.i
23	0.79 + 0.84i	1.4 + 1.0i	2.0 + 3.0i	0.57 + 0.38i	6. + 15.i	2.4 + 3.8i	4.7 + 8.3i	4.3 + 11.3i
24	7.2 + 4.8i	13.1 + 4.5i	21. + 14.i	4.7 + 1.4i	76. + 98.i	23. + 18.i	50. + 37.i	50. + 62.i
25	0.12 + 0.12i	-0.11 + 0.59i	2.2 + 3.0i	0.37 + 0.19i	0.6 + 5.5i	3.9 + 2.3i	7.7 + 9.4i	7.5 + 7.4i
26	0.59 - 0.11i	0.029 + 0.029i	2.4 + 5.1i	0.62 + 0.27i	5.3 + 5.9i	5.8 + 5.4i	8. + 17.i	11. + 15.i
27	3.0 + 2.2i	5.1 + 2.4i	9.1 + 9.1i	2.2 + 0.9i	29. + 46.i	12. + 11.i	24. + 26.i	24. + 35.i
28	0.19 + 0.37i	0.27 + 0.62i	0.9 + 2.2i	0.24 + 0.24i	0.4 + 6.9i	1.6 + 2.3i	2.8 + 6.3i	2.4 + 6.5i
29	5.5 + 0.6i	5.9 + 5.3i	46. + 29.i	6.9 + 0.4i	75. + 75.i	67. + 17.i	150 + 90i	150 + 70i
30	2.3 + 3.9i	5.4 + 5.8i	11. + 12.i	2.3 + 1.6i	17. + 67.i	12. + 12.i	30. + 29.i	21. + 39.i
31	9.4 + 7.7i	17. + 8.i	26. + 24.i	6.3 + 2.8i	90 + 150i	29. + 30.i	63. + 63.i	60. + 98.i
32	7.4 + 7.5i	15. + 11.i	35. + 24.i	6.5 + 2.4i	70 + 150i	39. + 21.i	98. + 60.i	83. + 83.i

Table 7.13: Part 4 of partial sum $M_{1,2}$ of the first two weighted projectors of the full EIES data set

	1	2	3	4	5	6	7	8
1	-2.2 - 2.2i	21. + 29.i	2.5 - 1.1i	-0.6 - 2.5i	1.5 + 0.8i	0.6 + 2.4i	3.1 - 0.4i	-40. + 16.i
2	29. + 21.i	-22. - 22.i	6.8 + 0.6i	-2.1 + 3.2i	1.7 - 0.3i	-7.0 - 0.9i	14. - 0.7i	-24. - 70.i
3	-1.1 + 2.5i	0.6 + 6.8i	0.53 + 0.53i	-0.29 - 0.54i	0.40 + 0.19i	-0.84 + 0.01i	0.9 + 1.2i	4.9 - 3.5i
4	-2.5 - 0.6i	3.2 - 2.1i	-0.54 - 0.29i	0.21 + 0.21i	-0.63 - 0.26i	-0.20 - 0.35i	-0.72 - 0.54i	9.8 + 9.1i
5	0.8 + 1.5i	-0.3 + 1.7i	0.19 + 0.40i	-0.26 - 0.63i	0.64 + 0.64i	0.48 + 0.74i	-0.02 + 0.86i	-4.5 - 10.1i
6	2.4 + 0.6i	-0.9 - 7.0i	0.01 - 0.84i	-0.35 - 0.20i	0.74 + 0.48i	0.29 + 0.29i	0.11 - 1.37i	-3.9 + 8.4i
7	-0.4 + 3.1i	-0.7 + 14.i	1.2 + 0.9i	-0.54 - 0.72i	0.86 - 0.02i	-1.37 + 0.11i	1.9 + 1.9i	2.1 - 8.3i
8	16. - 40.i	-70. - 24.i	-3.5 + 4.9i	9.1 + 9.8i	-10.1 - 4.5i	8.4 - 3.9i	-8.3 + 2.1i	-120 - 120i
9	5.2 - 3.5i	5.1 + 12.5i	1.30 + 0.18i	-0.2 + 2.5i	-1.1 - 3.3i	-0.81 + 0.17i	3.0 - 0.3i	-10. - 24.i
10	5.2 + 1.0i	-18. - 15.i	-0.22 + 0.76i	0.79 - 0.44i	0.5 + 2.2i	1.32 + 0.19i	-1.11 + 0.71i	-21. - 20.i
11	-16. + 14.i	-9. - 30.i	-2.1 + 0.7i	-0.18 + 0.54i	-1.6 + 0.04i	-6.4 - 8.1i	-0.4 + 1.4i	106. + 70.i
12	4.2 + 1.6i	-23. - 17.i	-0.06 + 0.41i	1.03 - 0.69i	0.6 + 2.7i	0.25 - 0.86i	-0.67 + 0.16i	-17. - 3.i
13	1.7 + 3.9i	-2.8 - 1.0i	0.93 + 0.62i	0.02 - 0.30i	0.14 + 0.82i	-0.82 - 0.03i	1.6 + 1.0i	-4.6 - 12.6i
14	6.0 + 5.5i	-18. - 10.i	0.88 + 0.80i	0.47 - 0.93i	0.9 + 2.7i	-0.72 + 0.41i	1.02 + 0.86i	-14. - 22.i
15	14. + 7.i	-21. - 10.i	2.3 + 0.2i	-0.11 - 0.47i	1.9 + 2.5i	-1.7 + 1.4i	3.8 - 0.5i	-27. - 33.i
16	2.1 + 5.4i	-7.0 + 5.4i	1.4 + 0.7i	-0.41 - 1.31i	1.4 + 1.5i	-1.5 + 0.3i	2.1 + 1.4i	-3.8 - 8.2i
17	-4.7 + 1.8i	1.22 - 0.08i	-0.22 + 0.23i	-0.26 + 0.05i	-0.19 - 0.52i	-1.1 - 2.0i	0.24 + 0.77i	19. + 20.i
18	0.7 + 3.3i	-0.6 + 4.5i	1.4 + 0.4i	-0.48 + 0.43i	0.15 - 0.72i	-1.9 - 1.5i	3.1 + 0.9i	1.5 + 1.9i
19	-2.6 + 2.3i	-0.2 - 5.4i	-0.24 + 0.16i	0.047 - 0.129i	-0.25 + 0.35i	-0.56 - 1.14i	-0.10 + 0.39i	11. + 9.i
20	0.4 + 2.1i	-2.7 + 1.9i	0.40 + 0.34i	0.03 - 0.58i	0.35 + 0.75i	-0.55 + 0.27i	0.49 + 0.62i	-0.6 - 5.3i
21	2.6 + 3.1i	-5.9 - 4.3i	0.50 + 0.48i	0.26 - 0.39i	0.19 + 1.23i	-0.36 + 0.44i	0.63 + 0.54i	-6. - 15.i
22	5.2 + 3.2i	-13. - 22.i	-1.10 + 0.14i	1.0 - 1.7i	0.6 + 4.2i	2.0 + 2.8i	-3.2 - 0.5i	-14. - 29.i
23	1.7 + 2.5i	-4.8 + 0.2i	0.51 + 0.29i	-0.03 - 0.72i	0.68 + 1.08i	-0.39 + 0.45i	0.59 + 0.52i	-4.6 - 7.0i
24	14. + 8.i	-64. - 54.i	-0.52 + 0.62i	2.2 - 1.9i	2.3 + 7.5i	0.05 - 1.5i	-2.0 - 0.6i	-31. - 11.i
25	0.04 + 2.6i	0.4 + 9.7i	0.51 + 0.94i	-0.87 - 0.90i	1.32 + 0.19i	0.25 + 0.58i	0.6 + 2.2i	-0.5 - 12.7i
26	2.7 + 4.2i	-0.9 + 5.1i	1.18 + 0.18i	-0.42 - 0.57i	0.77 + 0.59i	-1.4 + 0.9i	2.0 + 0.3i	-0.3 - 11.4i
27	4.1 + 0.6i	0.8 - 13.0i	0.30 - 0.54i	0.19 + 1.26i	-0.84 - 0.32i	0.004 - 0.24i	1.1 - 1.5i	-7.3 - 6.1i
28	0.1 + 1.4i	2.9 + 11.0i	0.92 + 0.39i	-0.39 - 0.37i	0.44 - 0.23i	-0.73 + 0.47i	1.5 + 0.9i	-1.9 - 7.2i
29	-10.9 + 5.2i	80. + 42.i	-3.0 - 1.3i	-7.1 - 6.4i	7.0 - 0.1i	9. + 12.i	-7.4 + 2.4i	38. - 23.i
30	-31. - 5.i	-4. - 30.i	-6.3 - 1.3i	1.24 + 0.19i	-2.7 - 1.1i	-1.4 - 10.6i	-8.6 - 1.0i	100 + 150i
31	-5.4 - 5.0i	29. + 64.i	2.4 + 1.2i	-1.8 - 1.3i	1.4 - 3.2i	0.5 + 3.1i	3.0 + 4.0i	-18. - 20.i
32	-28. + 13.i	3. - 65.i	-5.1 - 2.8i	0.8 + 1.8i	-4.4 - 0.4i	-8. - 13.i	-3.5 - 4.5i	160 + 170i

Table 7.14: Part 1 of the partial sum $M_{3,6}$ of the first two weighted projectors of the full EIES data set

	9	10	11	12	13	14	15	16
1	-3.5 + 5.2i	1.0 + 5.2i	14. - 16.i	1.6 + 4.2i	3.9 + 1.7i	5.5 + 6.0i	7. + 14.i	5.4 + 2.1i
2	12.5 + 5.1i	-15. - 18.i	-30. - 9.i	-17. - 23.i	-1.0 - 2.8i	-10. - 18.i	-10. - 21.i	5.4 - 7.0i
3	0.18 + 1.30i	0.76 - 0.22i	0.7 - 2.1i	0.41 - 0.06i	0.62 + 0.93i	0.80 + 0.88i	0.2 + 2.3i	0.7 + 1.4i
4	2.5 - 0.2i	-0.44 + 0.79i	0.54 - 0.18i	-0.69 + 1.03i	-0.30 + 0.02i	-0.93 + 0.47i	-0.47 - 0.11i	-1.31 - 0.41i
5	-3.3 - 1.1i	2.2 + 0.5i	0.04 - 1.6i	2.7 + 0.6i	0.82 + 0.14i	2.7 + 0.9i	2.5 + 1.9i	1.5 + 1.4i
6	0.17 - 0.81i	0.19 + 1.32i	-8.1 - 6.4i	-0.86 + 0.25i	-0.03 - 0.82i	0.41 - 0.72i	1.4 - 1.7i	0.3 - 1.5i
7	-0.3 + 3.0i	0.71 - 1.11i	1.4 - 0.4i	0.16 - 0.67i	1.0 + 1.6i	0.86 + 1.02i	-0.5 + 3.8i	1.4 + 2.1i
8	-24. - 10.i	-20. - 21.i	70. + 106.i	-3. - 17.i	-12.6 - 4.6i	-22. - 14.i	-33. - 27.i	-8.2 - 3.8i
9	3.8 + 3.8i	-4.9 - 7.6i	8. + 22.i	-3.3 - 4.7i	0.07 - 0.31i	-4.0 - 4.1i	-4.0 - 2.6i	0.8 - 1.4i
10	-7.6 - 4.9i	0.46 + 0.46i	-2.8 - 3.3i	1.5 - 1.6i	-1.2 - 1.0i	0.71 - 1.02i	-1.0 - 3.8i	0.57 + 0.41i
11	22. + 8.i	-3.3 - 2.8i	-25. - 25.i	-10.6 - 6.5i	-4.9 + 0.9i	-9.9 - 6.3i	-10. - 15.i	-9.6 - 4.6i
12	-4.7 - 3.3i	-1.6 + 1.5i	-6.5 - 10.6i	-2.2 - 2.2i	-2.2 - 0.6i	-1.8 - 1.3i	-4.0 - 5.0i	-0.79 - 0.81i
13	-0.31 + 0.07i	-1.0 - 1.2i	0.9 - 4.9i	-0.6 - 2.2i	0.22 + 0.22i	0.03 - 0.66i	-0.51 - 0.38i	1.15 + 0.64i
14	-4.1 - 4.0i	-1.02 + 0.71i	-6.3 - 9.9i	-1.3 - 1.8i	-0.66 + 0.03i	-0.28 - 0.28i	-2.4 - 1.8i	0.93 + 0.97i
15	-2.6 - 4.0i	-3.8 - 1.0i	-15. - 10.i	-5.0 - 4.0i	-0.38 - 0.51i	-1.8 - 2.4i	-3.8 - 3.8i	2.4 - 0.6i
16	-1.4 + 0.8i	0.41 + 0.57i	-4.6 - 9.6i	-0.81 - 0.79i	0.64 + 1.15i	0.97 + 0.93i	-0.6 + 2.4i	1.6 + 1.6i
17	4.3 + 4.4i	-0.22 - 1.32i	-2.1 - 4.1i	-1.6 - 1.9i	-0.72 + 0.41i	-1.5 - 1.5i	-1.4 - 2.1i	-1.4 - 1.0i
18	4.1 + 5.8i	-2.9 - 4.3i	-0.7 - 2.5i	-3.7 - 5.2i	-0.29 + 0.33i	-2.5 - 3.4i	-2.7 - 2.9i	0.6 - 1.3i
19	2.2 + 1.1i	-0.15 - 0.14i	-1.7 - 6.0i	-0.73 - 1.08i	-0.53 - 0.01i	-0.62 - 0.79i	-0.4 - 1.8i	-0.86 - 0.51i
20	-0.78 - 0.61i	0.19 + 0.74i	-0.4 - 3.5i	-0.04 + 0.33i	0.27 + 0.59i	0.42 + 1.04i	-0.3 + 1.6i	0.43 + 1.08i
21	-1.7 - 2.4i	-0.49 + 0.13i	-0.8 - 4.2i	-0.13 - 0.79i	0.006 + 0.036i	0.23 + 0.14i	-0.56 - 0.26i	0.74 + 0.85i
22	-10. - 14.i	3.7 + 7.0i	-6.1 - 11.0i	4.9 + 5.3i	0.20 - 0.92i	4.5 + 4.4i	3.6 + 1.7i	0.7 + 2.9i
23	-1.8 - 1.1i	0.39 + 0.96i	-2.3 - 5.1i	0.04 + 0.16i	0.27 + 0.40i	0.78 + 0.84i	-0.03 + 1.21i	0.80 + 0.97i
24	-11. - 12.i	-3.2 + 5.2i	-31. - 31.i	-6.3 - 4.4i	-5.8 - 2.1i	-4.6 - 3.6i	-10. - 15.i	-2.7 - 2.5i
25	-4.2 + 1.3i	4.1 - 0.8i	-0.36 + 0.47i	4.2 - 0.06i	1.4 + 0.7i	4.1 + 0.8i	3.5 + 3.2i	2.4 + 2.4i
26	0.87 - 0.38i	-0.48 + 0.15i	-3.5 - 4.3i	-1.26 + 0.02i	0.94 + 0.78i	0.33 + 0.90i	-0.2 + 2.4i	1.3 + 1.1i
27	2.7 - 0.9i	-3.4 - 2.7i	-1.5 + 0.01i	-2.7 - 3.5i	-0.7 - 1.7i	-2.3 - 3.7i	-0.9 - 5.9i	0.04 - 2.7i
28	-0.1 + 1.8i	0.26 - 0.73i	2.8 + 0.7i	0.30 - 0.12i	1.03 + 0.92i	0.87 + 0.91i	0.4 + 3.3i	1.4 + 1.3i
29	-22. - 12.i	41. + 16.i	-10.7 - 2.9i	43. + 28.i	16. + 0.7i	42. + 20.i	53. + 37.i	14. + 15.i
30	18. + 12.i	0.4 + 5.2i	-14. - 22.i	-7.0 + 1.1i	-7.3 + 0.2i	-9.5 - 2.8i	-8. - 13.i	-15. - 7.i
31	-5.9 + 9.4i	6.1 - 1.7i	27. + 20.i	8.8 + 4.4i	5.9 + 3.9i	8.4 + 6.9i	8. + 20.i	6.6 + 7.0i
32	42. + 10.i	-9.3 + 2.4i	-39. - 48.i	-21. - 5.i	-8.7 - 1.0i	-19. - 9.i	-14. - 25.i	-18. - 13.i

Table 7.15: Part 2 of the partial sum $M_{3,6}$ of the first two weighted projectors of the full EIES data set

	17	18	19	20	21	22	23	24
1	1.8 - 4.7i	3.3 + 0.7i	2.3 - 2.6i	2.1 + 0.4i	3.1 + 2.6i	3.2 + 5.2i	2.5 + 1.7i	8. + 14.i
2	-0.08 + 1.22i	4.5 - 0.6i	-5.4 - 0.2i	1.9 - 2.7i	-4.3 - 5.9i	-22. - 13.i	0.2 - 4.8i	-54. - 64.i
3	0.23 - 0.22i	0.4 + 1.4i	0.16 - 0.24i	0.34 + 0.40i	0.48 + 0.50i	0.14 - 1.10i	0.29 + 0.51i	0.62 - 0.52i
4	0.05 - 0.26i	0.43 - 0.48i	-0.129 + 0.047i	-0.58 + 0.03i	-0.39 + 0.26i	-1.7 + 1.0i	-0.72 - 0.03i	-1.9 + 2.2
5	-0.52 - 0.19i	-0.72 + 0.15i	0.35 - 0.25i	0.75 + 0.35i	1.23 + 0.19i	4.2 + 0.6i	1.08 + 0.68i	7.5 + 2.3i
6	-2.0 - 1.1i	-1.5 - 1.9i	-1.14 - 0.56i	0.27 - 0.55i	0.44 - 0.36i	2.8 + 2.0i	0.45 - 0.39i	-1.5 + 0.05i
7	0.77 + 0.24i	0.9 + 3.1i	0.39 - 0.10i	0.62 + 0.49i	0.54 + 0.63i	-0.5 - 3.2i	0.52 + 0.59i	-0.6 - 2.0i
8	20. + 19.i	1.9 + 1.5i	9. + 11.i	-5.3 - 0.6i	-15. - 6.i	-29. - 14.i	-7.0 - 4.6i	-11. - 31.i
9	4.4 + 4.3i	5.8 + 4.1i	1.1 + 2.2i	-0.61 - 0.78i	-2.4 - 1.7i	-14. - 10.i	-1.1 - 1.8i	-12. - 11.i
10	-1.32 - 0.22i	-4.3 - 2.9i	-0.14 - 0.15i	0.74 + 0.19i	0.13 - 0.49i	7.0 + 3.7i	0.96 + 0.39i	5.2 - 3.2i
11	-4.1 - 2.1i	-2.5 - 0.7i	-6.0 - 1.7i	-3.5 - 0.4i	-4.2 - 0.8i	-11.0 - 6.1i	-5.1 - 2.3i	-31. - 31.i
12	-1.9 - 1.6i	-5.2 - 3.7i	-1.08 - 0.73i	0.33 - 0.04i	-0.79 - 0.13i	5.3 + 4.9i	0.16 + 0.04i	-4.4 - 6.3i
13	0.41 - 0.72i	0.33 - 0.29i	0.01 - 0.53i	0.59 + 0.27i	0.036 + 0.006i	-0.92 + 0.20i	0.40 + 0.27i	-2.1 - 5.8i
14	-1.5 - 1.5i	-3.4 - 2.5i	-0.79 - 0.62i	1.04 + 0.42i	0.14 + 0.23i	4.4 + 4.5i	0.84 + 0.78i	-3.6 - 4.6i
15	-2.1 - 1.4i	-2.9 - 2.7i	-1.8 - 0.4i	1.6 - 0.3i	-0.26 - 0.56i	1.7 + 3.6i	1.21 - 0.03i	-15. - 10.i
16	-1.0 - 1.4i	-1.3 + 0.6i	-0.51 - 0.86i	1.08 + 0.43i	0.85 + 0.74i	2.9 + 0.7i	0.97 + 0.80i	-2.5 - 2.7i
17	-0.15 - 0.15i	0.25 + 1.20i	-0.82 - 0.49i	-0.67 - 0.18i	-0.74 - 0.26i	-2.7 - 3.8i	-0.89 - 0.71i	-4.3 - 7.9i
18	1.20 + 0.25i	2.0 + 2.0i	-0.63 - 0.40i	- 0.48i	-1.2 - 0.8i	-6.7 - 6.1i	-0.46 - 1.18i	-11. - 16.i
19	-0.49 - 0.82i	-0.40 - 0.63i	-0.61 - 0.61i	-0.28 + 0.02i	-0.29 - 0.06i	-0.58 - 0.07i	-0.41 - 0.18i	-1.7 - 4.5i
20	-0.18 - 0.67i	-0.48	0.02 - 0.28i	0.38 + 0.38i	0.36 + 0.57i	1.2 + 1.4i	0.30 + 0.62i	-0.27 + 0.96i
21	-0.26 - 0.74i	-0.8 - 1.2i	-0.06 - 0.29i	0.57 + 0.36i	0.20 + 0.20i	1.3 + 2.5i	0.46 + 0.57i	-0.6 - 1.5i
22	-3.8 - 2.7i	-6.1 - 6.7i	-0.07 - 0.58i	1.4 + 1.2i	2.5 + 1.3i	15. + 15.i	1.9 + 2.7i	15. + 17.i
23	-0.71 - 0.89i	-1.18 - 0.46i	-0.18 - 0.41i	0.62 + 0.30i	0.57 + 0.46i	2.7 + 1.9i	0.62 + 0.62i	0.17 + 0.58i
24	-7.9 - 4.3i	-16. - 11.i	-4.5 - 1.7i	0.96 - 0.27i	-1.5 - 0.6i	17. + 15.i	0.58 + 0.17i	-14. - 14.i
25	-0.47 + 0.69i	-0.5 + 2.6i	0.50 - 0.16i	1.07 + 0.45i	1.8 + 0.05i	5.3 - 3.3i	1.6 + 0.7i	11.3 + 0.2i
26	-0.35 - 0.81i	0.47 + 0.45i	-0.34 - 0.26i	0.72 + 0.29i	0.55 + 0.57i	-0.37 + 0.94i	0.53 + 0.60i	-4.5 + 0.1i
27	0.39 + 0.04i	1.3 - 2.3i	-0.66	-0.22 - 0.76i	-1.2 - 1.4i	-5.1 + 0.01i	-0.48 - 1.25i	-7.7 - 9.1i
28	0.92 + 0.11i	1.4 + 2.0i	0.54 - 0.04i	0.49 + 0.29i	0.49 + 0.44i	-1.1 - 1.8i	0.45 + 0.42i	0.10 + 0.12i
29	-11.2 - 1.4i	-1.3 + 5.0i	3.6 - 1.8i	6.4 + 2.9i	20. + 3.i	54. + 7.i	12. + 8.i	120 + 80i
30	-4.5 - 2.7i	-6.5 - 2.0i	-4.7 - 2.0i	-5.9 - 1.1i	-4.6 + 0.2i	-2.5 - 3.0i	-6.6 - 3.1i	-14. - 11.i
31	6.0 + 2.9i	8.0 + 11.4i	5.1 + 0.8i	1.8 + 1.3i	3.6 + 2.1i	-0.8 - 10.7i	2.6 + 2.1i	23. + 17.i
32	-7.4 - 7.1i	-3.2 - 8.3i	-10.1 - 3.6i	-7.2 - 2.0i	-7.7 - 0.8i	-21. + 2.i	-9.8 - 4.9i	-57. - 34.i

Table 7.16: Part 3 of the partial sum $M_{3,6}$ of the first two weighted projectors of the full EIES data set

	25	26	27	28	29	30	31	32
1	2.6 + 0.04i	4.2 + 2.7i	0.6 + 4.1i	1.4 + 0.1i	5.2 - 10.9i	-5. - 31.i	-5.0 - 5.4i	13. - 28.i
2	9.7 + 0.4i	5.1 - 0.9i	-13.0 + 0.8i	11.0 + 2.9i	42. + 80.i	-30. - 4.i	64. + 29.i	-65. + 3.i
3	0.94 + 0.51i	0.1+ 1.18i	-0.54 + 0.30i	0.39 + 0.92i	-1.3 - 3.0i	-1.3 - 6.3i	1.2 + 2.4i	-2.8 - 5.1i
4	-0.90 - 0.87i	-0.57 - 0.42i	1.26 + 0.19i	-0.37 - 0.39i	-6.4 - 7.1i	0.19 + 1.24i	-1.3 - 1.8i	1.8 + 0.8i
5	0.19 + 1.32i	0.59 + 0.77i	-0.32 - 0.84i	-0.23 + 0.44i	0.1 + 7.0i	-1.1 - 2.7i	-3.2 + 1.4i	-0.4 - 4.4i
6	0.58 + 0.25i	0.9 - 1.4i	-0.24 + 0.004i	0.47 - 0.73i	12. + 9.i	-10.6 - 1.4i	3.1 + 0.5i	-13. - 8.i
7	2.2 + 0.6i	0.3 + 2.0i	-1.5 + 1.1i	0.9 + 1.5i	2.4 - 7.4i	-1.0 - 8.6i	4.0 + 3.0i	-4.5 - 3.5i
8	-12.7 - 0.5i	-11.4 - 0.3i	-6.1 - 7.3i	-7.2 - 1.9i	-23. + 38.i	150 + 100i	-20. - 18.i	170 + 160i
9	1.3 - 4.2i	-0.38 + 0.87i	-0.9 + 2.7i	1.8 - 0.1i	-12. - 22.i	12. + 18.i	9.4 - 5.9i	10. + 42.i
10	-0.8 + 4.1i	0.15 - 0.48i	-2.7 - 3.4i	-0.73 + 0.26i	16. + 41.i	5.2 + 0.4i	-1.7 + 6.1i	2.4 - 9.3i
11	0.47 - 0.36i	-4.3 - 3.5i	0.01- 1.5i	0.7 + 2.8i	-2.9 - 10.7i	-22. - 14.i	20. + 27.i	-48. - 39.i
12	0.06 + 4.2i	0.02 - 1.26i	-3.5 - 2.7i	-0.12 + 0.30i	28. + 43.i	1.1 - 7.0i	4.4 + 8.8i	-5. - 21.i
13	0.7 + 1.4i	0.78 + 0.94i	-1.7 - 0.7i	0.92 + 1.03i	0.7 + 16.i	0.2 - 7.3i	3.9 + 5.9i	-1.0 - 8.7i
14	0.8 + 4.1i	0.90 + 0.33i	-3.7 - 2.3i	0.91 + 0.87i	20. + 42.i	-2.8 - 9.5i	6.9 + 8.4i	-9. - 19.i
15	3.2 + 3.5i	2.4 - 0.2i	-5.9 - 0.9i	3.3 + 0.4i	37. + 53.i	-13. - 8.i	20. + 8.i	-25. - 14.i
16	2.4 + 2.4i	1.1 + 1.3i	-2.7 + 0.04i	1.3 + 1.4i	15. + 14.i	-7. - 15.i	7.0 + 6.6i	-13. - 18.i
17	0.69 - 0.47i	-0.81 - 0.35i	0.04 + 0.39i	0.11 + 0.92i	-1.4 - 11.2i	-2.7 - 4.5i	2.9 + 6.0i	-7.1 - 7.4i
18	2.6 - 0.5i	0.45 + 0.47i	-2.3 + 1.3i	2.0 + 1.4i	5.0 - 1.3i	-2.0 - 6.5i	11.4 + 8.0i	-8.3 - 3.2i
19	-0.16 + 0.50i	-0.26 - 0.34i	- 0.66i	-0.04 + 0.54i	-1.8 + 3.6i	-2.0 - 4.7i	0.8 + 5.1i	-3.6 - 10.1i
20	0.45 + 1.07i	0.29 + 0.72i	-0.76 - 0.22i	0.29 + 0.49i	2.9 + 6.4i	-1.1 - 5.9i	1.3 + 1.8i	-2.0 - 7.2i
21	0.05 + 1.8i	0.57 + 0.55i	-1.4 - 1.2i	0.44 + 0.49i	3. + 20.i	0.2 - 4.6i	2.1 + 3.6i	-0.8 - 7.7i
22	-3.3 + 5.3i	0.94 - 0.37i	0.01 - 5.1i	-1.8 - 1.1i	7. + 54.i	-3.0 - 2.5i	-10.7 - 0.8i	2. - 21.i
23	0.7 + 1.6i	0.60 + 0.53i	-1.25 - 0.48i	0.42 + 0.45i	8. + 12.i	-3.1 - 6.6i	2.1 + 2.6i	-4.9 - 9.8i
24	0.2 + 11.3i	0.1 - 4.5i	-9.1 - 7.7i	0.12 + 0.10i	80 + 120i	-11. - 14.i	17. + 23.i	-34. - 57.i
25	1.4 + 1.4i	0.6 + 1.6i	-0.83 - 0.46i	-0.12 + 1.31i	0.2 - 2.0i	-2.2 - 3.9i	-3.2 + 3.5i	-4.7 - 3.0i
26	1.6 + 0.6i	1.0 + 1.0i	-1.3 + 0.7i	1.5 + 0.5i	5.0 + 6.2i	-7.2 - 7.5i	6.9 + 1.4i	-10.2 - 6.2i
27	-0.46 - 0.83i	0.7 - 1.3i	-0.52 - 0.52i	1.05 - 0.59i	-2. + 16.i	-0.5 + 5.9i	5.8 + 1.9i	-0.4 + 5.3i
28	1.31 - 0.12i	0.5 + 1.5i	-0.59 + 1.05i	0.74 + 0.74i	-1.8 - 6.8i	-0.2 - 5.1i	1.9 + 0.2i	-0.15 + 0.22i
29	-2.0 + 0.2i	6.2 + 5.0i	16. - 2.i	-6.8 - 1.8i	-73. - 73.i	-56. + 3.i	-71. - 29.i	-26. - 7.i
30	-3.9 - 2.2i	-7.5 - 7.2i	5.9 - 0.5i	-5.1 - 0.2i	3. - 56.i	-6.3 - 6.3i	-7. + 13.i	-18. - 41.i
31	3.5 - 3.2i	1.4 + 6.9i	1.9 + 5.8i	0.2 + 1.9i	-29. - 71.i	13. - 7.i	-14. - 14.i	28. + 26.i
32	-3.0 - 4.7i	-6.2 - 10.2i	5.3 - 0.4i	0.22 - 0.15i	-7. - 26.i	-41. - 18.i	26. + 28.i	-66. - 66.i

Table 7.17: Part 4 of the partial sum $M_{3,6}$ of the first two weighted projectors of the full EIES data set

List of Figures

List of Tables

Bibliography

[AB04] K.J. Arrow and R. Borzekowski. Limited network connections and the distribution of wages. The Federal Reserve Board: Finance and Economics Discussion Series, 2004–41, Aug 2004.

[ADDG+04] A. Arenas, L. Danon, A. Diaz-Guilera, P.M. Gleiser, and R. Guimera. Community analysis in social networks. *The European Physical Journal B*, 38:373–380, 2004.

[AGC03] M.K. Ahuja, D.F. Galletta, and K.M. Carley. Individual Centrality and Performance in Virtual R&D Groups: An empirical study. *Management Science*, 49(1):21–38, Jan 2003.

[ALB99] Reka Albert Albert Laszlo Barabasi. Emergence of scaling in random networks. *Science*, 286(5439):509–512, Oct 1999.

[BA02] A.-L. Barabasi and R. Albert. Statistical mechanics of complex networks. *Reviews of Modern Physics*, 74(1):47 – 97, Jan 2002.

[Bav48] A. Bavelas. A mathematical model for group structures. *Human Organization*, 7:16–30, 1948.

[BB01] A.L. Barabasi and G. Bianconi. Bose-einstein condensation in complex networks. *Physical Review Letters*, 86(24):5632 – 5635, Jun 2001.

[BBV04] A. Barrat, M. Barthélemy, and A. Vespignani. Weighted evolving networks: Coupling topology and weight dynamics. *Physical Review Letters*, 92:228701, Jun 2004.

[BF03] S. Borgatti and P.C. Foster. The network paradigm in organizational research: A review and typology. *Journal of Management*, 29(6):991–1013, 2003.

[BL01] P. Bonacich and P. Lloyd. Eigenvector-like Measurement of Centrality for Asymmetric Relations. *Social Networks*, (23):191 – 201, 2001.

[BL04] U. Brandes and J. Lerner. Structural similarity in graphs. *To appear in Proceedings of the 15th Intl. Symp. Algorithms and Computation (ISAAC '04)*, 2004.

[BR85] G.A. Barnett and R.E. Rice. Longitudinal Non-Euclidean Networks: Applying galileo. *Social Networks*, 7:287–322, 1985.

[BRRT01] A. Borodin, G.O. Roberts, J.S. Rosenthal, and P. Tsaparas. Finding authorities and hubs from link structures on the world wide web. In *Proceedings of the 10th International World Wide Web Conference*, pages 415–429, Hongkong, May 2001. ACM.

[BS00] J.L. Barlow and I. Slapnicar. Optimal perturbation bounds for the hermitian eigenvalue problem. *Linear Algebra and its Applications*, 309(1):19 –43, 2000.

[Bur79] A. Burghardt. *Einführung in die Allgemeine Soziologie*. WiSo Kurzlehrbücher Reihe Sozialwissenschaften. Verlag Franz Vahlen, München, 3. edition, 1979.

[Bus04] Bush-Cheney '04, Inc. Bush-Cheney '04. http://www.georgewbush.com/GetActive/ (16.08.2004), Feb 2004.

[CD02] J. Choi and J. Danowski. Making a Global Community on the Net – Global Village or Global Metropolis ?: A Network Analysis of Usenet Newsgroups. *Journal of Computer Mediated Communication: www.ascusc.org/jcmc/vol7/issue3/choi.html*, 7(3), Apr 2002.

[Chi98] N. Chino. Hilbert space theory in psychology. Bulletin of the faculty of letters No.28 Aichi Gakuin University, Japan, 1998.

[CS97] P. Cvetkovic, D. amd Rowlinson and S. Simic. *Eigenspaces of graphs*, volume 66 of *Encyclopedia of Mathematics and Its Applications*. Cambridge University Press, Cambridge, 1997.

[dF00] C. da Fonseca. The inertia of Hermitian block matrices with zero main diagonal. *Linear Algebra and its Applications*, 311(1):153 – 160, Feb 2000.

[Dic04] Merriam-Webster Online Dictionary. ”communication”. http://www.merriam-webster.com (14 Feb 2004), Feb 2004.

[DMM00] F.M. Dopico, J. Moro, and J.M. Molera. Weyl-type relative perturbation bounds for eigensystems of Hermitian matrices. *Linear Algebra and its Applications*, 309(1):3–18, 2000.

[DR01] P. Domingos and M. Richardson. Mining the network value of customers. In ACM Press, editor, *Proceedings of the 7th ACM SIGKDD International Conference on Knowledge Discovery and Data Mining*, pages 57–66, 2001.

[DS88] N. Dunford and J.T. Schwartz. *Linear Operators, Spectral Theory, Self Adjoint Operators in Hilbert Space (Wiley Classics Library)*. Wiley, New York, 1988.

[EB99] M.G. Everett and S.P. Borgatti. The centrality of groups and classes. *Journal of Mathematical Sociology*, 23(3):181–201, 1999.

[EMB02] H. Ebel, L.-I. Mielsch, and S. Bornholdt. Scale-free topology of e-mail networks. *e-publication: www.arXiv.org (05.05.2003)*, cond-mat(0201476), Feb 2002.

[FF62] L.R. Ford and D.R. Fulkerson. *Flows in networks*. Princeton University Press, Princeton, N.J., 1962.

[FF79] L. Freeman and S. Freeman. The networkers network: a study of the impact of a new communications medium on sociometric structure. *Social Science Research Reports*, (46), 1979.

[Fre84] L. Freeman. The impact of computer based communication on the social structure of an emerging scientific speciality. *Social Networks*, 6:201–221, 1984.

[Fre97] L. Freeman. Uncovering organizational hierachies. *Computational & Mathematical Organization Theory*, 3(1):5 – 18, 1997.

[Fre04] L. Freeman. Peronal communication. Email (27 Oct 2004), Oct 2004.

[Fri04] Friendster. Friendster. http://www.friendster.com (11 Oct 2004), Oct 2004.

[GDDG+02] R. Guimera, L. Danon, A. Diaz-Guilera, F. Giralt, and A. Arenas. Self-similar community structure in organisations. *e-publication: www.arXiv.org (29.04.2003)*, cond-mat(0211498), Nov 2002.

[GHW97] L. Garton, C. Haythornthwaite, and B. Wellman. Studying online social networks. *Journal of Computer Mediated Communication: www.ascusc.org/jcmc/vol3/issue1/garton.html*, 3(1), 1997.

[Gid95] A. Giddens. *Soziologie*. Nausner & Nausner, Wien, 1. edition, 1995.

[GKK01] K.-I. Goh, B. Kahng, and D. Kim. Spectra and eigenvectors of scale-free networks. *Physical Review E*, 64(5):1 – 5, Oct 2001.

[GKR98] D. Gibson, J. Kleinberg, and P. Raghavan. Inferring Web communities from Link Topology. In *Proceedings of the ninth ACM conference on Hypertext and hypermedia*, Conference on Hypertext and Hypermedia, pages 225 – 234. ACM, ACM-Press, Jun 1998.

[GN02] M. Girvan and M.E.J. Newman. Community structure in social and biological networks. *Proc. Natl. Acad. Sci. USA*, 99(12):7821–7826, Jun 2002.

[Gro04] D. Gross. It's who you know. Really. *The New York Times*, 22nd Aug. 2004, Aug 2004.

[GW95] L. Garton and B. Wellman. Social impacts of electronic mail in organizations: A review of research literature. *Communication Yearbook*, 18:434–453, 1995.

[Hay45] F.A. Hayek. The Use of Knowledge in Society. *The American Economic Review*, 35(4):519 – 530, 1945.

[Hel00] S. Helm. Viral marketing: Establishing customer relationships by word-of-mouse. *Electronic Markets*, 10(3):158–161, Jul 2000.

[Her02] C.P. Herrero. Ising model in small-world networks. *Physical Review E*, 65(66110):1–6, Jun 2002.

[HGS04] B. Hoser and A. Geyer-Schulz. Eigen System Analysis of Hermitian Adjacency Matrices of Perturbed Star Graphs. In Center for Methodology and University of Ljubliana Slovenia Informatics, Institute of Social Siences at Faculty of Social Siences, editors, *Sunbelt XXIV International Social Network Conference*, page 56. INSNA, Birografika BORI, d.o.o., Ljubliana, May 2004.

[HJ90] R. Horn and C.R. Johnson. *Matrix Analysis*. Cambridge University Press, Cambridge, 1990.

[HS74] M.W. Hirsch and S. Smale. *Differential Equations, Dynamical Systems, and Linear Algebra*. Pure and Applied Mathematics. Academic Press, San Diego, 1974.

[Hub65] C.H. Hubbell. An Input-output Approach to Clique Identification. *Sociometry*, 28(4):377–399, Dec 1965.

[Ips03] I.C.F. Ipsen. A note on unifying absolute and relative perturbation bounds. *Linear Algebra and its Applications*, 358:239 – 253, 2003.

[Jun99] D. Jungnickel. *Graphs, Networks and Algorithms*. Number 5 in Algorithms and Computation in Mathematics. Springer Verlag, Berlin, 1999.

[Kat53] L. Katz. A new status index derived from sociometric analysis. *Psychometrika*, 18(1):39–43, Mar 1953.

[Kat95] T. Kato. *Perturbation Theory for Linear Operators*. Springer, New York, 2nd edition, 1995.

[Ker04] Kerry-Edwards 2004, Inc. Kerry-Edwards 2004. http://volunteer.johnkerry.com/recruit/ (08.08.2004), Aug 2004.

[KH93] D. Krackhardt and J.R. Hanson. Informal networks: The company behind the chart. *Harvard Business Review*, 71(4):104–110, Jul 1993.

[Kle99] Jon M. Kleinberg. Authoritative sources in a hyperlinked environment. *JACM*, 46(5):604–632, sep 1999.

[Kre02] V.E. Krebs. Mapping networks of terrorist cells. *Connections*, 24(3):43 – 52, 2002.

[Lin04] LinkedIn. Linkedin. (https://www.linkedin.com/ 11 Oct 2004), Oct 2004.

[LM04] V. Latora and M. Marchiori. A measure of centrality based on the network efficiency. *e-publication: www.arXiv.org*, cond-mat(0402050):1–16, Feb 2004.

[Mat97] R. Mathias. Spectral perturbation bounds for positive definite matrices. *SIAM Journal on Matrix Analysis and Applications*, 18(4):959–980, 1997.

[Mey00] C.D. Meyer. *Matrix Analysis and Applied Linear Algebra*. Society for Industrial and Applied Mathematics, Philadelphia, 2000.

[NG03] M.E.J. Newman and M. Girvan. *Mixing patterns and community structure in networks*, volume 625 of *Lecture Notes in Physics*, pages 66–87. Springer, 2003.

[Ork04] Orkut. Orkut. http://www.orkut.com/ (11 Oct 2004), Oct 2004.

[PBMW98] L. Page, S. Brin, R. Motwani, and T. Winograd. The Page Rank Citation Ranking: Bringing Order to the Web. Technical report, Computer Science Department, Stanford University, Jan 1998.

[Pre00] J. Preece. *Online Communities: Designing Usability, Supporting Sociability*. Wiley, Chichester, 2000.

[PT03] H.W. Park and M. Thalwall. Hyperlink analyses of the world wide web: A review. *Journal of Computer-Mediated Communications*, 8(4), Jul 2003.

[Rhe00] H. Rheingold. *The Virtual Community*. MIT Press, Cambridge, 2000.

[RS00] W. Richards and A. Seary. Eigen analysis of networks. *Journal of Social Structure*, 1(2), Feb 2000.

[Sam48] P.A. Samuelson. Consumption theory in terms of revealed preference. *Economica*, 15(60):243–253, Nov 1948.

[Sch95] B. Schäfers. *Grundbegriffe der Soziologie*. Uni-Taschenbücher. Leske & Budrich, 4. edition, 1995.

[Sim00] H.A. Simon. *Administrative Behavior : A Study of Decision-Making Processes in Administrative Organizations*. Free Press, New York, 4 edition, 2000.

[SK99] M. Smith and P. Kollock. *Communities in Cyberspace*. Taylor, London, 1999.

[Smi02] R. Smith. Instant Messaging as a Scale-free Network. *e-publication: www.arXiv.org*, cond-mat(0206378), 19 2002.

[SR03a] A.J. Seary and W.D. Richards. *Spectral methods for analyzing and visualizing networks: An introduction*, pages 209–228. National Academies Press, Jan 2003.

[SR03b] M.R. Subramani and B. Rajagopalan. Knowledge-sharing and influence in online social networks via viral marketing. *Communications of the ACM*, 46(12):300–307, Dec 2003.

[Str01] S.H. Strogatz. *Nonlinear Dynamics and Chaos*. Perseus Book Group, Cambridge, MA, 1. edition, 2001.

[SW63] C.E. Shannon and W. Weaver. *Mathematical Theory of Communication*. University of Illinois Press, Chicago, 1963.

[TWH03] J.R. Tyler, D.M. Wilkinson, and B.A. Huberman. Email as spectroscopy: Automated discovery of community structure within organizations. *e-publication: www.arXiv.org (31.03.2003)*, cond-mat(0303264), 2003.

[Wel01] B. Wellman. Computer networks as social networks. *Science*, 293:2031–2034, Sep 2001.

[Wel02] B. Wellman. Designing the internet. *Communications of the ACM*, 45(5):91–96, May 2002.

[WF94] S. Wassermann and K. Faust. *Social Network Analysis, Methods and Applications*. Cambridge University Press, Cambridge, 1994.

[Wol03] Wolfram Research, Inc. *Mathematica*. Wolfram Research, Inc., Champaign, Illinois, 5.0 edition, 2003.

[YC02] B. Yaltaghian and M. Chignell. Re-ranking search results using network analysis: A case study with google. In IBM Centre for Advanced Studies Conference, editor, *Proceedings of the 2002 conference of the Centre for Advanced Studies on Collaborative research*, page 14, 2002.